A molecular analysis of the microtubule associated protein MAP65-1

Hsin Yu, Chang

A molecular analysis of the microtubule associated protein MAP65-1

By Hsin Yu Chang

Submitted in accordance with the requirements for the degree of

Doctor of Philosophy

University of Durham

School of Biological and Biomedical Sciences

September 2006

Declaration

The material in this thesis has not been submitted for a degree in Durham University or any other university. All original research within this thesis is the candidates own, apart from some experiments described in: (1) Chapter 4: In figure 4.1 and figure 4.4, transmission electron microscope images were taken by S. Sonobe; In section 4.3, Microtubule polymerisation assay was carried out in collaboration with A. Smertenko; In section 4.4, the experiments showing dimerization of AtMAP65-1 were done in collaboration with S. Fenyk and A. Smertenko. The images of *ple* mutant shown in Figure 4.5 were taken by S. Mullar. (2) Chapter5: In section 5.3, preparation of kinase samples and protein phosphorylation assay were carried out by A. Smertenko, S. Sonobe, and S. Fenyk. Results presented in the chapter 5.3.2 originate from the collaboration between A. Smertenko and L. Bogre.

Statement of copyright

Acknowledgements

I would like to thank my supervisor, Patrick Hussey, for his support and encouragement during my PhD. Many thanks to Dr. Andrei Smertenko for teaching me the techniques required and for all the scientific discussions during my study. Thanks to all the members in our lab for their kindness and giving me advice about my experiments and life in Durham. Thanks to ORS for providing me with a scholarship. Thanks to the Biomedical and Biological Sciences department for offering brilliant facilities and outstanding surroundings for research. Thanks to all my friends in Durham; you made my life in Durham full of fun. Here, I especially want to thank to my parents (張柏焜, 李美珠) whose support made the pursuit of my PhD possible, as well as my brothers (張智豪, 張益彰) for their encouragement. Thank you Ben Lyons for keeping me company through those up and downs during my PhD.

Abstract

Microtubules (MTs) play important roles in various cellular processes including cell division, organelle movement and the determination of cellular morphology. The dynamics and organization of microtubules are regulated by microtubule associated proteins (MAPs).

MAP65 bundles microtubules and forms crossbridges between microtubules *in vitro*. MAP65 belongs to a group of phylogenetically divergent proteins which includes yeast (*S. cerevisiae*) Ase1, insect (*D. melanogaster*) FEO, mammalian (*H. sapiens*) PRC1, and worm (*C. elegans*) SPD-1. All members of this group concentrate in the spindle midzone during anaphase and telophase and are important for successful cytokinesis. A gene family encoding nine MAP65-like proteins has been identified in *Arabidopsis thaliana*. These proteins have a sequence identity from 28% to 79%, suggesting that each protein might play a different role in microtubule organization. This study focuses on the MAP65-1 sub-group of MAP-65 proteins. Members of this sub-group can bind and bundle microtubules without affecting their dynamics *in vitro* and they co-localize with subsets of interphase microtubules, the preprophase band, the midzone of the anaphase spindle and the phragmoplast. Accumulation of MAP65-1 proteins in the anaphase spindle midzone suggests that it might crossbridge anti-parallel microtubules. However, the molecular mechanism of the MAP65-1 function is still unclear.

To study the dynamics of the interaction between MAP65-1 and microtubules *in vivo*, GFP: MAP65-1 chimeras were constructed and expressed in tobacco BY2 and *A. thaliana* plants. The localization of GFP was then analysed through the cell cycle and in different plant tissues. FRAP (fluorescence recovery after photobleaching) was used to study the MAP65-1 turnover. The data revealed that

MAP65 has a higher turnover than tubulin and that it can associate/dissociate randomly along microtubules. The expression of GFP: MAP65-1 in *A. thaliana* showed that MAP65-1 decorates microtubules in most of the tissues. These results suggest that the properties of MAP65-1 make it ideal for the maintenance of spatial organisation of dynamic microtubules *via* cross-bridging.

The location of the microtubule binding domain of MAP65-1 was mapped using truncated fragments and mutants. The results of these experiments demonstrate that the microtubule-binding domain lies in the C-terminal region of AtMAP65-1, whereas the dimerisation domain lies in the N-terminal region. However, a single amino acid substitution within the AtMAP65-1 microtubule binding domain (A409D and A420V) can significantly decrease the microtubule binding ability of AtMAP65-1 *in vitro*.

The cell cycle-specific binding of MAP65-1 to microtubules suggests that a specific mechanism controls this binding. Two possibilities were examined: (i) control of the protein level regulated through the cell cycle by specific degradation utilising the Destruction box and (ii) cell cycle-specific phosphorylation. Mutation of the Destruction box motif did not affect cell division or microtubule organization during the cell cycle, nor did it affect plant development. This suggests that MAP65-1 is not regulated in this way. However, MAP65-1 is hyperphosphorylated during prophase/metaphase and several phosphorylation motifs are predicted in the AtMAP65-1 protein. *In vivo* and *in vitro* experiments demonstrated that AtMAP65-1 is regulated by phosphorylation/dephosphorylation during the cell cycle by several distinct pathways including CDK and MAPK. Interestingly, over-expression of the non-phosphorylatable form of MAP65-1 induced excessive bundling of microtubules during mitosis, increased the number of pole-to-pole microtubule bundles in the mitotic spindle and caused a delay in mitosis. Therefore, precise control of microtubule bundling by MAP65-1 is essential for normal cell division.

List of Abbreviations

aa	amino acid
Ab	antibody
At	*Arabidopsis thaliana*
Agraobacterium	*Agrobacterium tumefaciens*
APC	Anaphase-promoting complex
Arabidopsis	*Arabidopsis thaliana*
AtKSS	*Arabidopsis thaliana* katanin–like protein small subunit
Ase1	Anaphase spindle elongation factor 1
AtMAP65	*Arabidopsis thaliana* microtubule associated protein of 65 kilo Daltons
AtPAKRP1	*Arabidopsis thaliana* phragmoplast-associated kinesin-related protein 1
ATP	Adenosine triphosphate
bot1	*botero1*
BY2	Bright yellow 2
bp	Base pair
BSA	Bovine serum albumin
°C	Degrees centigrade
cAMP	Cyclic guanosine mono-phosphate
cDNA	Complementary DNA
cdc	cell-division cycle
cdk	Cyclin-dependent kinase

CLIP170	Cytoplasmic linker protein 170
C-terminal	Carboxy –terminal
DMSO	Dimethylsulphoxide
DNA	Deoxyribonucleic acid
ds	Double stranded
DTT	Dithiothreitol
EB1	End binding 1
ECL	Enhanced chemiluiminescence
EDTA	Ethylenediaminetetraacetic acid
EGTA	Ethylene-glycol-bis (β-aminoethylether)-NNN'N'-tetra-acetic acid
erh3	*ectopic root hair3*
EtOH	Ethanol
FITC	Fluorescein isothiocyanate
Fra2	*Fragile fibre 2*
FRAP	Fluorescence recovery after photobleaching
GDP	Guanosine diphosphate
GA	gebberellin
Gem1	Gemini pollen 1
GFP	Green fluorescence protein
GTP	Guanosine triphosphate
hr	hour
hik	*hinkel*

IPTG	isopropyl-β-d-thiogalactoside
kbp	kilo base pair
kDa	kilo Dalton
kMTs	kinetochore microtubules
K fiber	kinetochore fiber
L	litre
LB	Luria-Bertani
MAP	Microtubule associated protein
MAPK	Mitogen-activated protein kinase
min	minute
MOR1	Microtubule oraganisator one
mRNA	Messenger ribonucleic acid
MS	Murashige and Skoog medium
MT	Microtubule
MTOCs	Microtubule organization centers
MW	Molecular weight
N-terminal	Amino-terminal
NtMAP65	*Nicotiana tabacum* microtubule associated protein of 65 kilodalton
OD_{260}	optical density at a wavelength of 260 nanometers
O/N	Overnight
PAGE	Poly acrylamide gel electrophoresis
PBS	Phosphate-buffered saline

PCR	Polymerase chain reaction
pI	Isoelectric point
PIPES	Piperazine-N,N'-bis (2-ethansulphonic acid)
PPB	Preprophase band
PRC1	Protein regulating cytokinesis 1
Ple	*pleiade*
RNA	Ribonucleic acid
rpm	Revolutions per minute
SDS	Sodium dodecyl sulphate
SDS-PAGE	Sodium dodecyl sulphate poly-acrylamide gel
spr1	*spiral1* mutant (Arabidopsis)
spr2	*spiral2*
TAE	Tris-acetate and EDTA
TAN1	TANGLED1
Taq	Thermos aquaticus
TBS	Tris-buffered saline
TBST	Tris-buffered Saline + Tween 20
TE	Tris/EDTA
TEMED	N,N,N,'N'-tetramethylethylenediamide
TKRP125	Tobacco kinesin-related polypeptide of 125kDa
UV	Ultraviolet light
WT	Wild type

X-Gal	5-bromo-4-chloro-3-indolyl-β-D-galactoside
zwi	*zwichel*

Table of contents

List of Figures

List of Tables

Publication List

Publications resulting from the work contained in this thesis:

Dynamic interaction of NtMAP65-1a with microtubules in vivo
Chang, H. Y., Smertenko, A.P., Igarashi, H., Dixon, D. P., Hussey, P. J.
Journal of Cell Science **118**, 3195-3201 (2005)

The *Arabidopsis* microtubule-associated protein AtMAP65-1: Molecular analysis of its microtubule bundling activity
Smertenko, A.P., **Chang, H.Y.**, Wagner, V., Kaloriti, D., Fenyk, S., Sonobe, S., Lloyd, C., Hauser, M.T. and Hussey, P.J.
Plant Cell, **16**, 2035-2047 (2004)

Mitotic progression is dependent on the reversible control of MAP65-1 activity
Smertenko*, A. P., Chang*, H. Y., Sonobe, S., Fenyk, S. I., Bogre, L., Hussey, P. J.
Jornal of Cell Science **119,** 3227-3237 (2006)
* APS and H-Y C contributed equally to this work.

Chapter1

Introduction

1.1 Cytoskeleton

The plant cytoskeleton is a dynamic network composed of microtubules (MTs) and actin filaments. It plays important parts in cell division, morphogenesis, intracellular transport, signal transduction, and cell wall formation.

1.2 Microtubules (MTs)

Microtubules (MTs) play important roles in various cellular processes including mitosis, organelle movements and the determination of cellular morphology (Hyams and Lloyd, 1993). Microtubules are composed of a heterodimer of α- and β-tubulin subunits and the structure of the tubulins shows a high degree of conservation across phylogeny (Burns and Surridge, 1994). α- and β-tubulin heterodimers are associated head-to-tail to form a protofilament. In general 13 protofilaments associate laterally to form a hollow tube, a microtubule, with an external diameter of 25 nm. Plant microtubules undergo dynamic reorganization through the cell cycle and in response to internal and external stimuli (Nick, 1998, Hussey, 2004). Plant microtubules also show different responses to anti-microtubule agents compared to mammalian microtubules. For instance, plant microtubules are more resistant to breakdown by colchicine. Also, anti-mitotic herbicides, dinitroaniline and the phosphorothioamidate have been

shown to bind to purified plant tubulin and inhibit plant microtubule assembly *in vitro*, but do not bind to the mammalian tubulins (Anthony and Hussey, 1999a). However, the extensive use of dinitroaniline herbicides has caused serious agriculture problems. Dinitroaniline and phosphorothioamidate resistant plants have been found to exist in natural surroundings (Anthony *et al.*, 1998; Yamamoto *et al.*, 1998; Zeng and Baird, 1999). Interestingly, this resistance has been shown to be the result of a single amino acid substitution in an α-tubulin: either Thr239 to Ile239 or Met268 to Thr268 (Anthony and Hussey,1999b). The threonine at 239 in α tubulin is positioned at the end of the long central helix close to the site of dimer-dimer interaction. The residue at 268, which is a methionine in plants and algae, and a proline in metazoans, is buried in the centre of the α-tubulin. These data suggest that each mutation causes herbicidal resistance through different mechanisms. Also, these mechanisms may involve increasing the stability of microtubules against the depolymerizing effects of the herbicide, changing the conformation of the α/β-tubulin dimer so that herbicide binding is less effective, or a combination of the two (Hussey *et al.*, 2004).

Another two *Arabidopsis* tubulin mutants, *lefty1* and *lefty2,* show the phenotype of left twisted roots and shoots, resulting from a single amino acid substitution at the interface of the α and β tubulin subunits in either α-tubulin 6 (TUA6) or α-tubulin 4 (TUA4) (Hashimoto, 2002; Thitamadee *et al.*, 2002). Right-handed helical cortical microtubule organization in the epidermal cells at the root elongation zone has also been shown in these mutants. However, abnormal

microtubule organization could not be seen in the mitotic microtubule arrays (Thitamadee *et al.*, 2002). The *lefty1/lefty2* double mutant showed helical growth in hypocotyls and radial cell expansion in the root elongation zone. The cortical microtubules in the *lefty* double mutant were more fragmented and random in orientation. The trichome in the *lefty* double mutant was less branched than wild type (Tatsuya *et al.*, 2004). The analysis of *lefty* mutants implies that microtubule organization is essential for anisotropic growth in elongating cells.

1.2.1 Dynamic instability of microtubules

Individual microtubules have been observed to undergo alternating periods of growth and shrinkage along their lengths, a process known as dynamic instability (Mitchison and Kirschner, 1984; Horio and Hotani, 1986). Microinjection of fluorescent tubulin or expression of MAP4-GFP chimeras in plant cells, coupled with measuring fluorescence recovery after photobleaching (FRAP) has shown that cortical microtubules demonstrate dynamic instability (Hush *et al.*, 1994; Yuan *et al.*, 1994; Marc *et al.*, 1998). Dynamic instability is characterized by four parameters: growth rate, shrinkage rate, frequency of transition from growth to shrinkage (catastrophe frequency), and frequency of transition from shrinkage to growth (rescue frequency) (Mitchison *et al.*, 1984). By altering dynamic instability parameters, cells can rearrange the microtubular network and quickly respond to stimuli, regulate cellular morphogenesis, and control cell division. Through microinjection studies, dynamic instability of microtubules was observed in higher plants (Zhang *et al.*, 1990). The interphase

plant microtubules grow at 5 μm/min, shrink at 20 μm/min, and display catastrophe and rescue frequencies of 0.02 and 0.08 events/sec respectively, exhibiting faster turnover than the mammalian microtubules (Dhonuckshe *et al.*, 2003).

The movement by loss of tubulin dimers from the minus end and addition at the plus end is called treadmilling (Margolis and Wilson, 1978; Shaw *et al.*, 2003). Treadmilling motility causes microtubule migration and plays a key role in the organization of the cortical array (Shaw *et al.*, 2003)

Microtubules are polar structures; the favoured assembly end is called the (+) end and the end that assembles more slowly is the (-) end. Both α- and β-tubulin bind GTP (guanosine 5'-triphosphate) to regulate polymerization. The α- tubulin subunit binds one molecule of GTP and does not hydrolyze it, whereas the β- tubulin subunit binds GTP and hydrolyzes it to GDP during or shortly after polymerization (Burns and Surridge, 1994). This GTP hydrolysis weakens the binding affinity of tubulin for adjacent molecules, thereby favouring depolymerization and resulting in the dynamic behaviour of microtubules.

1.2.2 Microtubule organizing centre (MTOC)

Most eukaryotic cells possess a specialized organelle, the microtubule-organization center (MTOC), which controls microtubule assembly and spatial organization. A typical MTOC in animal and algal cells is the

centrosome, whereas in fungi the spindle pole body (SPB) plays this role. The centrosome is a compound structure composed of a centriole pair embedded in an amorphous matrix with astral microtubule radiating from it. The pericentriolar material is important in the nucleation of microtubules and in spindle pole formation in mitosis. Microtubules always have their minus ends attached at the centrosome and their plus ends directed outwards (Heidemann *et al.*, 1980). γ-tubulin localization is restricted to the minus ends of microtubules at the MTOCs in eukaryotic cells, where it is thought to play an essential role in microtubule nucleation (Oakley *et al.*, 2000). The γ-tubulin ring complex (γ-TuRCs) initiates the nucleation of microtubules and recruits tubulins from the cytoplasm to the MTOC (Shiebel *et al*, 2000). The smallest complex unit capable of microtubule nucleation, the γ-tubulin small complex (γ-TuSC), was identified in yeast and in Drosophila (Knop and Schiebel, 1997; Oegema *et al.*, 1999; Gunawardane *et al.*, 2000). The γ-TuSC contains γ-tubulin as a nucleator and two additional proteins, spindle pole body components Spc98p and Spc97p or their homologues. These proteins are essential for the nucleation activity of the complex. Spc98p interacts with γ-tubulin, and Spc97p interacts with Spc98p. Therefore, Spc98p or its homologue can be considered as a marker for microtubule nucleation complexes (Martin *et al.*, 1998; Tassin *et al.*, 1998)

Unlike other eukaryotic cells, plant cells do not have centrosome-like organelles to nucleate microtubules. It is believed that cortical microtubules are nucleated at multiple sites dispersed in the cortical layer of cytoplasm (Chan *et al.*, 2003;

Dhonukshe and Gadella, 2003; Shaw *et al.*, 2003), whereas the nucleus-associated microtubules may be nucleated at the nuclear surface (Stoppin *et al.*, 1994; Vantard *et al.*, 1990). However, the mechanism of microtubule nucleation in plant cells is still unclear. Therefore, several proteins have been used as a marker to study microtubule nucleation in plants (Panteris *et al.*, 2000; Erhardt *et al.*, 2002; Chan *et al.*, 2003).

Plant γ-tubulin mainly localizes to the cytoplasm during interphase in the cell cycle (Erhardt *et al.*, 2002), but cortical microtubule array localization has also been observed (Panteris *et al.*, 2000). In dividing cells, γ-tubulin localizes at a subset of mitotic microtubule arrays and the cytokinetic phragmoplast (Dibbayawan *et al.*, 2001). The other marker, SPC98 orthologues have been cloned and characterized in rice (*Oryza sativa*) and *Arabidopsis thaliana* (Erhardt *et al.*, 2002). AtSpc98p-GFP colocalizes with γ-tubulin at the isolated tobacco BY-2 nuclear surface and at the cell cortex. Microtubule nucleation at the nuclear surface can be inhibited by Spc98p and γ-tubulin antibodies. This suggests that the Spc98p/γ-tubulin-containing complex is required for microtubule nucleation in plant cells. However, Spc98p does not co-distribute with γ-tubulin along microtubule arrays (Erhardt *et al.*, 2002). This indicates that the γ-tubulin associated along the microtubules might have an alternative function (Erhardt *et al.*, 2002). Another marker, end-binding protein 1(EB1), is a member of a conserved family of microtubule-associated proteins, known to bind the plus ends of microtubules and regulate microtubule dynamics (Rogers *et al.*

2002; Tirnauer *et al.* 2002). *Arabidopsis* AtEB1a-GFP has been found to associate with and dissociate from the cortex (Chan *et al.*, 2003). This suggests that microtubules in the cortical array are formed by nucleation sites dispersed along the plasma membrane.

Interestingly, a "microtubule-dependent microtubule nucleation" model (Wasteneys *et al.* 1989), in which microtubules themselves participate in the deployment of their nucleation sites, has been discovered in plant cells recently (Murata *et al.* 2005). It has been shown that microtubules are nucleated as branches on the existent cortical microtubules in plant cells. γ-tubulin locates at the branch points, and microtubule nucleation in the cell-free system is prevented by inhibiting γ-tubulin function with a specific antibody. Therefore, it is believed that microtubules nucleated by γ-tubulin recruited from the cytosol to the sides of previous formed microtubules (Murata *et al.*, 2005). However, it is still unclear if the same microtubule nucleation mechanism can be applied in the other three microtubule arrays in plant cells.

1.2.3 The microtubule arrays

Although the sequences of α and β tubulin are highly conserved, the organization of microtubules is different in animal and plant cells. In higher plants, microtubules form four distinct arrays through the cell cycle: the interphase cortical array, the preprophase band (PPB), the mitotic spindle, and the phragmoplast (Figure 1.1) (Goddard *et al.*, 1994). Besides the spindle, the

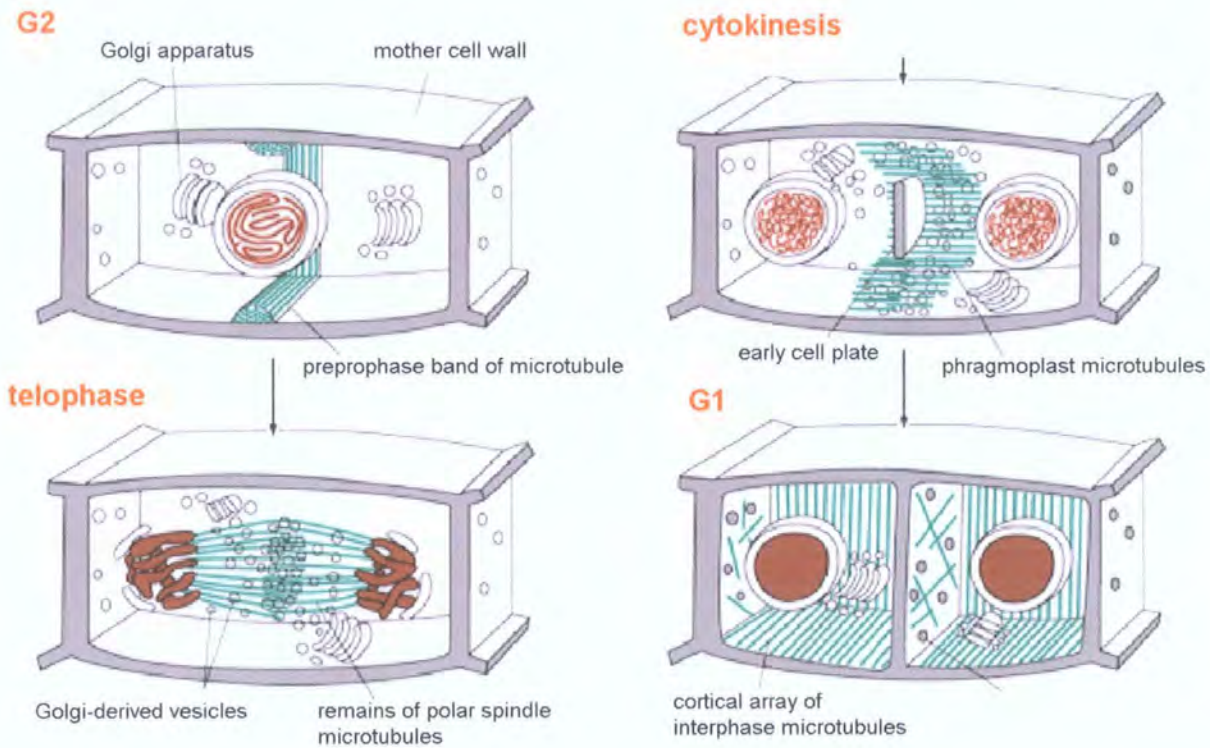

Figure 1-1. The special features of cytokinesis in a higher plant cell. The division plane is established before M phase by a band of microtubules and actin filaments (the preprophase band) at the cell cortex. At the beginning of telophase, after the chromosomes have segregated, a new cell wall starts to assemble inside the cell at the equator of the old spindle. The overlap microtubules of the mitotic spindle remaining at telophase form the phragmoplast and guide vesicles derived from the Golgi apparatus toward the center of the spindle. The vesicles are filled with cell-wall material and fuse to form the growing new cell wall, which grows outward to reach the plasma membrane and original cell wall at the site determined earlier by the preprophase band. The plasma membrane and the membrane surrounding the new cell wall fuse, completely separating the two daughter cells.

other arrays are absent in animal cells.

1.2.3.1 Interphase cortical microtubule array

Much research has been done into understanding the function of cortical microtubules in plant cells. In the 1960s, Paul Green found that colchicine-sensitive proteins of spindle fibre nature would be active in the control of wall texture and cell form (Green 1962). These "spindle fibres" were identified later as microtubules. In 1963, Ledbetter and Porter described for the first time plasma membrane-associated microtubules in transmission electron micrographs of plant cells. In tangential sections that cut through wall and cytoplasm, the microtubules showed similar orientation with the fibrous wall material and it was suggested the "tubules" were strong contenders for the role of orienting plant cell wall microfibrils (Ledbetter and Porter 1963). Since then, the relationship between cortical microtubules and cellulose microfibril orientation has been widely studied and several hypotheses have been established. Currently, the most accepted model is the "cellulose synthase constraint model" summarized by Giddlings and Staehelin (Giddings & Staehelin,1991). According to this theory, microtubules, through their close interaction with the plasma membrane, form barriers that constrain the paths of cellulose synthase complexes as they deposit cellulose chains in the cell wall. However, there are still some doubts about this model. For instance, the close relationship between microtubule orientation and the direction of cellulose deposition is not always maintained, especially in the transition from primary to

secondary wall formation. Nor is it certain that parallelism exists at all in helicoidal wall-forming cells (Giddlings and Staehelin 1991; Wasteneys 2004). Two temperature-sensitive mutants, *rsw-1* and *mor1-1,* have been used to test the cellulose synthase constraint model. The *rsw1* mutant of *Arabidopsis thaliana* is mutated in a gene encoding a cellulose synthase catalytic subunit. At temperatures above 28°C, cellulose levels are diminished, resulting in prominent root swelling (Arioli *et al.* 1999). The *mor1-1* mutant, identified in a screen for aberrant microtubule organization in leaf epidermal cells, is an allele of the large microtubule-associated protein of the MAP215 class (Whittington *et al.* 2001). Like *rsw1-1*, *mor1-1* mutants also undergo a characteristic root tip swelling at temperatures above 28°C. In the *rsw1-1* mutant, and in wild-type roots swelling after treatment with the cellulose synthesis inhibitor dichlorobienzonitril (DCB), microfibrils quickly lose parallel order, and eventually lose fibrillar appearance even though microtubules are clearly not the primary target (Sugimoto *et al.* 2001). Moreover, microtubule disruption in the *mor1-1* mutant or after treatment with the microtubule depolymerizing agent oryzalin generates radial swelling with no appreciable loss of parallel microfibril deposition (Sugimoto *et al.* 2003). These results suggest that microfibril orientation is correlated with levels of cellulose synthesis and that microtubule disorganization or complete depolymerization does not alter the ability for cellulose microfibrils to be deposited in parallel order. From the existing experimental results, Wasteneys proposes a new hypothesis, stating that cortical microtubules are required for the construction of microfibrils of sufficient

length to maintain anisotropic mechanical properties of rapidly expanding cell walls. The key concept behind the hypothesis is that short microfibrils will allow radial expansion through end-to-end separation in the lateral direction, whereas microfibrils of essentially unlimited length provide no scope for lateral separation and will thus only allow longitudinal wall expansion (Wastneys 2004).

1.2.3.2 Preprophase band (PPB)

The preprophase band (PPB) is formed at the end of the S phase and developed through the G2 phase. The band becomes thinner as the cell progresses to prophase, and it disappears completely before metaphase outset. Observation of MAP4-GFP localization during cell cycle progression allowed identification of four stages in PPB development: PPB initiation, PPB narrowing, PPB maturation, and PPB breakdown (Dhonukshe *et al.*, 2003). How the microtubules of the PPB function is still unclear; one idea is that the coincident localization of the PPB and the phragmoplast suggest that the PPB predicts the future cell division plane (Mineyuki *et al.*, 1990; Mineyuki 1999). However, not every somatic cell has a PPB, e.g. endosperm cells lack PPB but still form spindles (Smirnova and Bajer 1994). PPB removed cells can still form spindles, but its cell plate is disoriented (Mineyuki *et al.*, 1999; Murata and Wada 1991). It has also been shown that when microtubules of the PPB were depolymerized prior to PPB narrowing, the phragmoplast can still accurately target to and contact the former PPB site (Marcus *et al.*, 2005). These data suggest that there might be other factors at the PPB sites during the progression of prophase that mark the future sites of the

phragmoplast.

Interestingly, an actin depleted zone in the midzone of the spindles during prometaphase to anaphase is believed to participate in the demarcation of the division site at the final stage of cell division in higher plants (Hoshino *et al.*, 2003). The PPB, the actin-depleted zone, and the phragmopalst coincidently locate in the cell division plane, and hence are believed to play an important role in cytokinesis. However, there are a variety of molecules that have been detected at the PPB site, such as cyclin-dependent kinases (Stals *et al.*, 1997), γ-tubulin (Liu *et al.*, 1993), some kinases and phosphatases (Mineyuki *et al.*,1999; Weingartner *et al.*, 1992), MAF1 (Patel *et al.*, 2004), kinesin-like proteins (Asada *et al.*, 1997; Bowser and Reddy, 1997), and structural microtubule associated proteins such as TANGLED 1 (Smith *et al.*, 2001), AtMAP65-3 (Muller *et al.*, 2004), and MOR1 (Twell *et al.*, 2002). Their roles in cytokinesis still need to be clarified.

1.2.3.3 Spindle

Chromosome segregation is mediated by the spindle. Microtubules in the spindle have uniform polarity; the minus ends are at or near the poles and the plus ends extend toward the chromosomes (Heidemann and Mcintosh, 1980). The spindle consists of two sets of microtubules: kinetochore microtubules (kMTs), which extend from the spindle pole to the chromosomes (Rieder 1981); and the interpolar microtubules, which associate with polar microtubules of the

opposite hemisphere (Mastronarde *et al.*, 1993).

The microtubule-based mitotic spindle is highly dynamic (Mitchison *et al.*, 1986). During metaphase, kMTs display an additional treadmilling-like activity in which plus-ends grow at kinetochores while minus-ends disassemble at poles, achieving a balance that maintains a constant spindle length. (Mitchison *et al.*, 1986). Microtubule flux is a term describing the poleward movement of microtubules that is coupled to minus-end disassembly at the spindle pole (Maddox *et al.*, 2003). Flux is an evolutionarily conserved feature of all metazoan cells (Khodjakov *et al.*, 2005). The direct observation of flux suggested that chromosome movements may be powered by a "traction fiber", a model proposed in the 1950s (Ostergren, 1950). In the current version of this model (Figure 1.2), chromosomes are pulled polewards as kMT shorten as a result of reductions in the rate of tubulin incorporation at the kinetochore relative to that of microtubule depolymerization at the pole. It has been found that depolymerization of microtubules produces a force that might be needed for chromosome motion (Grishchuk *et al.*, 2005; Molodtsov *et al.*, 2005). However, Ganem *et al.* (2005) found that flux-free human cells do not hinder bipolar spindle assembly, chromosome alignment or mitotic progression. This result suggests that flux is not essential for spindle formation and chromosome movement. Therefore, how chromosomes move to the poles still needs to be clarified.

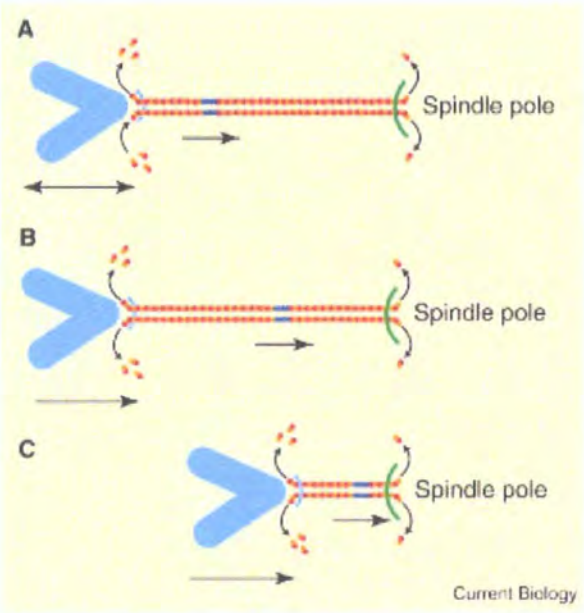

Figure 1.2 Dynamics of kinetochore fiber microtubules in vertebrate somatic cells.

(A) During metaphase tubulin subunits are continuously removed from the minus ends of microtubules at the spindle pole, while kinetochores switch between periods of tubulin polymerization and removing tubulin subunits from microtubule plus ends. As the result, chromosomes oscillate to and away from the pole, while microtubule lattice continuously fluxes poleward. (B–C). At the onset of anaphase kinetochores switch to continuous microtubule depolymerization. As a result, chromosomes move poleward on microtubules ('Pac-man') that at the same time are reeled to the pole via minus-end depolymerization ('Traction fiber'). (Image by Khodjakov and Kapoor 2005)

Kinetochores are paired, disk-like structures associated with centromeres of chromosomes. The paired nature of kinetochores facilitates the attachment of each chromosome to microtubules derived from both poles (Compton 2000). All microtubules associated with a given kinetochore form a tight bundle referred to as a kinetochore fiber (K fiber) (Compton 2000). Two possible mechanisms of K-fiber formation have been found: (a) K fibers form as microtubules growing from the spindle pole to search and capture kinetochores (Hayden *et al.* 1990) (b) K fibers self-assemble around chromatin in the absence of centrosomes (Heald *et al.*, 1997). These two mechanisms have been found to operate for the formation of the K fibers in animal cells (Rieder 2005). However, plant cells and many animal oocytes do not have centrosomes. In these cells, it is believed that microtubules nucleate around chromatin and their minus ends are organized together in the spindle poles by microtubule-based motor (dynein) (Heald *et al.*, 1996; Merdes *et al.*, 2000).

Recently, it has been observed that AtEB1a-GFP is sorted into two polar caps perpendicular to the PPB before nuclear envelope break down in *Arabidopsis thaliana* cells (Chan *et al.*, 2005). These bipolar caps of AtEB1a-GFP then transform and locate to the spindle poles after nuclear envelope breakdown However, in the cells without PPBs, the bipolar caps are missing and the bipolar spindles only emerged clearly after nuclear envelope breakdown (Chan *et al.*, 2005). From these observations and the fact that a prophase spindle exists in plant cells, this suggests that the search and capture model of K fiber formation

might also operate in plant cells (Chan *et al.*, 2005).

1.2.3.4 Phragmoplast

The phragmoplast is initiated during late anaphase. A phragmoplast complex is composed of two bundles of anti-parallel microtubules which overlap at their plus ends in the centre and actin filaments (Euteneuer *et al.*, 1982). However, recent evidence from electron tomography indicates that the anti-parallel microtubules terminate in a cell-plate assembly matrix without overlap of their plus ends (Austin *et al.*, 2005). Golgi-derived vesicles are transported to the equator of the phragmoplast by the microtubules (Samuels *et al.*, 1995). This transport might be assisted by microtubule motor proteins that have yet to be identified (Asada and Shiboaka 1994). Once cell-plate formation begins in its equatorial zone, the phragmoplast changes into a ring-like structure and centrifugally expands, maintaining localization of the microtubules at the leading edge of the cell plate. To examine how phragmoplast microtubules move centrifugally toward the cortex, Yasuhara treated tobacco BY-2 culture cells with a microtubule stabilization drug, taxol, during telophase (Yasuhara *et al.*, 2002). As a result, the phragmoplast expansion was inhibited and abnormal thick cell plates that result from the increased accumulation of vesicles were formed. The requirement for microtubule depolymerization during phragmoplast expansion indicates that the supply of tubulins from the pre-existing microtubules on the inner side of the phragmoplast forces the lateral expansion of the phragmoplast by constructing new microtubules arrays at its outer edge. Thus, the

phragmoplast appears to possess an activity that can initiate microtubule polymerization at its outer edge.

1.3 Microtubule associated proteins (MAPs)

Among the hundreds of proteins that interact with microtubules, there is a group of proteins called microtubule-associated proteins (MAPs). Traditionally, a protein was considered to be a MAP if it could be co-purified *in vitro* with microtubules as a result of direct binding. Nowadays, the label "MAP" is often used generally to describe any protein that is associated with microtubules, for instance, proteins that have an indirect or transient interaction with microtubules, proteins that have *in vivo* co-localization with microtubules, or proteins that have homology to a known MAP (Sedbrook 2004). So far, several MAPs have been isolated in plants (e.g. Wasteneys, 2000; Sedbrook 2004; Ketelaar *et al.*, 2004; Lloyd and Hussey, 2001).

1.3.1 Isolation and characterization of MAP65 protein

In animal cells, the basic procedure used to purify brain MAPs is by successively polymerizing and depolymerizing microtubules. Proteins then co-purified after several cycles are defined as microtubule-associated proteins. But in plant cells, very low amounts of microtubular proteins are obtained through the same procedure because of the vacuoles. Vacuoles contain protease and phenols that will affect the protein extraction. To solve this problem, Jiang and Sonobe (1992) made protoplasts from tobacco BY-2 suspension cells and removed the

vacuoles to generate miniprotoplasts. Plant MAPs could be isolated by cycling taxol stabilized microtubules from the miniprotoplasts. Since then, several MAPs have been isolated from plants.

1.3.2 MAP65 family

The MAP65 family is a group of proteins with approximate molecular weights of 65KD, which constitutes the most abundant group of proteins in the microtubule preparations of tobacco (Jiang and Sonobe 1993) and carrot (Daucus carota) (Chan *et al.*, 1996). Corresponding MAP65 cDNAs have been cloned (NtMAP65-1, Smertenko *et al.* 2000; DcMAP65-1, Chan *et al.* 2003b), and a gene family of nine members has been identified in *Arabidopsis thaliana* (Hussey *et al.*, 2002). The Arabidopsis MAP65s share 28-79% sequence identity, and their predicted molecular masses vary from 54 to 80kDa (Hussey *et al.*, 2002). An antibody raised against biochemically purified tobacco MAP65 decorates all microtubule arrays (Jiang and Sonobe, 1993), while antibodies raised to one isotype, recombinant NtMAP65-1, recognizes only a subset of interphase microtubules and in particular the anaphase spindle midzone and at the midline of the cytokinetic phragmoplast (Smertenko *et al.*, 2000). The localization suggested that MAP65 cross-links antiparallel microtubules (Smertenko *et al.*, 2000). Biochemically purified MAP65 proteins have been found to bind and bundle microtubules in *vitro* (Jiang and Sonobe 1993). Consistent with this observation, NtMAP65-1a protein was also able to increase the turbidity of tubulin solution *in vitro* (Smertenko *et al.*, 2000). Recently, it was

observed that recombinant AtMAP65-1 does not promote microtubule polymerization (Wicker-Peanguant *et al.*, 2004; Smertenko *et al.*, 2004). Instead, it induces microtubule bundling *in vitro* and forms 25 nm crossbridges between microtubules (Wicker-Peanguant *et al.*, 2004; Smertenko *et al.*, 2004). In contrast, Mao *et al.* (2005) showed that AtMAP65-1 promotes tubulin polymerization, enhances microtubule nucleation, and decreases the critical concentration for tubulin polymerization (Mao *et al.*, 2005). The effect of the presence of MAP65 on the cold stability of microtubules is also controversial. AtMAP65-1a does not stabilize microtubules against cold-induced microtubule depolymerization (Smertenko *et al.*, 2004), while NtMAP65-1b confers cold stability to microtubules bundle *in vitro* (Mao *et al.*, 2005; Wicker-Peanguant *et al.* 2004). Moreover, the bundling effect of NtMAP65-1b results from the interaction of the protein with the C-terminal part of tubulin (Wicker-Planquart *et al.*, 2004).

Chan *et al.* (1996) used taxol-stabilised brain microtubules to isolate MAP from detergent-extracted cytoskeletons prepared from carrot suspension cells. From this preparation, three electrophoretically separable bands of 60kDa, 62kDa, 68kDa, and two proteins of less than 100 kDa were detected on 1D SDS gels (Chan *et al.*, 1996). These three polypeptides were found to be antigenically related; hence they are referred to be "MAP65 family." Monospecific antibodies raised against these three MAP65 bands stained all four microtubule arrays in carrot cells, similar with the MAP65 localization in tobacco BY2 cells (Jiang and Sonobe, 1933). The single 60 kDa protein was chromatographically purified by

Rutten *et al.* (1997). This 60 kDa protein stabilizes brain microtubules against the depolymerization caused by the cold and calcium treatment, but does not bundle microtubules *in vitro*. Furthermore, it stimulates tubulin polymerization only when tubulin is just above the self-polymerization concentration (Rutten *et al.*, 1997). Later on, Chan *et al.* (2003b) isolated the 60 kDa, 62 kDa, and 68 kDa proteins of MAP65 using sucrose density gradients separation. Only the 62kDa band was found to be present in elongating cells containing only cortical microtubules, indicating that this isoform of MAP65 is responsible for the cross-bridging activity and maintaining the cortical microtubules during cell elongation (Chan *et al.*, 2003b).

MAP65 has been found to be involved in plant embryo development. Somatic embryogenesis of *Picea abies* (gymnosperm) was used as a model system to study the role of the MAP65 in the plant embryo development (Von Arnold *et al.*, 2002; Smertenko *et al.*, 2003). In the normal embryonic cell line, MAP65 has been found binding to the cortical microtubules at all stages of embryo development analyzed. However, different isoforms of MAP65, 63 kDa and 65 kDa, have been shown in *Picea abies* embryos. The 63 kDa isoform was prevalent in the normal embryonic cell line, whereas the 65 kDa isoform was the main isoform in the development-arrested cell line (Smertenko *et al.*, 2003). These results suggested that a critical quantity of the 63 kDa isoform is essential for cell differentiation.

The nine AtMAP65 proteins have sequence identity from 28% to 79% (Figure 1.3) (Hussey *et al.*, 2002). Each protein might play a different role in microtubule organization (Van Damme *et al.*, 2004). For instance, AtMAP65-1 and AtMAP65-6 share 44% sequence identity and act differently *in vitro* (Mao *et al.*, 2005). The AtMAP65-1 protein induces the formation of large microtubule bundles by forming cross-bridges between microtubules evenly along the whole length of microtubules, whereas the AtMAP65-6 protein only forms cross-bridges at regional sites between microtubules. The microtubule network induced by AtMAP65-6 forms a mesh-like network and is more resistant to high concentrations of NaCl than the bundles induced by AtMAP65-1. AtMAP65-6 does not enhance microtubule polymerization and nucleation *in vitro*, and it does not stabilize microtubules against cold treatment and dilution. Moreover, the localizations of AtMAP65-1, AtMAP65-3, AtMAP65-4, AtMAP65-5, AtMAP65-6, and AtMAP65-8 are different during the cell cycle (Van Damme *et al.*, 2004; Mao *et al.*, 2005). Purified anti-AtMAP65-6 antibodies revealed that AtMAP65-6 was associated with mitochondria in *Arabidopsis* cells (Mao *et al.*, 2005).

AtMAP65-3 plays an essential role in cytokinesis and has distinct localization in plant cells. From a genetic screen for defects in root morphology and embryo morphogenesis a mutant was selected having a phenotype of multinucleated cells and incomplete cell walls (Sorensen *et al.*, 2002; Söllner *et al.*, 2002; Müller *et al.*, 2002). The mutant was called *pleiade* (*ple*) and all identified alleles were found to be single amino acid substitution recessive mutations. Some of the

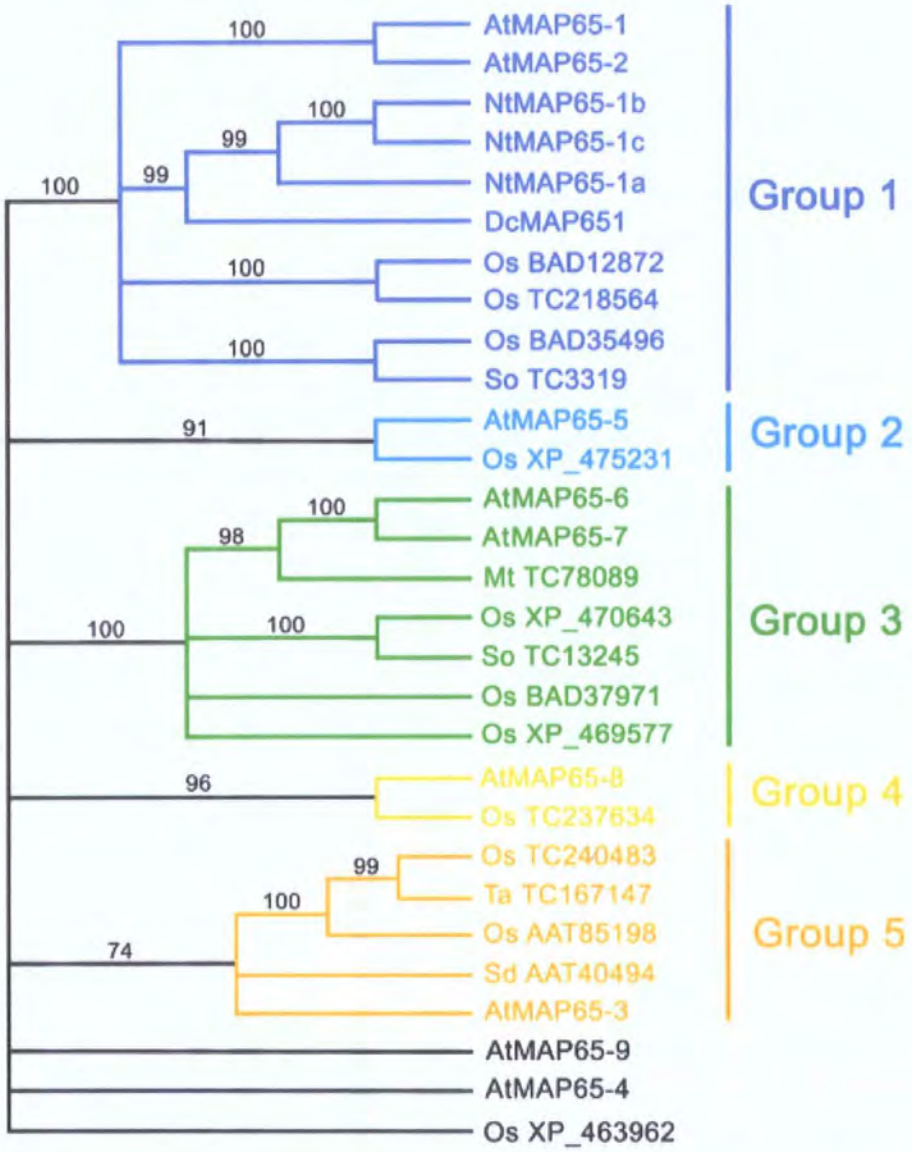

Figure 1.3 Phylogenetic tree of known MAP65 proteins from *A. thaliana*, *O. saliva*, *N. tabacum* **and other plant species.**

mutations result in C-terminal truncations of AtMAP65-3. AtMAP65-3/PLE does not co-localize with the interphase microtubules and only localizes to a subset of mitotic microtubule arrays. It binds to the preprophase band, the anaphase spindle midzone and the phragmoplast midline but not to the prophase, metaphase, and early anaphase spindles. In the *ple* mutants the anaphase spindle is normal, and the cytokinetic phragmoplast can form but is distorted; not only is it wider, but the midline is also unusually expanded (Muller *et al.*, 2004). Interestingly, AtMAP65-3/PLE is expressed in all organs in the plant, but the cytokinesis defect is only observed in root tissues, indicating that there is likely to be redundancy in function between members of *AtMAP65* gene family in different plant organs.

Expression of GFP chimeras with AtMAP65-1, AtMAP65-3, AtMAP65-5, and AtMAP65-8 in tobacco BY-2 cells reveals differential localization of these proteins (Van Damme *et al.*, 2004). AtMAP65-1-GFP shows thick bundles of cortical microtubules and concentrated dot–like structures that were attached to the end of the microtubules. In the phragmoplast, AtMAP65-1-GFP is excluded from the phragmoplast midline and associated along the microtubules. AtMAP65-3-GFP shows thin bundles of cortical microtubules and strong endocytic microtubule bundles wrapped around the nucleus and formed extensions that were connected to the cortical microtubules of the cell poles. Similar structures could also be observed in transgenic BY-2 cells transformed with other MAP65 constructs; and the GFP-MBD and TUA6-GFP controls.

AtMAP65-5 also decorates cortical microtubules, and the labeling pattern resembled the cortical array visualised by MBD-GFP. The AtMAP65-5-GFP fluorescence signal is much stronger in the phragmoplast than in the PPB and the spindle. AtMAP65-5-GFP is concentrated in the mid-zone of the phragmoplast. AtMAP65-8 decorates cortical microtubules discontinuously, indicating that AtMAP65-8-GFP is associated with a subpopulation of microtubules in the cortical array. AtMAP65-8-GFP does not decorate the phragmoplast midline, but labels the whole phragmoplast and the outer extreme ends of the phragmoplast near the nuclear surface where the microtubule minus-ends are located (Van Damme *et al.*, 2004).

There are MAP65 homologues in other organisms including PRC1(mammalian) (Mollinari *et al.*, 2002), Ase1 (Yeast) (Schuyler *et al.*, 2003), Feo(Drosophila)(Fiammetta *et al.*, 2004) , and SPD-1 (C. elegans) (*O'Connell et al.*, 1998).

Mammalian PRC1 stabilises the spindle midzone (Jiang *et al.*, 1998; Mollinari *et al.*, 2002). PRC1 is also a mitotic substrate for cyclin dependant protein kinase (CDK) (Jiang *et al.*, 1998). PRC1 binds and bundles microtubules *in vivo* and *in vitro* (Jiang *et al.*, 1998). Overexpression of PRC1 extensively bundles interphase microtubules, but does not affect early mitotic spindle organization (Mollinari *et al.*, 2002). PRC1 has two Cdk phosphorylation motifs, and a CDK phosphorylation null mutant caused extensive bundling of the prometaphase

spindle (Jiang *et al.*, 1998). Suppression of PRC1 by siRNA causes failure of microtubule interdigitation between half spindles and the absence of the spindle midzone (Mollinari *et al.*, 2002). It has been found that the N-terminal region of PRC1 is important for localization to the cleavage furrow and to the centre of the midbody, whereas the central conserved region is required for microtubule binding and bundling activity (Mollinari *et al.*, 2002). Interestingly, KIF4, a member of kinesin-4 family, has been found to interact with PRC1 and restrict localization of PRC1 to a narrow region in the centre of the anaphase spindle (Kurasawa., 2004).

Ase1p (anaphase spindle elongation 1) was first identified in budding yeast. Ase1p locates at the anaphase spindle midzone, where the microtubules overlap (Chan *et al.*, 1999; Mollinari *et al.*, 2002; Schuyler *et al.*, 2003; Verbrugghe and White, 2004; Verni *et al.*, 2004). Ase1 bundles microtubules *in vitro*. The deletion mutant is viable but fails to form overlapping anti-parallel microtubule bundles, leading to interphase nuclear positioning defects and premature mitotic spindle collapse (Schuyler *et al.*, 2003; Isabelle *et al.*, 2005; Akira *et al.*, 2005). FRAP data shows that during interphase Ase1p is highly dynamic at overlapping microtubule minus ends, while during mitosis Ase1p has a very slow rate of turnover at microtubule plus ends at the spindle midzone (Isabelle *et al.*, 2005; Schuyler *et al.*, 2003). It has also been found that Ase1 acts as a regulatory component in the cytokinesis checkpoint that operates to inhibit nuclear division when the cytokinesis apparatus is perturbed (Akira *et al.*, 2005). PRC1 and Ase1

share two notable sequence features: a consensus cyclin-dependent kinsae phosphorylation site and a sequence that is similar to a mitotic cyclin destruction box. However, it has been found that Ase1 is targeted for proteolysis by the anaphase-promoting complex (Juang *et al.*, 1997).

Drosophila FEO is especially enriched at the central-spindle midzone. The deletion of Feo causes aberrant central spindles. In Feo-depleted cells, the morphology of prophase, metaphase, or early anaphase are normal, but telophases display thin microtubule bundles of uniform width instead of robust hourglass-shaped central spindles. The phenotype of Feo-depleted telophases suggests that Feo interacts with the plus ends of central spindle microtubules so as to maintain their precise interdigitation during the anaphase-telophase microtubule elongation and antiparallel sliding (Fiammetta *et al.*, 2004).

C. elegans spd-1(oj5) is a temperature-sensitive maternal-effect embryonic-lethal mutation isolated in a screen for cell division mutants (*O'Connell et al.*, 1998). When *spd-1(oj5)* homozygote hermaphrodites are shifted to the restrictive temperature (25°C) at the four cell stage in embryo development, they produce 100% dead embryos. The spindles in these embryos are bent or broken at anaphase in cell division. In the *spd-1(oj5)* mutant, the microtubules in the spindle mizone are missing, but cytokinesis is completed by most of the cells. The *spd-1* gene has been cloned and found to be a member of the MAP65 protein family. SPD-1 bundles microtubules *in vivo* and localizes at

the spindle midzone (Verbrugghe *et al.*, 2004). All together, these data suggest that SPD-1 plays an important role in spindle midzone assembly (Verbrugghe *et al.*, 2004).

1.3.3 MAP190

Tobacco MAP190 was purified by its co-purification with cycling plant microtubules and its ability to bind F-actin (Igarashi *et al.*, 2000). Therefore, MAP190 is believed to be involved in the interaction between actin filaments and microtubules. MAP190 locates in the nucleus before nuclear envelope breakdown, and in the spindle and phragmoplast during cell division. After the re-formation of the nuclear membrane, MAP190 is sequestered into the daughter nuclei. However, MAP190 does not localize to the cortical microtubule array or preprophase band. Hence it is believed that MAP190 is regulated through the cell cycle. MAP190 contains a calmodulin-like domain in the C-terminus (Hussey *et al.*, 2002). This conserved motif suggests that MAP190 might link microtubules and actin in the plant cells in response to calcium ions (Igarashi *et al.*, 2000; Hussey *et al.*, 2002).

1.3.4 MOR1/GEM1

To identify factors regulating cortical microtubule organization, Whittington *et al.* (2001) used immunofluorescence microscopy to screen chemically mutagenized seedlings of *A. thaliana* for aberrant microtubule patterns. A mutant, which has the phenotype of temperature-sensitive cortical microtubule shortening and

disorganization, was found and named as *mor1* (*microtubule organization1*). Using ecotype specific markers, *MOR1* was identified as a 14 kb gene consisting of 53 exons and sharing sequence similarity to the human microtubule associated protein TOGp (Charrasse *et al.*, 1998), *Xenopus* MAP215 (Gard and Kirschner, 1987), *Drosophila* MSPS (Cullen *et al.*, 1999), *Dictyostelium* DdCP224 (Graf *et al.*, 2000), yeast STU2 (Wang and Huffaker, 1997) and Dis1 (Ohkura *et al.*, 1988; Garcia *et al.*, 2001), and *C. elegans* ZYG-9 protein (Hirsh and Vanderslice 1979). From the sequence analysis, at least ten putative HEAT repeats were found in *MOR1*, which represent sites of likely protein-protein interaction (Whittington *et al.*, 2001). The *mor1* mutant alleles (*mor1-1* and *mor1-2*) which contain substitutions in the HEAT repeat nearest to the N-terminus show a phenotype of short and disorganized cortical microtubules under restrictive temperature conditions (above 28°C) and restoration of parallel cortical microtubule after a few minutes of reaching the permissive temperature (21°C). Morphological defects including left-handed twisting of organs, isotropic cell expansion and impaired root hair polarity have also been found in *mor1* seedlings growing at 31°C . This result indicates that MOR1 is required throughout development in all plant organs (Whittington *et al.*, 2001). The MOR1 cDNA encoded a protein with a predicted mass of 217 kD. MOR1 protein was found to bind microtubules *in vivo*, localizing to cortical microtubules and to areas of overlapping microtubules in the phragmoplast (Whittington *et al.* 2002). From the RT-PCR analysis, MOR1 is expressed in roots, cotyledons, rosette leaves, stems, open flowers and green siliques. However, the microtubule

mitotic arrays were not affected in the *mor 1* mutants (Whittington *et al.*, 2002). Twell and colleagues identified a cytokinesis-defective mutant *gem1*, which is synonymous to MOR1 (Twell *et al.*, 2002). The *gem1* mutant-alleles *gem1-1* and *gem1-2* homozygotes are lethal and 50% of pollen from the heterozygotes failed to form the cell plate during mitosis. The MOR1/GEM1 carboxy-terminal domain, which binds to microtubules *in vitro*, is absent in *gem1-1* and *gem1-2* mutants (Twell *et al*, 2002). The result indicates that the C-terminus of MOR1/GEM1 is important for phragmoplast organization. The analysis of *mor1* and *gem1* mutants indicates that MOR1/GEM1 plays an essential role in both the cortical microtubule array and the phragmoplast (Whittington *et al.*, 2002; Twell *et al.*, 2002; Eleftheriou *et al.*, 2005).

Two protein homologues of MOR1/GEM1 were isolated and characterized in tobacco. TMBP200 was isolated from telophase BY-2 cells (Yasuhara *et al.*, 2002), and MAP200 was isolated from mostly interphase BY-2 cells (Hamada *et al.*, 2004). TMBP200 bundles microtubules and forms 10nm microtubule cross-bridges, whereas MAP200 does not. The different microtubule cross-bridge abilities between TMBP200 and MAP200 might be attributable to post-translational modification (Hamada *et al.*, 2004). MAP200 has been found to promote tubulin polymerization and increase the number and the length of microtubules *in vitro* (Hamada *et al.*, 2004). MAP200 and tubulin dimers have been found to form a complex *in vitro*. This complex may accelerate tubulin polymerization (Hamada *et al.*, 2004). Similar complexes have also been found

in *Xenopus*, it is composed of XMAP215 and tubulin dimers and is believed to promote tubulin polymerizaion. Therefore, the complex of MAP200 and tubulin oligomers might function as microtubule-nucleating complexes.

In animal cells, the stimulatory effect of XMAP215 is antagonized by the central motor kinesin, XKCM1 (Tournebize *et al.*, 2000). According to Hussey and Hawkins (2001), the N-terminal repeat of MOR1 could negate the effect of a destabilizing kinesin, either by binding directly to it or by competing for the microtubule binding site. Since XMAP215 has recently been reported to anchor nascent minus ends of microtubule asters formed *in vitro* (Popov *et al.*, 2002), a further possibility is that its plant homolog, MOR1, could itself have a direct effect on microtubule nucleation by helping to anchor growing ends at the cell cortex.

1.3.5 MAP70

To identify plant specific MAPs, Korolev *et al.* (2005) isolated microtubules by inducing the polymerization of endogenous tubulins contained within an extract of *Arabidopsis* protoplasts and identified the proteins attached to microtubules. Among these proteins, a 70 kDa protein was identified and named as AtMAP70. The AtMAP70 family is composed of five closely related *Arabidopsis* proteins, which have no known homologues in other eukaryotes. The GFP: AtMAP70 fusion protein decorates all four microtubule arrays in both transiently infected *Arabidopsis* and stably transformed tobacco BY-2 cell lines. However, AtMAP70

does not decorate the phragmoplast midline. When a GFP: AtMAP70 expressing cell line was treated with the microtubule stabilizing drug taxol, both microtubules and MAP70 formed thicker bundles, while treatment with the microtubule depolymerization drug oryzalin resulted in disruption of both microtubules and GFP: AtMAP70. Interestingly, GFP: AtMAP70 decoration of microtubules was not affected by the actin depolymerization drug, cytochalasin D. The drug treatment and the fact that AtMAP70 binds to microtubules *in vitro* suggest that AtMAP70 is a microtubule associated protein. AtMAP70-1 contains four predicted coiled-coil domains and truncation studies identified a central domain that targets the fusion protein to microtubules *in vivo* (Korolev *et al*, 2005).

1.3.6 SPIRAL1

The *Arabidopsis* mutant *spiral 1* (*spr1*) shows right-handed helical growth in roots and etiolated hypocotyls (Furutani *et al.*, 2000). These root phenotypes can be suppressed by microtubule depolymerization drugs, such as propyzamide, oryzalin, and enhanced by cold treatment. The cortical microtubule arrays of elongating *spr1-1* epidermal root cells have been found to be arranged in helices with a left-handed pitch, whereas in the ground tissue of etiolated hypocotyls, a mixture of transverse, oblique, and longitudinal arrays are observed (Furutani *et al.*, 2000). Moreover, propyzamide treatment creates right-handed helical microtubule arrays in wild type and *spr1-1* elongating root cells. These results suggest that SPR1 is essential for anisotropic cell expansion by affecting cortical microtubule organization. The *SPR1* gene encodes a plant-specific 12 kD

protein and belongs to a six member gene family in *Arabidopsis*. SPR1: green fluorescent protein (SPR1-GFP) fusion locates to the cortical microtubules, the preprophase band, the mitotic spindle, and the phragmoplast in *Arabidopsis* seedlings (Sedbrook *et al.*, 2004). SPR1 has a repeated motif at both ends, separated by a predicted rod-like domain, suggesting that it may act as an intermolecular linker (Sedbrook *et al.*, 2004). All together, SPR1 is a plant-specific microtubule-localized protein that influences directional cell expansion (Nakajima *et al.*, 2004; Sedbrook *et al.*, 2004).

1.3.7 SPIRAL2

spiral2 (*spr2*) is an *Arabidopsis* right-handed helical mutant with prominent counter-clockwise twisting in leaf petioles and flower petals (Furutani *et al.*, 2000), and is allelic to two classic twisting mutants, *tortifolia1* (Burger *et al.*, 1971) and *convoluta* (Relicahova *et al.*, 1976). The *SPR2* gene encodes a plant–specific 94 kD protein containing HEAT-repeat motifs that are implicated in protein-protein interaction. SPR2 is thought to be a MAP because of its ability to bind to microtubules *in vivo* and *in vitro*. SPR2-GFP locates to the cortical microtubule, the PPB, the spindle, and the phragmoplast in *Arabidopsis* and tobacco cells (Shoji *et al.*, 2004; Bushmann *et al.*, 2004). SPR2 is a MAP required for proper microtubule function during anisotropic growth of cells.

1.3.8 Tangled 1 (TAN1)

tangled1 is a recessive mutant of maize with the majority of cells in all leaf tissue

layers dividing in abnormal orientations (Smith *et al.* 1996). In *tangled1* mutant cells, the microtubule arrays involved in cell division are formed and appear structurally normally, but the orientations of these structures are abnormal. Abnormally oriented cell divisions can be attributed to the failure of phragmoplast to be guided to the former PPB site (Cleary and Smith, 1998). *Tan1* gene encodes a microtubule binding protein, TAN1. Antibodies against TAN1 preferentially decorate the PPBs, the spindles, and the phragmoplast, but not the interphase microtubules. The lack of association of TAN1 proteins with microtubules in interphase cells suggests that their interaction is regulated in a cycle-dependent manner (Smith *et al.* 2001). Therefore, TAN1 protein participates in the orientation of cytoskeletal structures in dividing cells through the association with microtubules. Moreover, the TAN1 protein distantly relates to the basic microtubule-binding domain of vertebrate adenomatous polyposis coli (APC) protein (Smith *et al.* 2001). APC proteins are activators of a guanine nucleotide exhange factor that in turns activates a small GTPase. The discovery of TAN shows that small GTPases may play roles in specifying division planes in plant cells.

1.3.9 End-binding MAPs

1.3.9.1 Microtubule plus-end-tracking proteins (+TIPs)

In the late 1990s, a new family of MAPs that preferentially accumulate at the plus ends of microtubules was identified (Perez *et al.*, 1999). In this work, the movement of a cytoplasmic linker protein 170 (CLIP-170) linked to GFP was

observed in living mammalian cells. The fusion protein formed a comet-like structure that tracked the plus ends of growing microtubules (Perez *et al.*, 1999), and this property is now the defining characteristic of the group of proteins called +TIPs. From the BLAST searches, it has been found that plants might lack CLIPs (Sherryl R. *et al.*, 2004). However, when mammalian CLIP-170 is expressed in plant cells, it tracks microtubule plus ends, indicating that the pathway that regulates binding of CLIP-170 to microtubules is conserved in plants (Dhonukshe and Gadella, 2003).

1.3.9.2 End-binding protein 1 (EB1)

End-binding protein 1(EB1) is a member of a conserved family of MAPs that in other eukaryotic cells is known to bind the plus ends of microtubules and regulate microtubules dynamics (Rogers *et al.* 2002; Tirnauer *et al.* 2002). EB1 was originally identified as a binding partner of the tumor suppressor protein adenomatous polyposis coil protein, APC in humans (Su *et al.* 1995). In *Arabidopsis* plants three EB1-like genes have been identified (Mathur *et al.*, 2003). In transgenic *Arabidopsis thiliana*, the GFP-AtEB1b fusion protein has been found localizing not only to microtubule plus ends but also to motile, pleiomorphic tubulovesicular membrane networks that surround other organelles and frequently merge with the endoplasmic reticulum. The dual localization pattern of AtEB1 suggests links between microtubule plus end dynamics and endomembrane organization during polarized growth of plant cells (Mathur *et al.*,

2003; Van *et al.*, 2004). Through the cell cycle, AtEB1-a and AtEB1-b label the microtubule plus end as a comet in the cortical array, mitotic spindle, and phragmoplast (Chang *et al.* 2003; Van *et al.*, 2004). However, the microtubule minus end labeling of AtEB1a-GFP is controversial. Although EB1 has been shown to localize at the plus ends of microtubules in different organisms (Rogers *et al.*, 2002; Timauer et sl., 2002; Chan *et al.*, 2003; Piehl *et al.*, 2004), AtEB1-GFP could also be found localizing at the minus ends of microtubules in the transient infected *Arabidopsis thiliana* suspension cells (Chan *et al.* 2003). However, this microtubule minus end localization is missing in the AtEB1-GFP expressed tobacco BY2 cell lines (Van Damme *et al.*, 2004).

1.3.10 Microtubule motor proteins: kinesin and kinesin-like proteins

Kinesins are microtubule-based motor proteins with a conserved kinesin motor domain. They move along microtubules by using the energy released from ATP hydrolysis. In the *Arabidopsis* genome (*Arbidopsis thaliana*), there are at least 61 genes encoding kinesins. Most Arabidopsis kinesins are evolutionarily divergent from their counterparts in animals and fungi (Lee *et al.*, 2004). *Arabidopsis* kinesins form a number of subfamilies. For example, BIMC/Kinesin-5 and the NCD/Kinesin-14 subfamilies in *Arabidopsis* are similar to those in fungi and animals, while other kinesins in *Arabidopsis* are very different in plants. Some *Arabidopsis* kinesins are associated with microtubules,

mitochondria, Golgi stacks, or vesicles. Therefore, kenesins contribute directly or indirectly to cell division and cell growth.

Members of the kinesin protein superfamily share a catalytic core domain of about 350 amino acids containing an ATP-binding site and a microtubule-binding site. The catalytic core is often juxtaposed with an α-helical domain of smaller than 50 amino acids, which is called the neck region (Endow, 1999). The catalytic core plus the neck form a kinesin motor domain. Kinesins are grouped into several subfamilies by phylogenetic analyses of their motor domains (Schoch *et al.*, 2003; Dagenbach and Endow, 2004).

1.3.10.1 KATA/ATK1

The *Arabidopsis* KAT genes encode KATA, KATB, and KATC (Mitsui *et al.*, 1993) proteins. KATA/ATK1 was shown to be a microtubule minus end-directed kinesin (Marcus *et al.*, 2002). In the *atk1-1* mutant, male meiotic cells have broad spindles, which lack focused poles in metaphase I and II. Consequently, chromosome segregation is abnormal and the fertility of the male is reduced (Chen *et al.*, 2002). It has been shown that the *atk1* mutant lacks microtubule accumulation at the predicted spindle pole during prophase and has reduced spindle bipolarity during prometaphase. However, all abnormalities are rectified by anaphase and chromosome segregation appears normal. The *atk1-1* phenotype could be caused by the lack of microtubule-bundling activities in the spindle. KATA/ATK1 and three other kinesins may contain a

microtubule-binding site at their N terminus due to the sequences similarity (Lee *et al.*, 2004).

1.3.10.2 The calmodulin-binding kinesin: KCBP/ZWI

Genetic screens of *Arabidopsis* plant for altered trichome morphogenesis have lead to the identification of a mutant, *zwichel* (*zwi*) (Hulskamp *et al.*, 1994). The normal wild type trichomes have large, single epidermal cells with a stalk and three or four branches, whereas the trichomes in *zwichel* mutant have a short stalk with one or two branches depending on the severity of the allele. The *ZWI* gene has been identified as a member of the kinesin superfamily of microtubule motor proteins and is identical to a kinesin-like calmodulin-binding protein (KCBP) (Oppenheimer *et al.*, 1997; Reddy *et al.*, 1996). *KCBP/ZWI* is a single gene in the *Arabidopsis* genome that encodes unique calmodulin-binding kinesin (Reddy *et al.*, 2000). KCBP contains a C-terminal motor domain and has a calmodulin-binding site. KCBP binds microtubules in an ATP-dependent manner and exhibits microtubule-stimulated ATPase activity. Calmodulin inhibits binding of KCBP to microtubules, and the extent of inhibition is dependent on the concentration of calcium and calmodulin (Deavours *et al.*, 1998). The phenotype can be suppressed by the application of a microtubule stabilization agent, taxol, which indicates KCBP/ZWI may play a role in stabilizing microtubules (Mathur *et al.*, 2000). Recent studies show that the cotton *Gossypium hirsutum* kinesin (GhKCBP) decorates cortical microtubules and mitotic microtubule arrays in cotton fibers, which suggests that KCBP/ZWI may stabilize microtubules in the

interphase cell and affect cell division (Preuss *et al.*, 2003).

1.3.10.3 The Actin-binding KCH kinesins

GhKCH1 has been identified from cotton (*Gossypium hirsutum*) fibers as an actin-binding kinesin (Preuss ML *et al.*, 2004). GhKCH1 has a centrally located kinesin catalytic core, a signature neck peptide of minus end-directed kinesins, and a unique calponin homology (CH) domain at its N terminus. GhKCH1 and other CH domain-containing kinesins (KCHs) belong to a distinct branch of the minus end-directed kinesin subfamily. So far the KCH kinesins have been found only in higher plants. GhKCH1's N-terminal region including the CH domain interacted directly with actin microfilaments. In cotton fibers, GhKCH1 decorates cortical microtubules in a punctate manner. It has been suggested that GhKCH1 might play a role in mediating dynamic interaction between microtubules and actin microfilaments in cotton fibers. Localization of GhKCH1 on cortical microtubules was independent of the integrity of actin microfilaments. Thus, GhKCH1 may play a role in organizing the actin network in cooperation with the cortical microtubule array. These data also suggest that flowering plants may employ unique KCHs to coordinate actin microfilaments and microtubules during cell growth.

1.3.10.4 AtPAKRP1

AtPAKRP1 stands for *Arabidopsis thaliana* phragmoplast-associated kinesin-related protein 1. AtPAKRP1 localizes to the spindle midzone during late

anaphase and at the phragmoplast midline during telophase. It is believed to have a function in establishing and maintaining the bipolar structure of the phragmoplast (Lee *et al.*, 2000). AtPAKRP2 first appears in a punctuate pattern among interzonal microtubules during late anaphase. When the phragmoplast microtubule array appears in a mirror pair, AtPAKRP2 becomes more concentrated near the division site, and an additional signal can be detected elsewhere in the phragmoplast. In contrast, the previously identified AtPAKRP1 protein is associated specifically with bundles of microtubules in the phragmoplast at or near their plus ends. Localization of the tobacco homolog(s) of AtPAKRP2 was altered by treatment of brefeldin A in BY-2 cells. AtPAKRP1 might play a role in establishing and/or maintaining the phragmoplast microtubule array, while AtPAKRP2 may contribute to the transport of Golgi-derived vesicles in the phragmoplast.

1.3.10.5 KRP125

TKRP125, tobacco kinesin-related polypeptide of 125kDa, has been purified from isolated phragmoplasts of synchronized tobacco BY2 cells (Asada *et al.*, 1994) and found to belong to the bimC subfamily. An antibody against a short peptide from the motor domain of TKRP125 inhibits the GTP- or ATP-dependent translocation of the phragmoplast microtubules in membrane-permeabilized BY-2 cells, which suggests a function in the formation and/or maintenance of the bipolar structure of the phragmoplast (Asada *et al.*, 1997). The expression of TKRP125 is cell cycle-dependent. TKRP125 is not present in cells at the G_1

phase, but appears in the S phase and accumulates during the G_2 phase and M phase. TKRP125 is distributed along cortical microtubules during S phase, PPB and perinuclear microtubules in the premitotic cells (Asada *et al.*, 1997). TKRP125 is distributed along spindle microtubules and accumulates at the equatorial plane of the spindle as the spindle elongates. In dividing cells, TKRP125 colocalizes with phragmoplast microtubules (Asada *et al.*, 1997).

The D-box consensus sequence is R-XX-L-XXXX-N (Glotzer *et al.*, 1991; King *et al.*, 1996; Fang *et al.*, 1998) and the KEN-box consensus sequence is K-E-N-XX-N/D where X can be any residue (Pfleger and Kirschner, 2000). The destruction box and KEN-box sequences are thought to be recognized by the anaphase promoting complex (APC). The anaphase-promoting complex/cyclosome (APC/C) is a multisubunit ubiquitin-protein ligase that targets for degradation cell-cycle regulatory proteins during exit from mitosis and in the G1 phase of the cell cycle. TKRP125 sequences contain a D-box-like motif and a KEN-box-like motif and is found to be regulated by the ubiquitin-proteasome degradation pathway during M/G_1 transition (Oka *et al.*, 2004). TKRP125 carrot homologue, DcKRP120, has been identified and found to contain the conserved motor region. The localization of DcKRP120 in plant cells is similar to that of TKRP125 (Barroso *et al.*, 2000).

1.3.11 Microtubule severing protein: Katanin

Katanin, a microtubule-severing protein, couples ATP hydrolysis to disassemble

microtubules into tubulin subunits. Animal katanin is a heterodimer of 60 kDa (P60) and 80 kDa (P80) subunits and requires ATP hydrolysis for its microtubule-severing activity (McNally and Vale, 1993). P60 has been found to be a member of the AAA (ATPase associated with various cellular activities) protein family, which hydrolyses ATP in a microtubule-dependent manner and is sufficient to sever microtubules *in vitro* (McNally *et al.*, 2000). In animal cells, katanin is thought to be involved in the release of microtubules from centromsomes and the regulation of the number of microtubule ends in the mitotic spindle (Buster *et al.*, 2002).

In *Arabidopsis*, mutations in katanin P60 have been isolated as *fragile fibre2* (*fra2*) (Burk *et al.*, 2001), *botero1* (*bot1*)(Bichet *et al.*, 2001), *ectopic root hair3* (*erh3*) (Webb *et al.*, 2002), and *lue1* (Bouquin *et al.*, 2002). These loci encode a 60kDa microtubule-associated ATPase katanin ortholog is called AtKSS, which stands for *Arabidopsis thaliana* katanin–like protein small subunit (McClinton *et al.*, 2001). AtKSS has been found to sever microtubule *in vitro* in the presence of ATP (Stoppin *et al.*, 2002).

fra2 (fragile fibre2) has been identified by screening for Arabidopsis mutants with reduced mechanical strength in the inflorescence stem (Burk *et al.*, 2001). The mutant shows the phenotype of aberrant cortical microtubule orientation and distorted cellulose microfibrils that in turn leads to defects in cell elongation. In *fra2*, the disappearance of perinuclear microtubule array and the establishment

of transverse cortical microtubule array in interphase and elongating cells are delayed (Burk and Ye., 2002).

The *bot1 (botero1)* mutant has shorter and broader cells in the non-tip-growing cell types examined (Bichet *et al.*, 2001). In wild type *Arabidopsis*, cortical microtubules in cells near the division zone of the meristem were loosely organized but became more highly aligned in transverse arrays in the elongation zone. In *bot1*, the cortical microtubule arrays failed to reorient after cessation of mitosis and remained distorted throughout the elongation zone. The *bot1* phenotype also indicates that there is a link between the orientation of cortical microtubule arrays and growth anisotropy (Bichet *et al.*, 2001).

erh3 (*ectopic root hair3*) develop hair cells in non-hair positions, whereas non-hair cells form in hair locations (Webb *et al.*, 2002). From this mutant, it is believed that AtKSS is required for a microtubule-dependent cell wall biosynthetic process that is involved in the spatial organisaiton of positional information in the root. In other words, microtubules are required for the orientation of spatial determinant of cell fate in epidermal cells, in which AtKSS is required (Webb *et al.*, 2002).

lue1 was isolated in a bio-imaging screen for *Arabidopsis* mutants exhibiting inappropriate feedback regulation of the gibberellin (GA) biosynthetic gene (Bouguin *et al.*, 2003). From this mutant, it is suggested that microtubule function

and/or AtKSS activity are involved in feedback control of GA synthesis. Because GA treatment increased AtKSS mRNA levels, GA modulation of AtKSS function might affect microtubule organization. Moreover, this work also showed that AtKSS interacts with a katanin p80 ortholog and with a close FRA1-, kinesin-like homolog (Bouguin *et al.*, 2003).

1. 4 Protein kinases

1.4.1 Cyclin-dependent kinases (CDK)

Cyclin-dependent protein kinases (CDKs) belong to the serine/threonine kinase family. The binding of cyclin activates CDKs during the cell cycle. Yeasts have a single CDK responsible for cell-cycle control that possesses the sequence PSTAIRE (single amino-acid code) within its cyclin-binding domain (Jeffrey *et al.*,1995; Morgan, 1995). This CDK is conserved in all eukaryotes and is hence referred to by its fission yeast name of *cdc2*. It has been found that CDK can phosphorylate peptides containing KSP (Lys-Ser-Pro) sequences, which are characterized by two polypeptide motifs, KSPXK and KSPXX (Taranath *et al.*, 1993). However, in higher eukaryotes there are multiple additional CDKs that have roles at different points in the cell cycle. These CDKs are not conserved between animals and plants and have variant sequences in their cyclin-binding domain. In *Arabidopsis,* there are four types of CDK: CDKA, CDKB, CDKC, and CDKE (Joubes *et al.*, 2000). CDK is inactive unless bound to an appropriate cyclin. Cyclins are a diverse group of proteins with low overall homology that share a large, rather poor conserved region responsible for their interaction with

the CDK; this region is referred to as the cyclin core. According to the sequence similarity to animal cyclins, plant cyclins have been classifed as A-, B-, C-, D-, H-, and L-type cyclins (Renaudin *et al*, 1996; Yamaguchi *et al.*, 2000; Barroco *et al.*, 2003). An enzyme complex called *SCF*, named after its three main protein subunits, is responsible for the ubiquitylation and destruction of cyclins that control S-phase initiation. In M phase, the *anaphase-promoting complex* (*APC*) is responsible for the ubiquitylation and proteolysis of cyclins and other regulators of mitosis. A and B type cyclins possess a "destruction box" motif that is responsible for the degradation of these proteins by the anaphase promoting complex (APC) during metaphase. D-type cyclins are conjugated to ubiquitin by an SCF complex and then directed to the proteasome degradation pathway (Renaudin *et al*, 1996; Yamaguchi *et al.*, 2000; Barroco *et al.*, 2003). The activity of the basic CDK-cyclin module is potentially controlled not only through the expression level of cyclins and CDK, but also by activation and inhibitory phosphorylation.

1.4.2 MAPKs (mitogen-activated protein kinases)

MAP kinase is a serine/threonine protein kinase, which is activated in response to cell stimulation by various growth factors. It mediates cellular responses by phosphorylating various protein targets including transcription factors that regulate expression of important cell-cycle and differentiation specific proteins. It is also involved in the regulation of cytoskeletal rearrangements. Most of these rearrangements are achieved via MAPK-mediated phosphorylation of target

cytoskeleton-associated proteins. On the other hand, both stimulated and stressed cells use the cytoskeleton as a sensor for changes during cell division or differentiation resulting in the activation of MAPK signaling pathways (Irigoyen *et al.*, 1997; Gachet *et al*, 2001). MAPKs are conserved throughout eukaryotes, and individual organisms have multiple MAPK cascades. In general, , each cascade depends on a MAPK kinase kinase (MAPKKK), which phosphorylates and activates a MAPK kinase (MAPKK), which, in turn, activates a MAPK by phorphorylation (Chen *et al.*, 2001). In higher plants, various homologs of components that might participate in MAPK cascades have been identified (Ichimura *et al.*, 2002) and various stimuli have been shown to activate MAPKs (Jonak *et al.*, 2002). MAPK cascades also influence various aspects of cell division (Pages *et al.*, 1993; Minshull *et al.*, 1994; Wang *et al.*, 1997; Takenaka *et al.*1997, 1998; Wright *et al.*, 1999; Graves *et al.*, 2000). The studies of MAPKs of animals and plants suggest that a MAPK cascade controls cytokinesis. Several MAPKs were found activating at late M phase and localizing in the spindle midzone and the phagmoplast midline in plant cells or the midbody in animal cells (Calderini *et al.*, 1998; Shapiro *et al.*, 1998; Zecevic *et al.*, 1998; Bogre *et al.*, 1999; Nishihama and Machida 2001; Nishihama *et al.*, 2001,2002; Soyano *et al.*, 2003). Tobacco *NPK1* cDNA has been isolated and identified as a homolog of MAPKKKs (Nishihama and Machida, 2000). *NPK1* consists of two major domains: the kinase domain at the amino (N)-terminal, and the regulatory domain at the carboxyl (C) half which negatively regulates the kinase activity (Nishihama and Machida, 2000). NPK1 has been found to localize in the nuclei

at interphase and in the equatorial region of phragmoplast at anaphase (Nishihama and Machida, 2000; Ishikawa *et al.*, 2002). NPK1 is activated by the interaction with kinesin-like protein, NACK1, at late M phase. This interaction has been found necessary for cell plate formation (Ishikawa *et al.*, 2002).

1.5 Summary

This study is focused on the *Arabidopsis thaliana* microtubule associated protein MAP65-1. MAP65-1 has been found to form 25 nm crossbridges between microtubules and stabilize microtubules *in vitro* (Wicker-Peanguant *et al.*2004; Smertenko *et al.*, 2004; Mao *et al.*, 2005). However, the molecular mechanism of this protein is still unknown. In this study, a few questions have been asked. Does MAP65-1 form polymers? Where does the microtubule binding domain locate? How does MAP65 move on the microtubules *in vivo*? What is the turnover rate of MAP65-1 *in vivo*? Moreover, MAP65-1 binds to a subset of microtubule arrays but not to the prometaphase and metaphase spindles. This suggests that MAP65 is regulated in the cell cycle manner. What is the mechanism to regulate MAP65 through cell cycle? To answer these questions, biochemistry and molecular cell biology experiments have been carried out. In chapter 3, GFP-MAP65-1 has been expressed *in vivo* and the dynamic property of MAP65-1 has been revealed. In chapter 4, MAP65-1 dimerization domain and microtubule binding domain have been identified. The regulation of MAP65-1 through cell cycle is discussed in chapter5.

Chapter 2

Materials and methods

2.1 Materials

2.1.1 E. *coli* strains

XL-1 Blue MRF' strain

Genotype: *rec A1 end A1 gynA96 thi-1 hsdR19 suoE44 relA1 lac[F' proAB lac^q ZDM15 Tn 10(Tet^R)*

BL21 DE3

Genotype:*F-amp T hsdS_B (r^B-m^B-) gal dcm(DE3)*

BL21 DE3 pLysS

F- Genotype: *amp T hsdS_B (r^B-m^B-) gal dcm(DE3) pLysS (Cam^R)*

BL21 Tuner™

Genotype: *F-amp T hsdS_B (r^B-m^B-) gal dcm lacY1(DE3)*

BL21 DE3 Rosetta

Genotype: *F-amp T hsdS_B (r^B-m^B-) gal dcm (DE3) pRARE(Cam^R)*

2.1.2 *Agrobacterium* strains

LBA4404

T Genotype: iAch5, rif, pAL4404, spec & strep, (Hoekema *et al.*, 1983).

C58C3

Genotype: This is an industrial strain with the C58 background, specific genotype is unknown, resistant to Nalidixic acid and streptomycin.

2.1.3 *Arabidopsis* line

Columbia-0, obtained by LEHLE SEEDS.

2.1.4 pGreenII-N-GFP vector

pGreenII-N-GFP vector contains the pGreenII backbone, the nos-Kan (NptII under the nos promoter for kanamycin resistance), the 35S-CaMV promoter, the N-terminal EGFP, and the 35S terminator. Target genes were sub-cloned downstream of GFP into SalI and XbaI or XhoI and EcoRI sites respectively.

2.2 Methods

2.2.1 Nucleic acids methods

2.2.1.1 Plasmid miniprep

E.coli strain cells containing derived plasmid were spread onto a LB agar (Luria-Bertaki, 10 g/L NaCl, 10 g/L Tryptone, 5 g/L Yeast Extract, 20 g/L Micro agarose, pH7.0) plate supplemented with the corresponding selection marker. The culture was incubated at 37 °C, overnight. Several colonies from the plate were inoculated into separate sterile 13ml tissue culture tubes containing 4 ml LB Broth (Luria-Bertaki, 10 g/L NaCl, 10 g/L Tryptone, 5 g/L Yeast Extract, pH7.0) with corresponding antibiotics and incubated at 37 °C, shaking at 225-250 rpm overnight. GenElute^{TM} Plasmid Miniprep Kit (SIGMA, Cat. No.PLN350) was then used to extract plasmid DNA from *E.coli* according to the manufacturer's instructions.

2.2.1.2 Restriction digests

To check the identity of the vector and/or specific DNA fragments, a restriction digest reaction with specific nucleases was performed. A typical restriction digestion was made in a final volume of 20µl and the mixture contained 1µg DNA, 2 units of enzyme, 1 x enzyme buffer. The reaction mixture was incubated at 37 °C for two hours.

2.2.1.3 Exchange buffer

To remove the solution used in the digestion reaction, the following buffer exchange method was used. 600µl of PB buffer (Quiagen) was added to the digestion mixture and then loaded onto the GenElute Miniprep Binding Column (SIGMA, Cat. No. G6415). The tube was centrifuged at 14,000 xg for 2minutes. Flow-through liquid was discarded, and 750µl of Column Wash Solution

(SIGMA, Cat. No.W3886) was added to the column. Then the column was centrifuged at 14,000 xg for 2 minutes. The column was dried by centrifugation at 14,000 xg for 1 minute and transferred to a fresh collection tube. DNA was eluted with 100 µl of sterile distilled H_2O, added to the column and centrifuged at 14,000 xg for 2 minutes.

2.2.1.4 Dephosphorylation of the vector

After digestion with restriction enzymes, the vector was dephosphorylated if required by adding 4U of calf intestinal alkaline phosphatase (Promega,Cat.No. M1821) into the digestion mixture at 37°C for 30 minutes. To inactivate the phosphatase, 100µl chloroform was added to the tube containing the reaction mixture and vortexed for several seconds. The tube was centrifuged at 14,000 xg for 5 minutes. The upper layer of the solution containing DNA was collected. Then, buffer was exchanged by the method described in 2.2.1.3.

2.2.1.5 Agarose gel electrophoresis

DNA samples were separated by size using electrophoresis in submerged agarose gels. A typical agarose gel contained 1% (w/v) agarose (Sigma) in 1x TAE buffer (20mM glacial acetic acid, 40mM Tris acetate, 1mM EDTA, pH 7.2) and 0.5µg/ml ethidium bromide. Then the gel was submerged in 1xTAE buffer in the electrophoresis tank. DNA size markers and DNA samples were mixed with 6x loading buffer (0.25% (w/v) Fast orange, 15% (w/v) Ficoll) and loaded into the gel. Electrophoresis was at 50-100 V for 20 minutes. The DNA bands were then detected and photographed by using a Bio-Rad Gel Doc 1000 imaging system.

2.2.1.6 Gel-purification of DNA

DNA samples were separated using agarose gels and specific DNA fragments were excised from the gel. DNA was recovered from agarose gels using DNA Ultrafree-DA column (Milipore) following the manufacturer's instructions.

2.2.1.7 Ligation of DNA fragments

The specific DNA fragments were joined together by a ligation reaction using T4 DNA ligase. The relative concentration of vectors and inserts were predicted from the agarose gel electrophoresis images. The ratio between DNA vector and insert for optimum ligation was varied for different reactions, but typically a ratio of 1:2 (vector:insert) was used for most of the ligation mixtures. The ligation reaction also contained 2x rapid ligation buffer and 5 units of T4 DNA ligase and was incubated for 2 hours at room temperature (22-23°C).

2.2.1.8 Polymerase chain reaction (PCR)

DNA fragments were amplified by polymerase chain reaction. The reaction mixture contained DNA template (10ng-100ng), specific oligonucleotide forward primers 0.5 mM, reverse primer 0.5mM, 2.5mM $MgCl_2$, 0.2mM of dNTP (dATP, dGTP, dCTP, and dTTP),1x reaction buffer, 1 unit of BIOTAQ Red DNA polymerase (Bioline), and deionized water added to a final volume of 50μl. The reaction was performed in an HYBAID Omn-E series thermocycler. A typical PCR program consisted of 1 cycle at 94°C for 2 minutes, followed by 33 cycles of 1 minute at 94°C, 1 minute at 55-60°C, and 1kb of PCR fragment per minute at 72°C. Finally, samples were incubated in the PCR at 72°C for 10 minutes.

2.2.1.9 Mutagenesis of DNA through PCR

Point mutations in the DNA sequences were introduced using the QuikChange® XL Site-Directed Mutagenesis Kit (Stratagene,Cat. No.200517) following the manufacturer's instructions.

2.2.2 Preparation of competent cells

2.2.2.1 Preparation of XL1-Blue cells:

XL-Blue cells were cultured in Psi Broth medium supplemented with 12.5mg/ml tetracycline at 37 °C with agitation (200-220 rpm) until OD_{550} reached 0.4-0.5. The bacterial culture was chilled on ice for 15 minutes and centrifuged at 5000 xg for 5 minutes. The pellet was suspended in 40 ml TfbI (30mM Potassium acetate, 100mM Rubidium chloride, 10mM Calcium chloride, 50mM Manganese chloride, and 15% (v/v) Glycerol, pH5.8) and chilled on ice for 5 minutes, and then centrifuged at 5000 xg for 5 minutes. The pellet was suspended with 4 ml TfbII (10mM MOPS, 75mM Calcium chloride, 10mM Rubidium chloride, 15% (v/v) Glycerol, pH 6.5) and chilled on ice for 15 minutes. The cells were aliquoted and quickly frozen in liquid Nitrogen and stored at –80 °C. Frozen competent cells were thawed on ice just before use.

2.2.2.2 Preparaton of competent *E-coli* cells of the strains used for protein expression

Tuner™ and BL21 (DE3) were prepared in the same way as XL1-Blue cells, except that no antibiotic was added to the culture medium.

BL21(DE3) plyss and Rosetta™ cells were prepared in the same way as XL1-Blue cells, except that 35mg/ ml Chloramphenicol was added to the Psi Broth.

2.2.2.3 Preparation of *Agrobacterium tumefaciens* competent cells

Preparation of *Agrobacterium Tumefaciens* strain C58C3

Agrobacterium tumefaciens strain C58C3 cells were cultured in 5ml LB Broth

medium (100μg/ml streptomycin and 25μg/ml nalidixic acid), at 30 °C, overnight. A mixture containing100μl of the overnight culture was added to 50 ml of 2YT medium supplemented with 100μg/ml of streptomycin and 25μg/ml of nalidixic acid and incubated at 30 °C with continuous shaking (200 rpm) until OD_{600} reached 0.45. The culture was chilled on ice for 15 minutes. Cells were spun down at 4000g for 10 minutes at 4°C and resuspended in 50 ml of 10% (v/v) glycerol. The centrifugation step was repeated, but cells were suspended in 25ml of 10% (v/v) glycerol. Centrifugation and resuspension steps were repeated three times, each time the suspension volume was decreased by half. Finally cells were resuspended in 0.5ml of 10% (v/v) glycerol, aliquoted into eppendorfs, frozen in liquid nitrogen, and stored at –80 °C.

Preparation of *Agrobacterium tumefaciens* strain LBA4404

Agrobacterium tumefaciens strain LBA4404 competent cells were prepared in the same way as in 2.2.2.3, except that 100μg/ml streptomycin and 100μg/ml rifampicin were added to the culture medium.

2.2.3 Transformation

2.2.3.1 Transformation of *E-coli* competent cells

5μl of DNA was transferred into 50μl of freshly thawed XL1-Blue cells in an eppendorf and incubated on ice for 20 minutes. The eppendorf was incubated in a 42°C water bath for 40 seconds and then chilled on ice for 2 minutes. 0.8 ml of LB Broth was added to the eppendorf tube and cells were incubated at 37°C for 1 hour. The cells were plated on a LB agar plate containing selection antibiotics and incubated at 37°C for 18 hours.

2.2.3.2 Transformation of *Agobacteria* strains

2 µl of DNA was added to 40 µl of thawed *Agrobacterium tumefaciens* competent cells and mixed gently on ice. The cells were transferred to a chilled electroporation cuvette and electroporated at 1440 Volts, 1 pulse. 1000 µl of chilled 2YT was added to the cells in the cuvette and transferred into an eppendorf. The cells were allowed to recover at 30°C with shaking at 225-250 rpm for 3 hours, and then the cells were spun down at 5000 xg for 4 minutes. The pellet was resuspended in 100µl of LB Broth and plated on a LB agar plate supplemented with the appropriate selection markers. The plates with transfomred bacteria were incubated at 30°C for 48 hours.

2.2.3.3 Transformation of tobacco BY-2 suspension cells

4ml of a 3 day old tobacco BY-2 suspension culture was aliquoted into a 9cm sterile Petri dish. Then 100µl of *Agrobacterium Tumefaciens* LBA4404 overnight culture (OD_{550} reached 0.45) containing the desired construct was inoculated into the Petri dish. BY2 cells and agrobacterium were co-cultured for 42-48 hours at 26°C in the dark on a flat surface. Then the mixture was transferred into a 15ml tissue culture tube. BY-2 cells were washed by gentle pipetting with 5ml of BY-2 medium. The tissue culture tubes were centrifuged at 4,000 xg for 5 minutes. The supernatant was discarded and this washing was repeated 5 more times. After washing, BY2 cells were resuspended in 10 times cell volume of fresh BY2 medium and 1ml of the suspension was then spread onto a 9 mm Petri dish containing solid BY2 medium supplemented with 500µg/ml carbenicillin and 200 µg/ml of kanamycin. The plate was sealed with parafilm and incubated for 15-20 days at 26°C in the dark until the colonies appeared. The colonies were transferred into a sterile 25 compartment square Petri dish containing solid BY2 medium supplemented with 200 µg/ml of kanamycin.

2.2.3.4 Transformation of Arabidopsis plants

Arabidopsis thaliana var. Columbia plants were planted in 3.5" pots (6 plants per pot) with a plastic mesh placed over the soil. Plants were grown for 4 weeks until they were approximately 10-15 cm tall and displaying a number of immature, unopened buds. *Agrobacterium tumefaciens* strain C58C3 containing the desired construct was grown for 48 hours at 30°C in 200ml LB Broth (OD_{600} reached 0.8) (100µg/ml kanamycin, 25µg/ml nalidixic acid, 100µg/ml streptomycin). After centrifugation at 5000 xg for 4 minutes, the bacterial cell pellet was resuspended in 1 litre of a freshly made 5% (w/v) sucrose solution. The plants were dipped fully into the bacterial suspension and gently agitated for 10-15 seconds. After that the dipped plants were placed into transparent bags overnight to maintain the high humidity level. The following day, the plants were removed from the bags and placed in the greenhouse to grow. The dipping procedure was repeated 7 days after the first dipping. Seed were then collected from individual pots, sterilized and germinated on 1/2 MS10 agar with an appropriate antibiotic selection.

2.2.4 Protein analysis method

2.2.4.1 Extraction and purification of recombinant proteins

2.2.4.1.1 Expression of His-tagged proteins in *E-coli* cells

DNA fragments encoding the required protein were cloned into the expression vector-pET28-a, downstream of the sequence encoding six Histidine residues. The final plasmids were then transformed into *E-coli* BL21 strains and His-tagged proteins were expressed. The bacterial cells were grown overnight in 4ml LB broth media supplemented with the appropriate selection markers. The following day, the overnight culture was inoculated into the 2 litre culture and grown at 37°C with shaking at 200 rpm. When the culture OD_{600nm} reached 0.45,

expression was induced by adding IPTG to 1mM. The culture was further incubated at 37°C with shaking at 200 rpm for two hours.

2.2.4.1.2 Preparation of the Ni^{2+} affinity column

2ml of Ni^{2+}-NTA-Agarose chromatography resin was transferred to a column. The resin was washed with 3 column volumes of sterile H_2O and equilibrated with 3 volumes of protein extraction buffer (50 mM NaH_2PO_4, pH8.0, 300 mM NaCl, 5 mM β-mercaptoethanol).

2.2.4.1.3 Extraction of soluble proteins

Bacterial cells were pelleted by centrifugation at 5,000 xg for 10 minutes. The cell pellet was suspended in protein extraction buffer (50 mM NaH_2PO_4, pH8.0, 300 mM NaCl, 5 mM β-mercaptoethanol) supplemented with protease inhibitors (1 mM PMSF, 10 μg/ml of leupeptin and 10 μg/ml pepstatin A) and incubated on ice for 2 hours. Bacterial cell wall was disrupted by sonication with the Soniprep 150 (MSF, UK). 10 pulses were given at amplitude of 26 μm; the length of each pulse was 1 s/ml of extraction buffer). Bacterial lysate was centrifuged at 30,000 xg or 15 minutes and filtered through 0.2μm nitrocellulose membrane. Then protein extract was applied to the column containing Ni-NTA agarose resin (Quiagen, UK) and mixed with the resin for 15 minutes. The columns were washed three times with each 20 mM imidazole; 40mM imidazole; 60mM imidazole in the bacterial protein extraction buffer. The specifically bound proteins were eluted with 200 mM imidazole and proteins were dialysed against MTSB buffer (0.1M PIPES, pH6.8, 2 mM EGTA, 2 mM $MgSO_4$, 2 mM DTT, 50 mM NaCl and 10% glycerol).

2.2.4.1.4 Extraction of insoluble proteins

The procedures were the same as in 2.2.4.1.3 except that 6M urea was added into the protein extraction buffer (50 mM NaH_2PO_4, pH8.0, 300 mM NaCl, 5

mM β-mercaptoethanol), 4M urea was added into 20 mM imidazole wash buffer, 3M urea was added into 40mM imidazole wash buffer, and 2 M urea was added into 60M imidazole wash buffer, and 2 M urea was added into 200 mM imidazole elution buffer.

2.2.4.1.5 Protein refolding

Proteins were refolded by dialysis against buffer containing 15mM PIPES, pH7.0, 50mM NaCl , 2mM $MgCl_2$, 20% (v/v) glycerol, 5mM DTT, 0.05% (v/v) Tween 20 at 4°C, overnight.

2.2.4.2 Polyacrylamide gel electrophoresis

2.2.4.2.1 Preparation of 15% (w/v) polyacrylamide gel

SDS gel contains two parts: the stacking gel (30% (v/v) protogel (30% (w/v) acrylamide, 0.8%(w/v) bisacrylamide), 10% (w/v) SDS, 0.25M Tris-HCl, 10% (w/v) APS, 10μl TEMED, add H_2O to 2.5ml), the separation gel (30% (v/v) protogel (w/v), 10% (w/v) SDS, 0.75 M Tris-HCl, 10% (w/v) APS, 5μl TEMED, add H_2O to 7ml). The percentage of gel used depends on the size of the protein to be resolved.

2.2.4.2.2 One dimensional polyacrylamide gel electrophoresis (1D PAGE)

The protein samples were mixed 1:1 with two time's concentrated sample loading buffer (0.125 M Tris-HCl, 20% (v/v) glycerol, 10% (v/v) β-mercaptoethanol). Protein was denatured by heating at 95°C for 3 minutes. The SDS gel was placed in the gel electrophoresis chamber and filled with 1 X running buffer. Then the protein maker and samples were loaded in the gel lanes. The electrophoresis was run at 20 mA until the dye front reached the bottom edge. The protein was visualized by staining gel for 30 minutes at room

temperature with Coomassie Brilliant Blue solution (25% (v/v) EtOH, 7% (v/v) Acetic acid, 0.25% (w/v) coomassie brilliant blue R-250). The gel was then distained in solution containg 25% (v/v) EtOH and 7% (v/v) Acetic acid.

2.2.4.3 Western blotting

Protein was transferred from the SDS-PAGE gels onto 20μm pore size nitrocellulose membrane (BDH Electran) at 20 V electric current onvernight or alternatively at 50V for 2 hours using the liquid protein blotting system. The transfer buffer contained 38mM Glycine, 48mM Tris, 0.037% (v/v) SDS, 20% (v/v) methanol. The efficiency of the transfer was checked by staining the membrane with amido black solution (0.01 %(w/v) naphtol blue black in 0.01% (v/v) acetic acid). The membrane was destained by washing in distilled water and then air dried.

2.2.4.4 Colloidal silver staining of proteins on nitrocellulose membranes

Nitrocellulose membrane with proteins was washed intensively in distilled water for 30 minutes. Then the membrane was incubated in colloidal silver solution containing 2% (w/v) HOC(COONa)(CH2COONa)2.2H2O, 0.8% (w/v) $FeSO_4.7H_2O$, and 0.2% (w/v) $AgNO_3$ for 1-2 minutes. Membrane was washed in distilled water and air-dried. To increase the contrast, the membrane was treated with photographic fixing solution when required.

2.2.4.5 Microtubules co-sedimentation assay

Pig brain tubulin was rapidly defrosted from -80°C to 4°C using a 42 °C heating block. Then it was transferred onto ice immediately. Both tubulin and recombinant proteins were centrifuged at 150,000 xg for 15 min at 2°C to remove any aggregates. For the assays with non-stabilised microtubules, tubulin at a concentration of 20 μM was mixed with the specified concentration

of recombinant proteins, incubated at 32°C or 1°C for 15 min and centrifuged at 100,000 xg for 15 min (Backman TLX ultracentrifuge, rotor TLA120.1). The supernatant was collected and the pellet was washed and resuspended in SDS-PAGE sample buffer. For the experiments with stable microtubules, microtubules were polymerised with 10 μM taxol, mixed with recombinant proteins, incubated for 10 min at 32°C and centrifuged at 100 000 xg for 15 min at 32°C. In all the negative controls, i.e. when the microtubules were not added to the proteins, the reaction mixture was supplemented with MTSB buffer containing 10 μM taxol.

2.2.4.6 Tubulin polymerization assay

Pig brain tubulin was used at a concentration of 20 μM in all assays. The blank was set up with the cuvette containing tubulin in MTSB alone. Then GTP was added up to a final concentration of 1 mM followed by recombinant AtMAP65-1, mutants or Fragments 1-4. The turbidity was monitored at 350 nm and at 32°C on a Helios beta spectrophotometer equipped with Unicam Peltier temperature control unit (Thermospectronic, UK).

2.2.5 Fixation and microtubule staining in BY2 tissue culture cells

BY2 suspension culture cells were separated form the tissue culture medium using 100 μm mesh nylon cloth and fixed for 30 min at room temperature with 4% (v/v) paraformaldehyde in 0.1 M PIPES, pH 6.8, 5 mM EGTA, 2 mM $MgCl_2$, and 0.4% (v/v) Triton X-100. The fixative was washed away with PBS buffer and cells were treated for 5 min at room temperature with a solution of 0.8% (w/v) Macerozyme R-10 and 0.2% (w/v) Pectolyase Y-23 in 0.4 M mannitol, 5 mM EGTA, 15 mM MES, pH 5.0, 1 mM PMSF, 10 μg/ml leupeptin and 10 μg/ml Pepstatin A. Then the cells were washed in PBS buffer and attached to poly-L-lysine coated coverslips. The coverslips were then incubated for 30 min in 1%

(w/v) bovine serum albumin in PBS and incubated for 1 hour with primary antibody. The primary antibodies used were: rabbit anti-AtMAP65 diluted 1:500 and mouse anti-tubulin DM1A diluted 1:200 (Sigma). The specimens were then washed 3x10 min in PBS and incubated for 1 hour with secondary antibodies: goat anti-mouse TRITC conjugates and anti-rabbit FITC conjugates; both antibodies were diluted 1:200. After washing in the PBS buffer, the specimens were mounted in Vectashied (Vector Laboratories) mounting medium and examined with a Zeiss 510 confocal microscope.

2.2.6 Laser scanning confocal microscopy (LSCM)

Time lapse images were obtained by confocal laser scanning microscopy (Zeiss 510).

2.2.7 Measurement of the dynamics of NtMAP65-1a using FRAP

For taking the static NtMAP65-1a: GFP images, 7 day old *Arabidopsis* seedlings were collected from the agar plates and mounted in distilled water. For FRAP or time lapse studies, seedlings were partially immobilised by mounting in 1% (w/v) low gelling temperature agarose and observed immediately. BY-2 tissue culture cells were mixed with an equal volume of 1% (w/v) low gelling point agarose (Sigma, Dorset, UK) solution in BY-2 medium. The samples were observed using a Zeiss 510 inverted confocal microscope with the Argon/Crypton laser equipped with a 488 nm excitation filter and a 514 nm emission filter. The laser power was 6% maximum for the samples expressing both GFP: NtMAP65-1a and GFP: AtMAP65-1. The recovery of the fluorescence signal was measured during 20 minutes of the sample's lifetime.

For the statistical analysis of the FRAP data, the background value was measured outside the photobleached region and subtracted from the experimental FRAP values. The data collected from numerous cells (the

number is indicated for each of the experiments) were averaged and normalised by division by the mean value. The level of recovery was expressed as percentage of the fluorescence before photobleaching.

To calculate the time of 50% signal recovery, $t_{1/2}$, the FRAP curve from each of the experiments was fitted to an exponential recovery curve: $F(t) = F_\infty - (F_\infty - F_0)\, e^{-t\ kOFF}$ (Bulinski *et al.*, 2001), where F_0 is the fluorescence after the photobleaching, F_∞ is the fluorescence when the recovery reached the plateau stage, t is time and k_{OFF} is the first-order rate constant that describes the rate of recovery. The curve fit and calculation of k_{OFF} was done with Abscissa software version 3.2.1 (http://iapf.physik.tu-berlin.de/DZ/bruehl/). The $t_{1/2}$ was calculated as $\ln(2)/k_{OFF}$.

2.2.8 Maintenance of cell cultures and calli

Cells of *Nicotiana tabacum* L. cv. Bright yellow 2 (BY2) were maintained in liquid medium (30 g/l of sucrose, 4.3g/l Murashige and Skoog salts, 100mg/ml inositol, 1mg/l thiamine, 0.2mg/ml 2,4-dichlorophenoxyacetic acid, 225mg/l KH_2PO_4, pH5) on a shaker at 25°C. Cells were subcultured weekly (1:80) in to new medium. Calli were maintained on solid medium (contain in 0.7% (w/v) agarose) at 25°C and subcultured monthly. Transgenic lines had 200μg/ml kanamycin added to the medium or agar.

2.2.9 *Arabidopsis* seed sterilization

Arabidopsis seeds were immersed in 10% (v/v) sodium hypochlorite solution for 10 minutes and washed with distilled water three times.

2.2.10 Microtubule protein preparation

Miniprotoplast were prepared as described previously (Sonobe 1990; Jiang *et al.*, 1992) with slight modifications. To prepare protoplast, BY-2 cells of about 320g were incubated in an enzyme solution (1.5% (w/v) Sumizyme C, 0.15% (w/v) Sumizyme AP2 (Shin-Nihonkagaku Industries Ltd., Anjo, Japan), 0.45 M mannitol, pH 5.5) at 30 °C for 90 min. To prepare miniprotoplast, protoplasts were suspended in 400 ml of Percoll solutoin (30% Percoll (Pharmacia LKB Biotechnology AB, Uppsala, Sweden) supplemented with 20 mM $MgCl_2$ and 0.7 M mannitol, pH7.0) and centrifuged at 12,000 xg for 45 min. Miniprotoplasts were collected from the lower most layer and washed twice with a cold 0.6 M mannitol solution. 20g of miniprotoplasts were suspended in 60 ml of an ice-cold extraction buffer (50 mM PIPES, pH7.0, 20 mM EGTA, 2 mM $MgCl_2$, 25 μg/ml leupeptin, 1 mM PMSF, 2 mM DTT) and homogenized by an ultra sonic disrupter (ULTRASONIC DISRUPTER UD-201, Tomy Co. Ltd., Japan) on output 4, duty 50. The homogenate was centrifuged twice at 408,000 xg for 15 min at 2 °C. Resultant supernatant was used as a cytoplasmic extract. To polymerize tubulin, 20 μM taxol was added to the cytoplasmic extract and microtubule proteins were collected by centrifuged at 100, 000 xg for 10 min. Microtubule protein were resuspended in a depolymerizing buffer (25 mM PIPES, 1 mM $CaCl_2$, 0.4 M KCl, 2 mM GTP, 2 mM DTT, 1 mM PMSF, pH7.0) and incubated on ice for 60 min. The suspension was centrifuged at 163,000 xg for 15 min. The supernatant containing tubulin and MAPs was dialyzed against tubulin dialysis buffer (25 mM PIPES, 5 mM EGTA, 2 mM $MgCl_2$, 50 MM NaCl, 2mM DTT, 1mM PMSF, 0.1M GTP, pH7.0).

2.2.11 Phosphorylation assay

The reaction was started by adding the assay buffer (20 mM Hepes, PH7.5, 15mM $MgCl_2$, 5 mM EGTA, 1 mM DTT, 0.5 mg/ml histoneH1 (SIGMA type III),

and 2 μCi of [γ^{-32}P]ATP). The reaction was incubated at room temperature for 30 min and was terminated by the addition of 5μl of 4x SDS sample buffer. The samples were analyzed by SDS-PAGE and subsequent autoradiography.

Chapter 3

Dynamic interaction of MAP65-1 with microtubules *in vivo*

3.1 Introduction

The MAP65-1 group of proteins belongs to the MAP65-1 protein family (Figure 1.3) and forms a separate clade in the phylogenetic tree. Tobacco NtMAP65-1a decorates microtubules in the interphase cortical array, the preprophase band (PPB), the anaphase spindle and the phragmoplast. Interestingly, immunostaining data shows that there is specific localization of NtMAP65-1a to the anaphase spindle midzone and the phragmoplast midline (Smertenko *et al.*, 2000). Localization data suggests that NtMAP65-1 crosslinks anti-parallel microtubules (Smertenko *et al.*, 2000). However, the dynamics of MAP65 binding to microtubules and its redistribution during the cell cycle progression remains unknown. In this chapter, both GFP: NtMAP65-1a and GFP: AtMAP65-1 were constructed and expressed alternatively in tobacco BY-2 cells and *Arabidopsis thaliana* plants to test their functional conservation. The localization of GFP: NtMAP65-1a and GFP: AtMAP65-1 was recorded using a confocal microscope. Time-lapse images of GFP signal were taken throughout the cell cycle in tobacco BY2 cells. Decoration of microtubules was observed in *Arabidopsis* plants.

Plant microtubules undergo dynamic reorganization through the cell cycle and in response to internal and external stimuli (Nick, 1998, Hussey, 2004). The dynamics of plant microtubules both *in vitro* (Moore *et al.*, 1997) and *in vivo* (Hush *et al.*, 1994; Shaw *et al.*, 2003) have been shown to be higher than the dynamics of animal microtubules. The major microtubule protein is a heterodimer of αβ tubulin and the structure of the tubulins shows a high degree

of conservation across phylogeny (Burns and Surridge, 1994). The difference in the dynamic properties of plant and animal microtubules *in vitro* has been suggested to arise as a result of small differences in tertiary structure of the dimer arising from the small number of residue differences between animal and plant tubulins (Moore *et al.*, 1997). In animals, numerous structural microtubule associated proteins (e.g. tau, MAP1, MAP4) that are not present in plants modulate dynamics (Kreis and Vale, 1993), but so far no plant structural MAP has been shown to affect microtubule dynamics (Lloyd *et al.*, 2004).

In this chapter, the interaction of the GFP fused MAP65s with microtubules has been studied *in vivo* using the fluorescence recovery after photobleaching (FRAP) method. The turnover of the NtMAP65-1a and the AtMAP65-1 microtubule interaction is faster than microtubule treadmilling and faster than other known structural MAPs from animals. Analysis of the FRAP data suggests that MAP65-1 proteins translocate randomly along microtubules. All together, these data suggest that the properties of NtMAP65-1a (AtMAP65-1) make it ideal for temporally crossbridging microtubules in dynamic microtubule arrays so that their spatial organisation is maintained.

3.2 Localization of MAP65-1 in tobacco BY2 cells and *Arabidopsis* plants

3.2.1 Preparation of GFP fusions with NtMAP65-1a and AtMAP65-1

Full length red-shifted soluble modified GFP was subcloned into the Not I and Xho I sites of the pGreen II vector. A linker (Pro Ala Gln Ala Gln Ala Gln Ala Gln Ala Gln Ala Ser) was constructed between the GFP and the insertion sequences. Then full length NtMAP65-1a (Smertenko *et al.*, 2000) or AtMAP65-1 (Smertenko *et al.*, 2004) was sub-cloned downstream of GFP into the Sal I

and the XbaI or the XhoI and the EcoRI sites respectively (Fig.3.1). The sequences of GFP and NtMAP65-1a or AtMAP65-1 chimeras and their linker region in the pGreenII vector were confirmed by sequencing. Gene expression was under the control of the constitutive cauliflower mosaic virus (CaMV) 35s promoter.

The constructs were co-transformed with pSOUP vector into *Agrobacterium tumefaciens* strain C58C3 for the transformation of *Arabidopsis thaliana* plants and into LBA4404 for the transformation of tobacco BY-2 cells. *Arabidopsis* plants were transformed using the floral dipping method (Clough and Bent, 1998) and BY-2 cells were transformed by the co-incubation method (Geelen and Inze´, 2001). The seeds were geminated on 1/2 MS basic salt medium supplemented with 7.5% agar and 50 mg/l of kanamycin at 23 °C and 14 hours day/10 hours night light cycle. BY-2 cell transformants were selected on medium containing 200 mg/l of kanamycin and 500mg/l carbenicillin. The kanamycin-resistant colonies expressing GFP-NtMAP65-1a were subcultured and maintained in liquid medium containing 200 mg/l of kanamycin.

3.2.2 Localization of GFP: NtMAP65-1a and GFP: AtMAP65-1 in BY2 cells

Comparison of the wild type BY2 lines with cell lines expressing GFP: NtMAP65-1a or GFP: AtMAP65-1 showed no differences in cell growth and morphology. Therefore, overexpression of the GFP: NtMAP65-1a or GFP: AtMAP65-1 fusion proteins had no prominent effect on cell growth or proliferation. Five kanamycin-resistant lines were checked under the confocal microscope. All lines showed GFP signals associated with the microtubule cortical array, the preprophase band, the anaphase spindle, and the phragmoplast, but not with the metaphase spindle. Intriguingly, NtMAP65-1a was found to be concentrated at the anaphase spindle midzone and the

Figure 3.1 Schematic diagram of the GFP-NtMAP65-1a and GFP-AtMAP65-1 constructs.

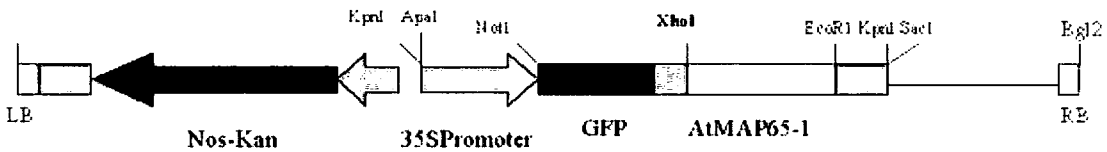

(A) Schematic diagram of GFP-AtMAP65-1 construct.

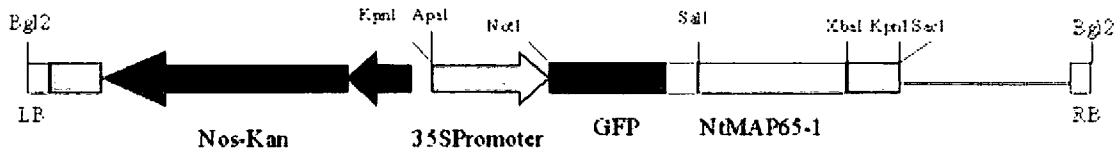

(B) Schematic diagram of GFP-NtMAP65-1a construct.

phragmoplast midline, an area where anti-parallel microtubules overlap, suggesting that MAP65 crosslinks these anti-parallel microtubules and maintains phragmoplast organization (Fig 3.2). Time-lapse images showed the relocation of GFP: NtMAP65-1a through different stages of the cell cycle (Fig3.3). Here a cell was imaged from the end of the G2 phase to the end of cytokinesis. The preprophase band forms around the nucleus during the G2 phase and highlights the beginning of mitosis. The preprophase band decoration by GFP: NtMAP65-1a first narrows and later gradually disappears, while most of the GFP signal remains mainly cytoplasmic. After nuclear envelope breakdown, the GFP signal is localized around condensing chromosomes, but still shows no binding to the microtubules of the prometaphase/metaphase spindle. However, during anaphase, a very bright GFP signal is detected in the midzone of the anaphase spindle and this persisted during phragmoplast formation. The signal weakens and then completely disappears during phragmoplast development and cell plate synthesis. Figure 3.2 D (82-132 seconds) shows an apparent concentration of GFP:NtMAP65-1a in the midzone at the early stages of phragmoplast formation; later the GFP signal is broadly distributed along phragmoplast microtubules (Figure 3.2D, 224 seconds) and eventually disappears from the cell plate region when microtubules disassemble (Figure 3-2D, 398 seconds). The cell plate has formed by this time and the phragmoplast has started to disassemble. The entire GFP signal is now located around the divided daughter nuclei and is detectable on the perinuclear microtubule array and on the reappearing transverse cortical microtubules. The localization of GFP: NtMAP65-1 during cell division is very similar to MAP4: GFP or tubulin: YFP, except that GFP: NtMAP65-1 does not decorate the prophase spindle and the metaphase spindle and accumulates in the midzone of the anaphase spindle and phragmoplast.

Five BY2 cell lines transformed with GFP: AtMAP65-1 were selected on kanamycin plates. The localization of GFP (see supplementary information

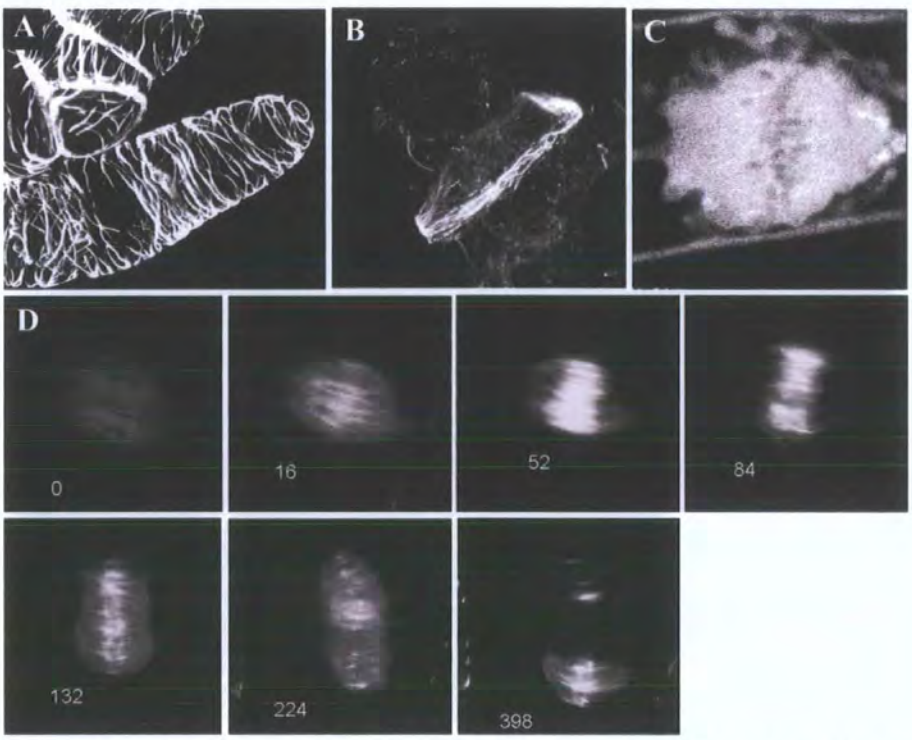

Fig 3.2 GFP-NtMAP65-1a decorates MT arrays throughout the cell cycle. GFP-NtMAP65-1 fusion protein was expressed in tobacco BY-2 cells under the the control of the 35S promotor.
(A)Cortical microtubule array in interphase cells
(B)Preprophase band
(C)Metaphase mitotic spindle; decoration is absent
(D)Phragmoplast (Numbers indicate the time in seconds)

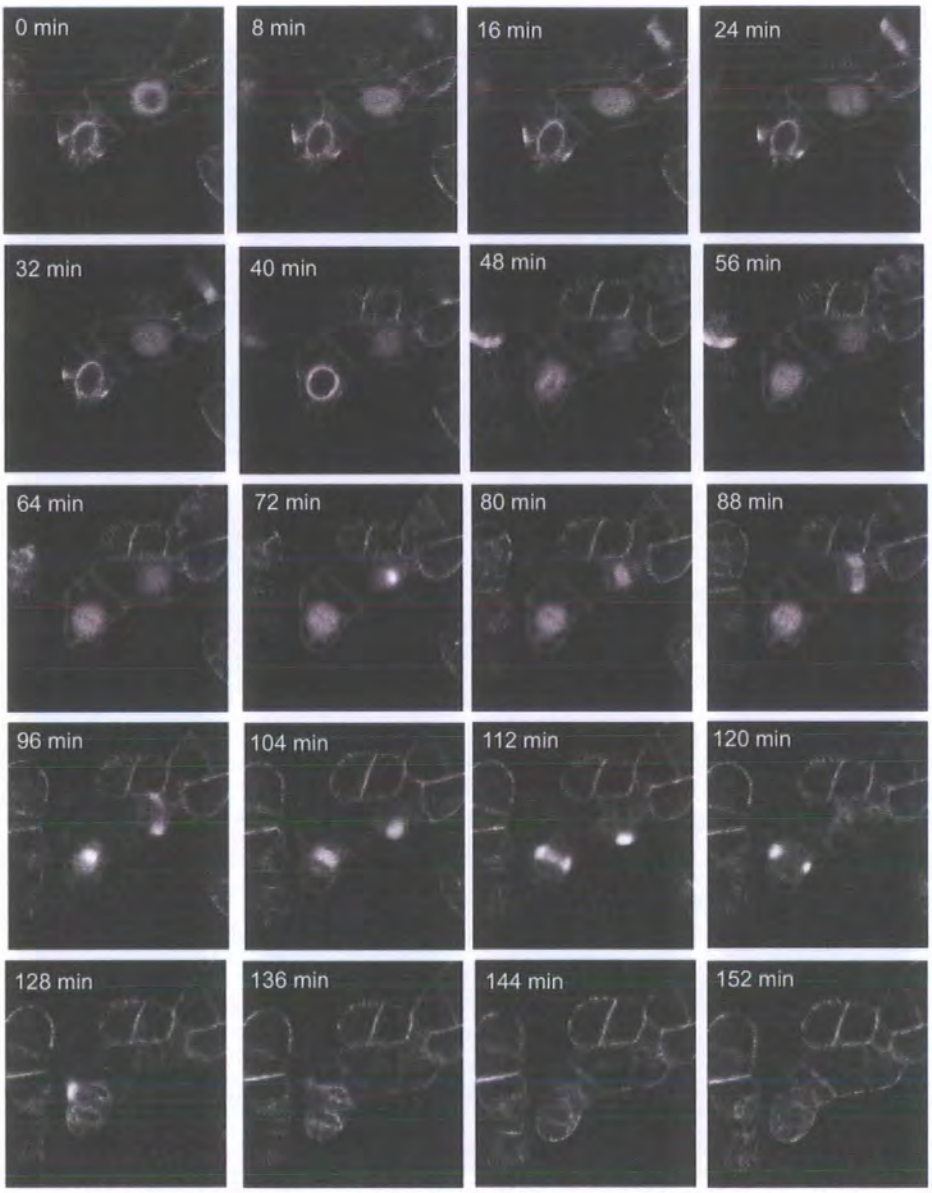

Figure 3.3 Time -lapse images of GFP-NtMAP65-1a throughout cytokinesis in BY-2 cells. The BY2 cell expressed GFP-NtMAP65-1a (arrow) was recorded from the G2 phase to the end of M phase. The image at 0 min showed the decoration of preprophase band. The PPB was narrowing down to a concentrated band and the signal broke down, MAP65-1a does not bind to MTs. At 96 min, a very strong GFP signal was observed in the middle of the dividing plane, in which the anaphase spindle mid zone was marked. At 104 min, phragmoplast was formed and expanded centrifugually toward the cell wall. At 128 min, phragmoplast disassambled and cytokinesis terminated. MAP65 was found around the newly formed nuclei.

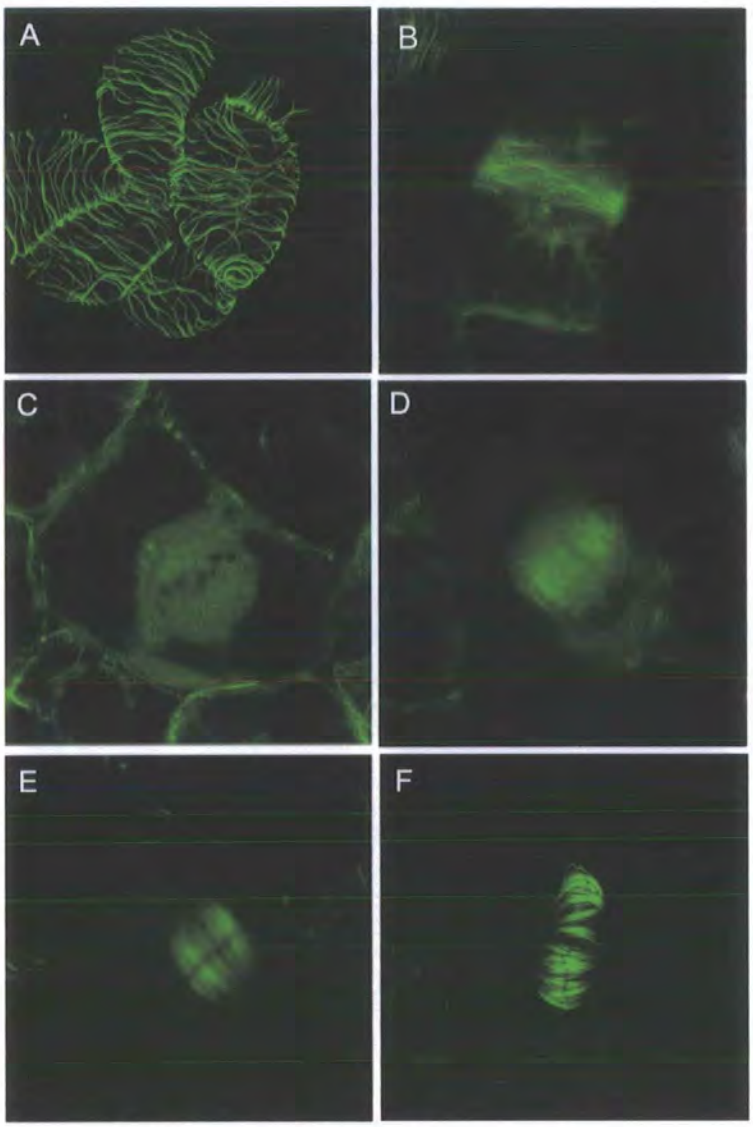

Figure 3.4 GFP: AtMAP65-1decorates MT throughout the cell cycle in BY2 cells.
The GFP: AtMAP65-1 construct was cloned into pGreen II vector and then trasnformed intoTobacco BY-2 cells via Agrobacterium. The fusion protein were expressed under the control of the CaMV 35s promotor in BY2 cells. (A)Interphase cortical mictubule array (B) Preprophase band (C)Metaphase,GFP: AtMAP65-1 did not decorate metaphase spindle (D)Anaphase spindle, (E)GFP: AtMAP65-1 shows a strong singal in the centre of the anaphase spindle (F) Phragmoplast, the cell plate was formed in the middle of the phragmoplast.

movie 1) in these lines during different stages of the cell cycle was the same as GFP: NtMAP65-1a, except that NtMAP65-1a decorated a broader region in the phragmoplast midzone. The similarity of their localization in BY2 cells also suggests that AtMAP65-1 and NtMAP65-1 are functionally conserved.

3.2.3 Localization of GFP: NtMAP65-1a and GFP: AtMAP65-1 in *Arabidopsis* seedlings

Four kanamycin-resistant plant lines for each GFP: NtMAP65-1a and GFP: AtMAP65-1 construct were analyzed. The fusion proteins decorated microtubules in leaves, hypocotyl cells, lateral roots, root hairs, and root tips in seven day old seedlings (Fig 3.6, Fig 3.7). The GFP: NtMAP65-1a and GFP: AtMAP65-1 showed a similar decoration of microtubules in the *Arabidopsis* plants. This shows the conservation in their functions again. Interestingly, the microtubule arrays, which include the cortical microtubule arrays, the PPB, the phragmoplast, can all be observed clearly in the root tips. The development of Arabidopsis plants was not affected by the expression of GFP-NtMAP65-1a fusion proteins. The second generation also germinated normally and no obvious phenotype was observed (Figure 3.5). Therefore, these plants can be used for investigation of MAP65-1 activity in different plant organs and tissues.

Although the 35S promoter was used to drive the expression of GFP: NtMAP65-1a, most of the root cells show no or very weak decoration of cortical microtubules in the root elongation zone. For example, in the root extension zone, GFP: NtMAP65-1a did not decorate cortical microtubules, but instead formed aggregate in the cells (Figure 3.7E). This suggests that the interaction between microtubules and GFP: NtMAP65-1a is very weak or that GFP: NtMAP65-1 is degraded in these cells. A similar result has been reported for Azuki bean, when MAP65 protein expression and interaction with microtubules was found to be higher in the cell with higher growth activity and lower in the

Fig 3.5 Comparision of wild type with GFP: AtMAP65-1 and and GFP: NtMAP65-1a Arabidopsis line. 20 days Arabidopsis plants grown on 1/2 MS agar medium (contains 1% sucrose). No difference was found between wild type, GFP: AtMAP65-1, and GFP: NtMAP65-1a lines.

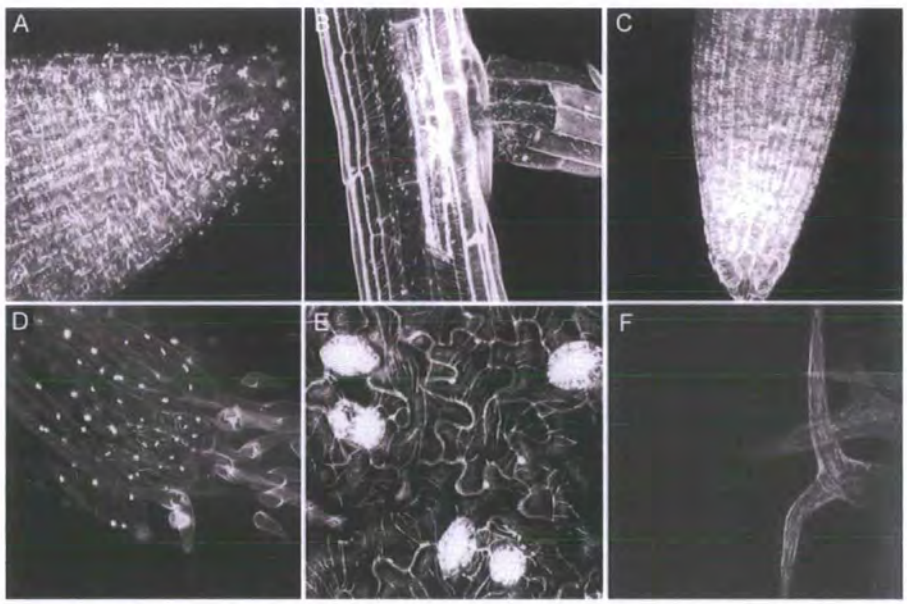

Fig 3.6 Localization of GFP:NtMAP65-1a in Arabidopsis seedlings. GFP:NtMAP65-1a fusion proteins were expressed and decorated MTs in 12 day Arabidopsis seedlings. (A) Root tip (B) Lateral root (C) Lateral root tip (D) Hypocotyle cells (E) Leaf epidermic cells (F) Trichomes

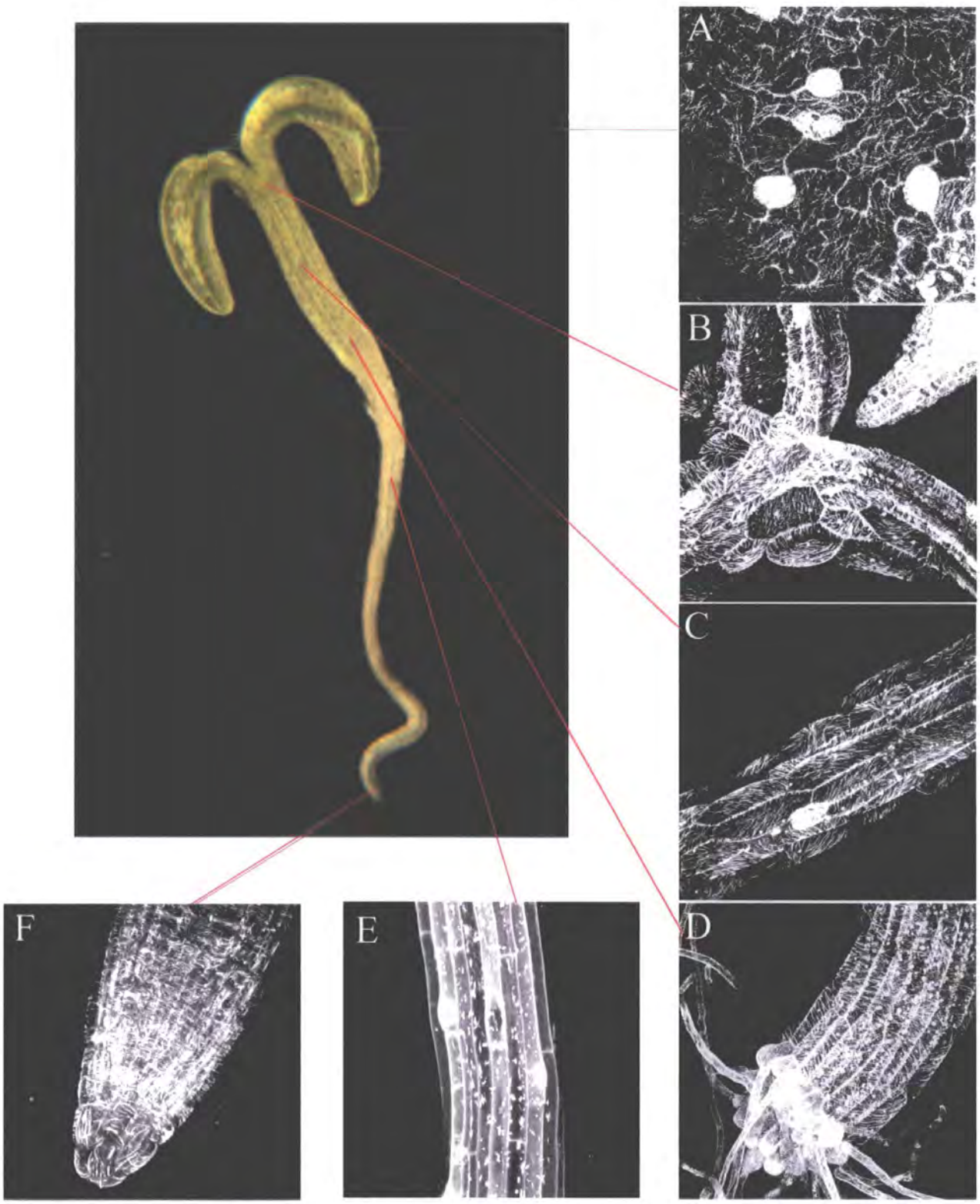

Figure 3.7 Localisation of GFP-AtMAP65-1 in Arabidopsis seedlings.
(A) Leaf epidermal cells(B) Hypocotyl (C) Hypocotyl
(D) Hypocotyl/root (E) Root (F) Primary root tip

cells with lower growth activity (Masahide *et al.*, 2000). In young proliferating cells (leaf epidermal cells, apical cells, primary root tip, and lateral roots), the decoration of microtubules by GFP: MAP65 protein was strong, while in other tissues e.g. root extension zone, the MAP65 binding to microtubules was weak or absent. These results suggest that regulation of MAP65 binding to microtubules is tissue specific or that the promoter does not express to the same level in each cell type.

3.3 Interaction of NtMAP65-1a and AtMAP65-1 with microtubules *in vivo*

3.3.1 Interaction between NtMAP65-1a and microtubules is dynamic

The *Arabidopsis* lines expressing GFP: NtMAP65-1a were used to study the dynamics of the MAP-65 interaction with microtubules *in vivo* by fluorescence recovery after photobleaching (FRAP). The FRAP method usually involves marking the protein of interest with a specific fluorescent group. This can be done either with a fluorescent ligand such as FITC or TRITC coupled to the protein *in vitro* and then microinjected into the cell or by expression of a protein linked to GFP. The fluorescent group is then bleached in a small area by a laser beam, and the time taken for proteins carrying an unbleached ligand or GFP to diffuse into the bleached area is measured. Here, GFP: NtMAP65-1 expressing tissues were tested. Root, cotyledon and hypocotyl cells were assessed for their suitability for these experiments. Hypocotyl epidermal cells were chosen as these have a very low level of autofluorescence and because of their large flattened shape many microtubules could be observed in a single focal plane. Moreover, they are easily immobilized in low gelling temperature agarose. For the FRAP experiments, a narrow patch of the cell containing several GFP-

fluorescing microtubules (Figure 3.8) was bleached with a laser pulse and the time required for the recovery of 50% of the signal ($t_{1/2}$) was estimated. This $t_{1/2}$ value represents the time taken for half of the GFP: NtMAP65-1 to be replaced and therefore a numerical estimation of the protein turnover. The selected area (outlined as a white rectangle in Figure 3.8A) was bleached for approximately 4.8 seconds. Subsequently, images were collected every 3.6 seconds (Figure 3.8 B) and the intensity of the GFP signal in the selected area was measured and plotted against time (Figure 3.8 C). The $t_{1/2}$ for the GFP: NtMAP65-1a was found to be 8.96 seconds (Number of cells analyzed for this value n=24). Considering the fact that tubulin:GFP in similar experiments has a $t_{1/2}$ of 58.95 seconds (Table 3.1), these data demonstrate that the GFP:NtMAP65-1a signal recovers faster then GFP: tubulin, hence the exchange of GFP:NtMAP65-1a on the microtubule surface must be independent of microtubule treadmilling. As a further comparison the $t_{1/2}$ of another GFP chimera that interacts with microtubules *in vivo*, MAP4: GFP, was determined and found to be 2.91±0.21 seconds (n=20).

3.3.2 MAP-65 molecules interchange at any site along the length of the microtubule.

So far our data suggest that the rate of GFP: NtMAP65-1a turnover in its association with microtubules is not dependent on microtubule treadmilling (as this rate is much faster than microtubule treadmilling). Therefore the signal may recover as the result of either active transport of MAP-65 along microtubules or the exchange of the MAP-65 molecules randomly along the length of the microtubules. To address these possibilities we examined the pattern of GFP: NtMAP65-1a recovery. A total of 18 microtubules were photobleached in different cells and their recovery monitored (shown for a representative microtubule in Figure 3.9). The microtubule recovers completely in 30 seconds after photobleaching (Figure 3.9A and B) indicating that this is sufficient time for

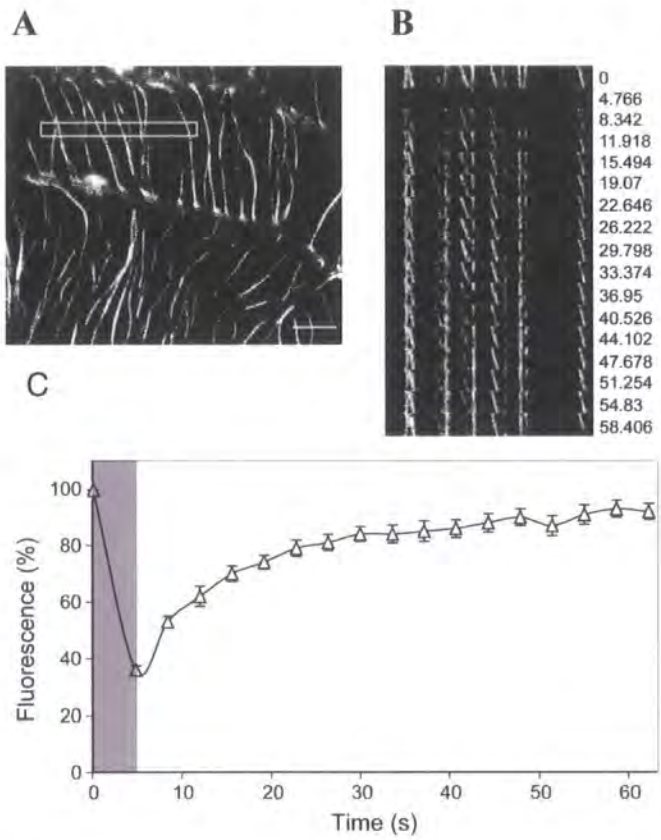

Figure 3-8. Recovery of GFP: NtMAP65-1a signal after photobleaching. A, The GFP:NtMAP65-1a signal in the hypocotyl of Arabidopsis 7 day old seedlings. The white rectangles outline the photobleached area. B.Time series (top to the bottom) of GFP:NtMAP65-1a signal recovery during a FRAP experiment within the area indicated by the rectangle in A. The numbers on the right hand side indicate the time in seconds when each of the frames was collected with 0 corresponding to the image before the photobleaching onset and 4.766 just after the photobleaching. C, Fluorescence recovery after photobleaching. The first measurement was taken just before the photobleaching and corresponds to point 0. The grey sector represents the duration of photobleaching, then 14 images were collected and measured at approximately 4.14 seconds intervals. The fluorescence signal was measured in 24 cells and expressed as the percentage of the signal before photobleaching. The error bars indicate standard deviation of the mean.

Table 3.1. Analysis of the FRAP data. The dissociation constants k_{off} and $t_{1/2}$ were estimated for GFP fusions in various cell types and at various cell cycle stages. 'N' column shows the number of cells analysed in each experiment and the 'Bound' column shows the fraction of NtMAP65-1a:GFP initially bound to the microtubules, expressed as percentages of total fusion protein.

	Cell type	k_{off}[1]	$t_{1/2}$ (s)	N	k_{off}[2]	Bound (%)
NtMAP65-1a						
Interphase	Hypocotyl	0.077	8.96±0.85	24		
Interphase	BY-2	0.100	6.95±0.91	23	0.094	80.7
PPB	BY-2	0.117	5.92±0.64	19	0.083	85.8
Metaphase	BY-2	0.960	0.72±0.21	23	nd[5]	nd[5]
Phragmoplast	BY-2	0.146	4.83±0.64	20	0.117	75.0
Oryzalin	BY-2	0.402	1.71±0.24	23		
AtMAP65-1						
Interphase	BY-2	0.117	5.93±0.86	20		
MBD-GFP						
Interphase	Hypocotyl	0.238	2.91±0.21	20		
Tubulin						
Interphase[3]	Hypocotyl		58.95			
Interphase[4]	Stamen hair		67±3.3			
Metaphase[4]	Stamen hair		31.4±6.1			
Phragmoplast[4]	Stamen hair		60.0±8.1			

[1]k_{off} estimated by single exponential fit; [2]k_{off} estimated by double exponential fit; [3]Shaw et al. 2003; [4]Hush et al., 1994; [5]Not determined due to values being below the threshold for diffusion seen in the oryzalin treated control cells.

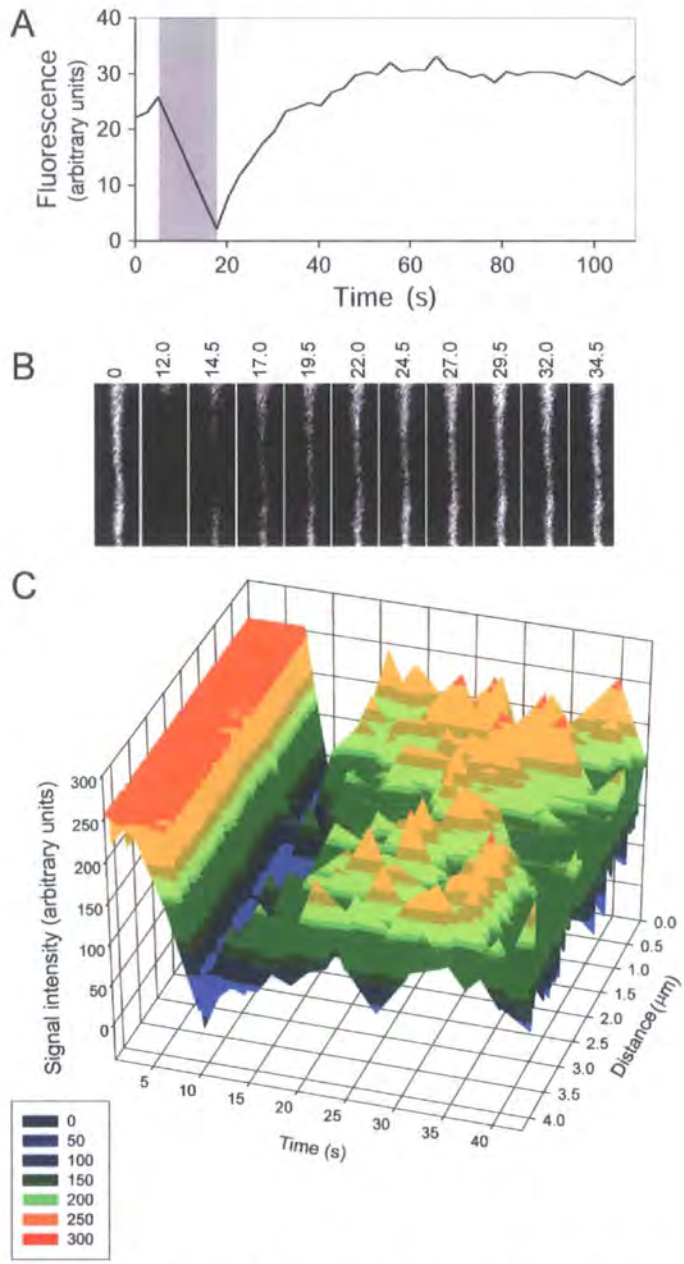

Figure 3.9 Random recovery of GFP:NtMAP65-1a signal over the microtubule length. The fluorescence redistribution after photobleaching 27 sections was measured and an example is shown in this figure A, The first measurement was taken just before the photobleaching and corresponds to point 0 (the image of the microtubule at this time point is represented in the part B point 0). The grey sector represents the duration of photobleaching then 35 images were collected and measured at approximately 2.5 second intervals. The fluorescence signal on the chart is expressed in arbitrary values.
B, Time series (left to right) of GFP:NtMAP65-1a signal recovery after photobleaching the microtubules shown in A. The numbers at the top of each image indicate time in seconds when each of the frames was collected with 0 corresponding to the image before the photobleaching onset and 12.0 just after the photobleaching. The images shown follow the microtubule to complete recovery and this occurred after 34.5 seconds.
C, The chart showing changes in time (x axes) of the distribution of the fluorescence signal (z axes) along the length of the microtubule (y axes) shown in A and B. The signal intensity is expressed in arbitrary values.

the exchange of most, if not all, of the attached GFP: NtMAP65-1a molecules. Moreover, the intensity of the GFP: NtMAP65-1a signal along the length of the microtubule at each time point was measured (Figure 3.9C). The results show that the signal recovers randomly suggesting that GFP: NtMAP65-1a is exchanged along the microtubule length rather than actively moved along the microtubule, possibly by sliding or by another motor driven transport.

3.3.3 Interaction of MAP65 with microtubules during mitosis.

In this chapter, the interaction of NtMAP65-1a with the microtubules has been analysed during the cell cycle in BY-2 cells using FRAP on the tobacco cell lines expressing GFP: NtMAP65-1a (Table 3.1). The $t_{1/2}$ was found to be similar for interphase microtubules (6.95±0.91 s, n=23) and for microtubules in the preprophase band (5.92±0.64 s, n=19). In the phragmoplast midzone the $t_{1/2}$ was slightly faster (4.83±0.64 s, n=23) than for the cortical arrays. In the metaphase spindle the $t_{1/2}$ was over two fold lower than in all other arrays (2.04±0.18 s, n=20). The recovery time has been compared in the metaphase spindle with the recovery time in cells where microtubules were depolymerised with the anti-microtubular drug oryzalin. No filamentous structures were visible in the majority of the cells following a 2 hours treatment with 10μM oryzalin (data not shown). Disruption of microtubules should cause MAP65 to become cytoplasmic so only free diffusion of GFP: NtMAP65-1a can occur. Indeed, the $t_{1/2}$ value in this case was found to be 2.01±0.14 seconds (n=23). This $t_{1/2}$ value is very similar to that in the metaphase spindle indicating that in this array the majority of the NtMAP65-1a are not bound to microtubules and do not form complexes that can slow its mobility.

3.4 Conclusions

The over expression of GFP-NtMAP65-1a or GFP-AtMAP65-1 in BY-2 cells/ *Arabidopsis thaliana* plants did not cause any phenotype and showed similar

localization. These results indicate the protein function is conserved between NtMAP65-1a and AtMAP65-1. From the confocal images of GFP-MAP65 in BY-2 cells, MAP65-1 was showed to decorate the cortical microtubule array, the PPB, the anaphase spindle, and the phragmoplast. The GFP signal was very strong in the anaphase spindle midzone and the phragmoplast midline where cell plate occurs. These results suggest that MAP65-1 might crosslink the microtubules in these structures. Interestingly, prophase spindle and metaphase spindle decoration was absent. MAP65-1 seemed cytoplasmic in the prophase and metaphase spindle area, and then appeared again in the midzone of the anaphase spindle and the phragmoplast. This observation suggests that MAP65 / microtubule interaction is regulated in a cell-cycle dependent manner. Moreover, the GFP-NtMAP65-1a and GFP-AtMAP65-1 BY2 cell lines didn't show any phenotype, which makes them a tool to analyze the dynamics of MAP65-1 *in vivo*.

The GFP: NtMAP65-1a and GFP: AtMAP65-1 *Arabidopsis* lines grew normally and produced normal seedlings. 7 day old seedlings were observed under the confocal microscope. The fusion protein was expressed everywhere in the plant, decorating microtubules in the root, root hairs, stem, leaves, and trichomes. However, in the root extension zone, instead of decorating cortical microtubule array, it showed aggregation in the cells.

From the FRAP result, the turnover of the NtMAP65-1a and the AtMAP65-1 microtubule interaction has been found to be faster than microtubule treadmilling and faster than other known structural MAPs from animals. The FRAP data suggests that MAP65-1 proteins translocate randomly along microtubules. The $t_{1/2}$ has been measured by FRAP and found to be similar for interphase microtubules and for microtubules in the preprophase band. In the phragmoplast midzone $t_{1/2}$ is slightly shorter than for the cortical arrays. In the metaphase spindle $t_{1/2}$ is over twice as short as in all other arrays.

Chapter 4

Molecular analysis of AtMAP65-1 microtubule bundling activity

4.1 Introduction

AtMAP65-1 (At5g55230) encodes a protein that shows 86% similarity to tobacco NtMAP65-1 (Smertenko *et al.*, 2000). The predicted open reading frame encodes a 587 amino acid protein of 65.8kDa molecular weight and a pI of 4.72. Full length AtMAP65-1 recombinant protein was purified and tested in the microtubule co-sedimentation assay and polymerization assay. To identify the microtubule binding domains in AtMAP65-1, AtMAP65-1 cDNA was divided into four fragments (Fragment 1, amino acids 1-150; Fragment 2, amino acids 151-339; Fragment 3, amino acids 340-494; Fragment 4, 495-587). Recombinant proteins were then purified and their effect on microtubules was analysed in the microtubule co-sedimentation and polymerization assay. To investigate the interaction of MAP65 with microtubules *in vivo*, GFP fusions were prepared with Fragment 5 (amino acid residues 1-339), Fragment 6 (residues 340-587), Fragment 7 (residues 1-496), Fragment 8 (residues 151-587) and Fragment 9 (residues 151-494). The localization of the proteins was analyzed in transformed tissue culture cells.

The *Arabidopsis PLEIADE* gene is synonymous with *AtMAP65-3,* a member of

the MAP65 gene family (Figure 1.2) (Müller *et al.*, 2004). The *pleiade* mutants were originally identified in a screen for root morphology defects (Müller *et al.*, 2002). The phenotype of these mutants is orchestrated by enlarged multinucleated cells with incomplete cross walls indicating that the defect is in cytokinesis (Müller *et al.*, 2002). Sequencing the genomic DNA of allele *ple-4* revealed a single point mutation, which causes the substitution of conserved alanine 421 for valine (Müller *et al.*, 2004). This residue is conserved in all nine AtMAP65 sequences. In this chapter, this conserved alanine at position 420 in AtMAP65-1 was substituted for valine. The A420V mutant protein showed a reduced capability in binding microtubules and did not induce bundling of microtubules *in vitro*. It suggests that A420/ A421 is essential for AtMAP65 to interact with microtubules.

4.2 AtMAP65-1 bundles microtubules, but does not promote microtubule polymerisation

The effect of AtMAP65-1 on microtubule polymerisation was assessed using a turbidimetric assay. AtMAP65-1 was added to a MAP-free porcine brain tubulin solution (final concentration 20 μM) at an AtMAP65-1 to tubulin dimer molar ratio of 1:2. The turbidity of the mixture was monitored at 350 nm. AtMAP65-1 induced a dramatic increase in the turbidity of the polymerising microtubule mixture compared to the control (Figure 4.1A). These data indicate two possibilities: AtMAP65-1 could increase the total amount of microtubule polymer or it could induce bundling of assembled microtubules. These processes are not

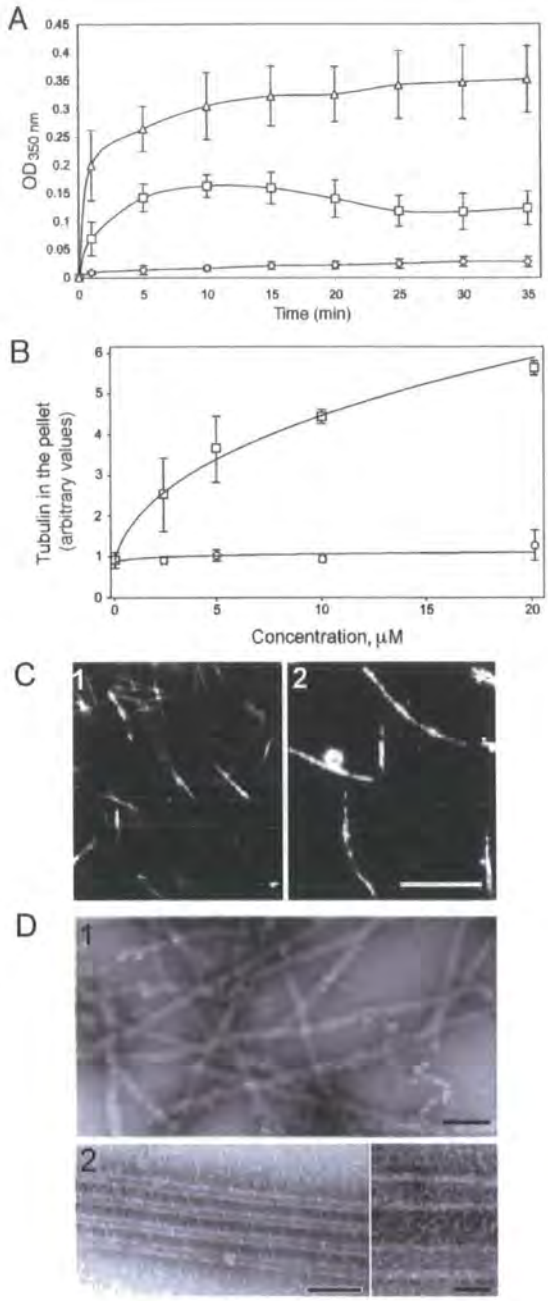

Figure 4.1 AtMAP65-1 bundles microtubules.
(A) Turbidity of the 20 μM tubulin solution (diamonds) and 20 μM tubulin solution after the addition of 10 μM AtMAP65-1 (squares) or 10 μM taxol (triangles) monitored at 350 nm and at 32 °C.(B) Amount of tubulin sedimented at 100 000xg in the presence of increasing concentration (0-20 μM) of AtMAP65-1(circles) or taxol (squares). Three independent experiments were performed and the error bars show the standard deviation. The x axis indicates concentration of taxol or AtMAP65-1.(C) Dark field microscopy images of microtubules polymerised in a 20 μM tubulin solution in the absence (panel 1) or presence (panel 2) of 10 μM AtMAP65-1 . Bar=10 μm.
(D)Transmission electron microscopy images of samples from the same experiments in (C) . Panel 1 microtubules without AtMAP65-1; Panel 2 microtubules with AtMAP65-1; the inset shows a higher magnification image of the microtubule bundle formed in the presence of AtMAP65-1. Scale bar corresponds to 100 nm (inset bar+= 20nm).

necessarily mutually exclusive as bundling can also stabilise microtubules, resulting in an increase of the total amount of microtubule polymer by preventing dynamic instability. To distinguish between these two possibilities, microtubules were polymerized in the presence of increasing concentrations of AtMAP65-1 and the amount of tubulin that cosediments with the AtMAP65-1 was analyzed. If AtMAP65-1 increases the total amount of microtubule polymer, the amount of tubulin in the pellet should increase proportionally to the point of saturation. However, the amount of tubulin in the pellet did not change significantly across the AtMAP65-1 range of 0 to 20 μM (Figure 4.1B). Taxol, a microtubule stabilising agent and capable promoter of microtubule polymerisation, also increases the turbidity of the tubulin solution (Figure 4.1A), but in contrast to AtMAP65-1, taxol increased the total amount of tubulin in the pellet in a concentration dependent fashion (Figure 4.1B). This result strongly suggests that AtMAP65-1 bundles but does not promote the polymerisation of microtubules. This conclusion was further confirmed by an analysis using dark field microscopy (Figure 4.1C). Addition of AtMAP65-1 to dynamic tobacco microtubules (shown in panel 1; average length 4.2±1.1 μm, n=89) caused the formation of long, thick microtubule bundles (panel 2; average length 11.5±4.4 μm, n=62). Examination of these bundles under the electron microscope showed that they are composed of parallel microtubules separated by 25 nm cross-bridges (Figure 4.1D). These data suggest that AtMAP65-1 does not promote microtubule polymerisation *in vitro*, but bundles polymerised microtubules *via* the formation of 25 nm cross-bridges.

One effect of microtubule bundling can be a reduction in the depolymerisation of microtubules, for example, by inhibiting catastrophe. To determine whether AtMAP65-1 affects depolymerisation, microtubules were first polymerised at 32°C for 10 minutes, and then AtMAP65-1 protein was added at a tubulin: AtMAP65-1 molar ratio of 2:1. The mixture was diluted with microtubule-polymerising buffer pre-warmed to 32°C, incubated for 10 min and the microtubules were pelleted at 100,000 xg and analysed on SDS-PAGE gels. Taxol at a concentration of 10 μM was used as a positive control to demonstrate the effect of a microtubule stabilising agent on the amount of tubulin polymer upon isothermal dilution. The results of three independent experiments are presented in Figure 4.2 A. No significant difference in the quantity of tubulin in the supernatant with or without AtMAP65-1 was observed: the total amount of tubulin polymer decreased five fold with the decrease in final tubulin concentration from 20 to 1μM. In contrast the amount of tubulin polymer in the presence of taxol decreased by only 10%.

In order to assess whether AtMAP65-1 changes the stability of microtubules, the effect of AtMAP65-1 on the cold-induced depolymerisation of microtubules was analyzed. Here, the turbidity of a tubulin solution (20 μM) was monitored at 350 nm after addition of GTP. Microtubules were polymerised at 32°C for 20 min, then AtMAP65-1 was added to a tubulin: AtMAP65-1 molar ratio of 2:1 and the reaction was allowed to proceed for another 30 min (Figure 4.2B). The

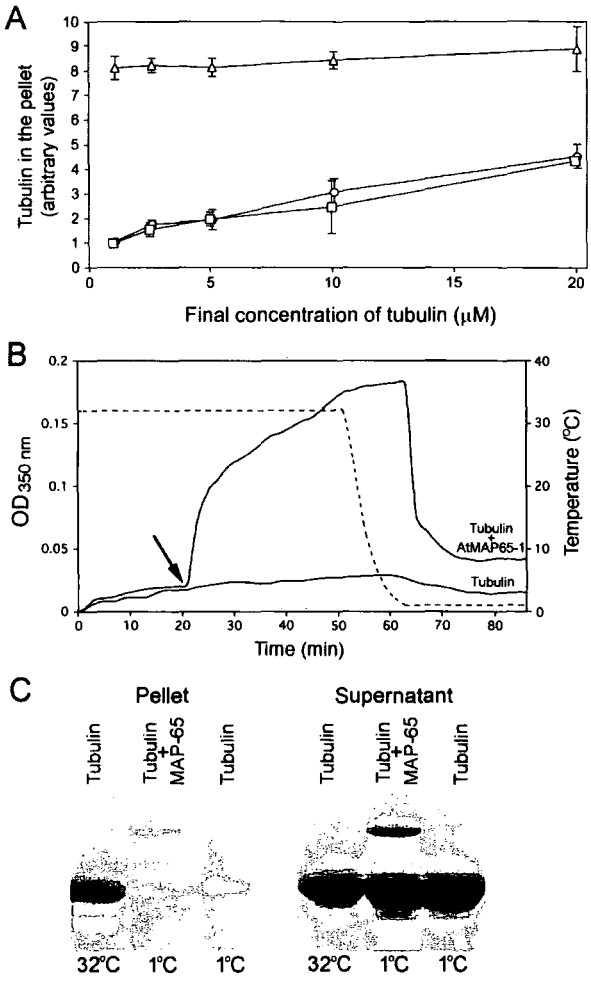

Figure 4.2 AtMAP65-1 does not affect microtubule dynamics. AtMAP65-1 does not stabilize the microtubule depolymerisation caused by dilution and cold treatment. (A) Amount of tubulin sedimented at 100,000 xg after dilution of the 20 μM tubulin mixture. Squares, tubulin only solution, circles,tubulin with 10 μM AtMAP65-1; triangles,tubulin with 10 μM taxol. (B) Turbidity of the 20 μM tubulin solution without, and with, the addition of 10 μM AtMAP65-1 (solid lines) at 32°C, and after decreasing the temperature. Temperature is indicated by the broken line. The arrow indicates the time at which AtMAP65-1 was added. (C) Coommassie stained SDS-PAGE gel of microtubule pellets and supernatants of a 20 μM tubulin solution incubated at 32°C for 10 min, a 20 μM tubulin solution with 10 μM AtMAP65-1 incubated at 32°C for 10 min and then at 1°C for 10 min and a 20 μM tubulin solution incubated at 32°C for 10 min and then at 1°C for 10 min. The final temperature of the reaction mixtures are indicated below the lanes.

addition of AtMAP65-1 induced an increase in the turbidity of the tubulin solution compared to the control. Subsequently, the temperature of the reaction was decreased to 1°C, with temperature readings collected every two minutes and plotted (shown as the broken line in Figure 4.2B). The drop in the absorbance indicates cold-induced microtubule depolymerisation and this only occurred when the temperature reached 1°C. However in the microtubule only and the microtubule: AtMAP65-1 samples, the minimal absorbance reading after microtubule depolymerisation was always above the starting point. This would indicate that a small proportion of the microtubules were intrinsically resistant to cold induced depolymerisation. To demonstrate this, the samples were centrifuged at 100000xg and the amount of tubulin in the pellet analyzed. The amount of tubulin in the pellet in both samples was similar (but less than in samples incubated at 32°C) which indicates that the majority of microtubules depolymerised regardless of being bundled by AtMAP65-1 (Figure 4.2C).

4.3 AtMAP65-1 forms dimers

Previously it was suggested that the 25-30 nm crossbridges between microtubules created using a carrot MAP65 enriched protein preparation were unlikely to be generated by monomeric MAP65 molecules (Chan *et al.*, 1999). Therefore, whether the recombinant AtMAP65-1 could form oligomers was assessed. Using two different methods here it is shown that AtMAP65-1 can form dimers. Firstly, chemical crosslinking of AtMAP65-1 with EDC produces a band of approximately 130kDa molecular weight on one dimensional

SDS-PAGE (Figure 4.3A). Secondly, in native acrylamide gel electrophoresis recombinant AtMAP65-1 runs at a position corresponding to 120-140kDa (Figure 4.3B). In both experiments the size of the complex indicates an AtMAP65-1 dimer. Moreover, the recombinant AtMAP65-1 was immobilized on an Ni-NTA resin column which was then loaded with a total cell extract of a tobacco BY-2 cell line expressing the HA-epitope tagged tobacco equivalent to AtMAP65-1, NtMAP65-1. Immunoblotting of the eluates from control (resin only) and AtMAP65-1 affinity columns with anti-HA antibodies demonstrated that the HA-epitope-tagged NtMAP65-1 interacted with AtMAP65-1 on the column (Figure 4.3C).

The affinity column AtMAP65-1 method was used to determine which fragment in the AtMAP65-1 was capable for dimer formation. Affinity columns were prepared with fragments 1, 2 3, and 4 (see above). The columns were again loaded with the BY2 cell extracts expressing the HA-tagged NtMAP65-1, eluted with 0.5 M NaCl and the washes immunoblotted with anti-HA. The results show that fragment 2 (i.e. amino acids 151-339) had the highest affinity for NtMAP65-1 (Figure 4.3 D). These data show that fragment 2 in the N-terminal half of the protein, which does not bind microtubules, is involved in dimerization of MAP65 (Smertenko *et al.* 2004).

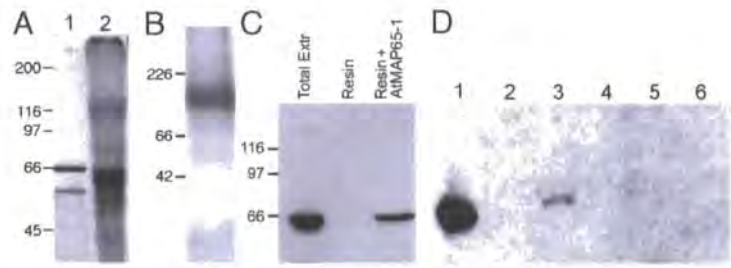

Figure 4.3 AtMAP65-1 can form dimers.

(A) AtMAP65-1 control (lane 1) and EDC crosslinked AtMAP65-1(lane 2) separated on a SDS-PAGE gel and stained with Coomassie.

(B) AtMAP65-1 run on a non-denaturing acrylamide gel and stained as in (A)

(C) Immunoblot probed with anti-HA epitope. Lane 1, a BY-2 cell total protein extract expressing NtMAP65-1:HA epitope tag. Lane 2, 0.5M NaCl eluate from control Ni-NTA column. Lane 3, 0.5M eluate from AtMAP65-1 affinity column.

(D) Immunoblot probed with anti-HA epitope. Lane 1, a BY-2 cell total protein extract expressing NtMAP65-1:HA epitope tag. Lane 2-5, 0.5M NaCl eluates from AtMAP65-1 Fragments 1-4 affinity columns. Lane 6, 0.5M NaCl eluate from control Ni-NTA column.

The numbers on the left of each gel are molecular weights of markers in kDa.

4. 4 Microtubule binding region of AtMAP65-1

AtMAP65-1 fragments were cloned, expressed and purified in bacteria, and then used to assess their microtubule binding capabilities using the cosedimentation assay (Figure 4.4 B, C). Fragments 3 and 4, but not Fragments 1 and 2, co-sedimented with taxol stabilized microtubules. In controls, none of the fragments were detected in the pellet in the absence of microtubules. These data indicate that the C-terminal half of AtMAP65-1 harbours the microtubule-binding region. These four fragments were assessed for microtubule-bundling activity using a turbidimetric assay. Figure 4.4D shows that none of the fragments were able to increase the turbidity of polymerising microtubules significantly compared to full-length AtMAP65-1 (Figure 4.4D) and dark-field microscopy confirms that no bundling occurs (Figure 4.4E). These results show that the microtubule-binding region alone is not sufficient to cause microtubule bundling and form the 25 nm crossbridges.

Taking into account that both fragments 3 and 4 of AtMAP65-1 could bind microtubules *in vitro*, it was hypothesised that the C-terminus (FR3+FR4) contained the microtubule -binding region and that it can bind to microtubules *in vivo*. A fragment of AtMAP65-1 consisted of Fragment 3+4 (Fragment 6) was linked to GFP and expressed as a fusion protein to test this hypothesis. The N-terminal region consisting of Fragment 1+2 (Fragment 5) (Figure 4.5) was used as the negative control in this experiment.

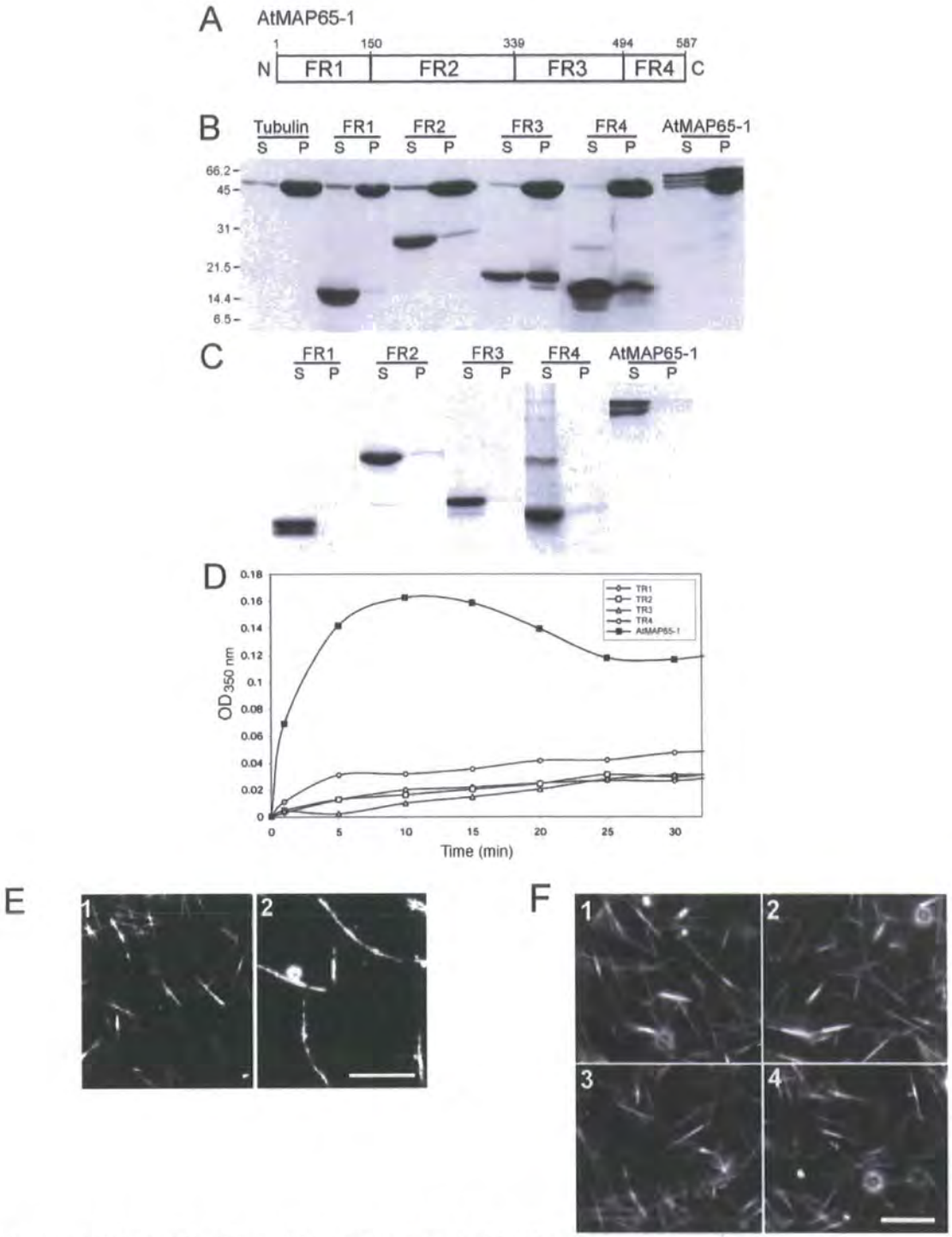

Figure 4.4 Identification of the microtubule binding domain of AtMAP65-1.
(A) Diagram showing the positions of the four AtMAP65-1 fragments (FR1, FR2, FR3 and FR4). The numbers indicate the positions of the first and the last amino acids of each fragment in the AtMAP65-1 full-length sequence. N and C indicate the amino and carboxy termini respectively. (B) Cosedimentation of AtMAP65-1 and fragments 1-4 with taxol-stabilised microtubules. Microtubules on their own or as a mixture with AtMAP65-1 or AtMAP65-1 fragments 1-4 were centrifuged at 100,000 xg, then the supernatants (S) and pellets (P) separated on an SDS-PAGE gel and stained with Coomassie. (C) Sedimentation of the same AtMAP65-1 and AtMAP65-1 fragments 1-4 (as in B) in the absence of microtubules. AtMAP65-1 and fragments 1-4 were analysed as in B. (D) Effect of AtMAP65-1 and fragments 1-4 (each 20 mM) on the turbidity of a 20 mM tubulin solution. The assay was performed at 32 °C and the turbidity was monitored at 350 nm. (E) Dark field microscopy images of microtubules polymerised in a 20 μM tubulin solution in the absence (panel 1) or presence (panel 2) of 10 μM AtMAP65-1 . Bar=10 μm. (F) Dark field microsopy images of a 20 mM tubulin solution polymerised in the presence of 10 mM AtMAP65-1 fragments 1-4 (panels 1-4 respectively). Scale bar corresponds to 1 mm.

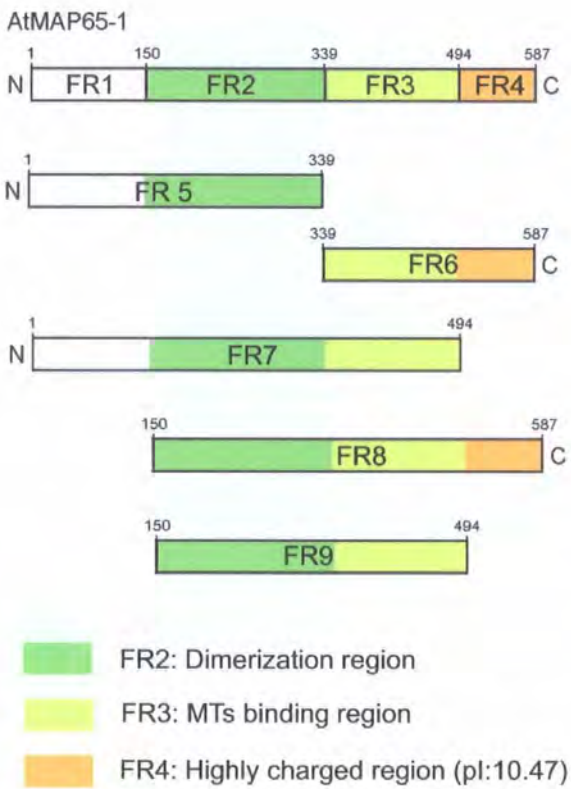

Fig 4.5 Scheme representing functional domain and fragments of AtMAP65-1. fragments (FR5, FR6, FR7, FR8 and FR9).The numbers indicate the positions of the first and the last amino acids of each fragment in the AtMAP65-1 full-length sequence. N and C indicate the amino and carboxy termini respectively.

Both fragments 5 and 6 showed a cytosolic localization and an aggregation around the nucleus during all cell cycle stages. Immunostaining with anti-tubulin and anti-GFP revealed that these aggregates around the nucleus did not co-localize with microtubule (Figure 4.6). These results suggest that the microtubule -binding domain of AtMAP65-1 alone is not sufficient for binding to microtubules *in vivo* (Figure 4.6). In contrast, fragments 7 and 8 which contained sequences in the N-terminus or C-terminus could interact with microtubules *in vivo*, but the binding was much weaker compared to the full length AtMAP65-1 (Figure 4.7). Fragment 9: GFP protein, which includes the dimerization region and one microtubule-interaction site, lacked any microtubule binding ability *in vivo.* Fragment 6 did not bind to microtubules *in vivo* perhaps because it did not have a dimerization domain, required for microtubule bundling. Fragments 7 and 8 contain both a dimerization domain and a microtubule-binding domain, hence they could bind to microtubules *in vivo*, though weaker than the full length AtMAP65-1. Interestingly, a microtubule-binding site and dimerization domain are not sufficient for the microtubule binding, as Fragment 9 showed no microtubule co-localization. Either only the C-terminus or the N-terminus was necessary for the interaction to be detectable. These data suggest that binding of MAP65 to microtubule depends on the protein's tertiary structure.

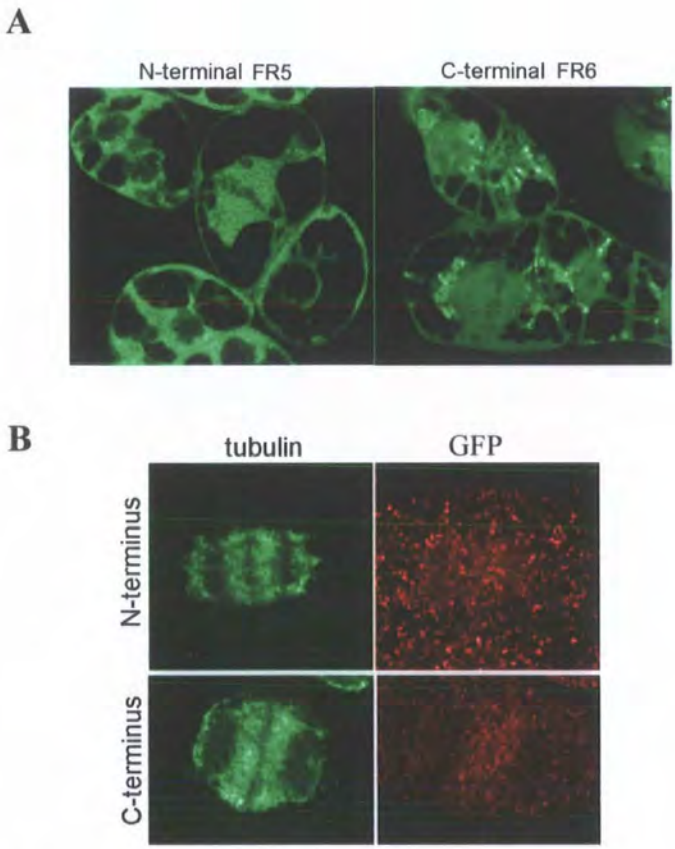

Fig 4.6 Localization of FR5 and FR6 in BY2 cells
(A) GFP-FR5 and GFP-FR6 fusion proteins expressed in BY2 cells. GFP signals was co-localized in the cytoplasm and no binding to MTs was observed. (B) Cells expreesing GFP-FR5 and GFP-FR6 anaphase cells were stainedwith anti-tubulin (green) and anti-GFP (red) anibody. No co-localization of tubulin and GFP was found.

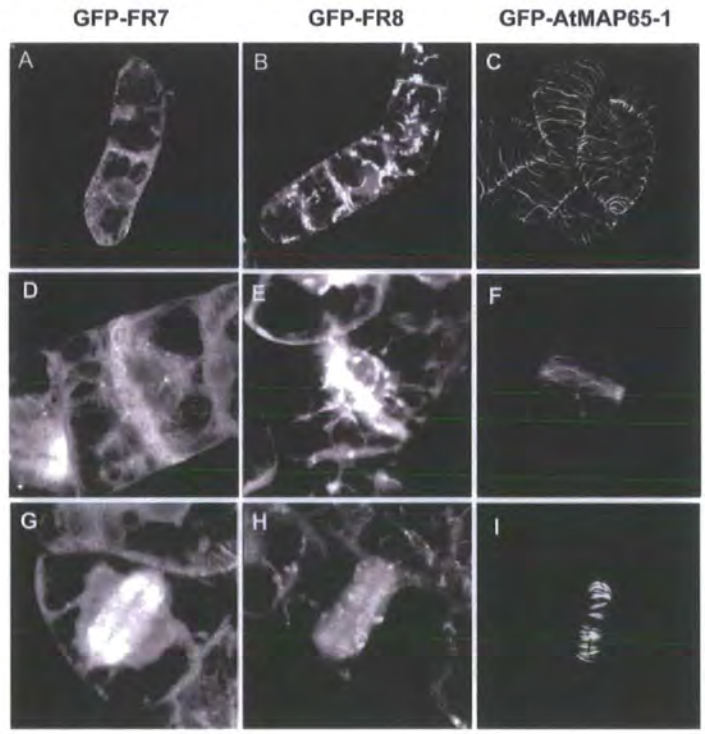

Figure 4.7 Comparision of GFP: FR7, GFP: FR8, and GFP: AtMAP65-1 localization in tobacco BY2 cells. GFP: FR7 and GFP: FR8 decorated MTs during interphase (A,B,C) and prophase (D,E,F), however did not concentrated at the division midzone (G,H, I).

4.5 Ala 420/421 is essential for AtMAP65 interaction with microtubules.

A recessive *Arabidopsis* mutant was isolated that is allelic to the published *pleiade* alleles *ple-1, ple-5* and *ple-6* (Sorensen *et al.*, 2002; Söllner *et al.*, 2002; Müller *et al.*, 2002). This mutant was named *ple-4* (Figure 4.8 A, B). Sequencing the genomic DNA at the *pleiade* loci revealed a single point mutation, which causes the substitution of alanine 421 for valine (Figure 4.8C). This residue is conserved in all nine AtMAP65 sequences and lies in Fragment 3 of AtMAP65-1 (Figure 4.8D). To mimick the *ple4* mutation in the AtMAP65-1 protein, the corresponding conserved alanine 420 was substituted for the hydrophobic valine by PCR using the QuikChange® XL Site-Directed Mutagenesis Kit (Stratagene,Cat. No.200517). The Ala 420 to Valine mutation was confirmed by DNA sequencing. The mutant was then cloned into NdeI/XhoI digested pET28a vectors (Novagen) and expressed in *E-coli*. The mutated protein was included in the microtubule co-sedimentation assay. The results show that A420V mutant protein has a reduced capability in binding microtubules (Figure 4.7E) and did not induce bundling of microtubules *in vitro*. This hydrophobic substitution must have caused some conformational change in the protein. There is another conserved alanine residue at position 409 but this is substituted by a hydrophobic valine in AtMAP65-8. This residue was selected for substitution to a charged amino acid, an aspartic acid. Again, the mutated protein did not bind and bundle microtubules. Competition binding studies using short synthetic peptides have been used to identify interaction sites between numerous

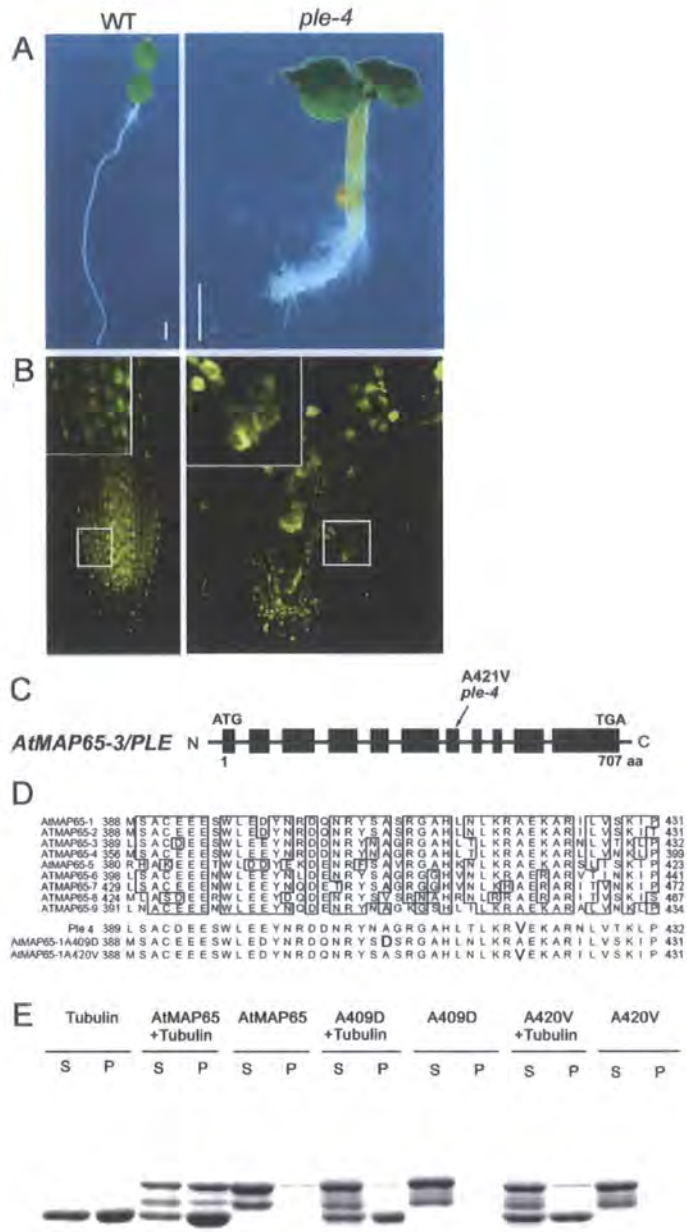

Figure 4.8 Ala409 and Ala420 are essential for AtMAP65-1 binding to microtubules.
(A) Arabidopsis wild type (WT) and pleiade-4 (ple-4) mutant allele.
(B) Nuclei in the roots of WT and ple-4 seven day old seedlings visualised with the DNA-specific dye, YO-PROTM; (C) The intron (thin line) and exon (thick line) map of AtMAP65-3/PLE with the position of the A421V mutation in the ple4 allele indicated. (D) Alignment of the most conserved region of all AtMAP65 proteins. The corresponding sequences encoded by the ple4 allele and AtMAP65-1/A409D and AtMAP65-1/A420V mutant proteins are also shown. (E) Microtubule co-sedimentation assay using AtMAP65-1 and AtMAP65-1/A409D and A420V mutants.
Supernatants (S) and pellets (P) were separated on an SDS-PAGE gel and stained with Coomassie.

proteins.

4.6 Conclusion

In this chapter, it is has been shown that a recombinant *Arabidopsis* MAP65, AtMAP65-1, can bind and bundle microtubules. However, it does not promote microtubule polymerisation or stabilise microtubules against cold-induced depolymerisation. AtMAP65-1 bundles the microtubules into a regular lattice structure and forms crossbridges of 25 nm. Fragmentation of AtMAP65-1 and analysis of mutants reveals that the microtubule-binding region is in the C-terminal half and that alanine residues at positions 409 and 420 play key roles. Moreover, the AtMAP65-1 dimerization region has been found in the N-terminal half. When the GFP-AtMAP65-1 fragments are expressed in BY2 cells, the binding domain alone is not sufficient to bind microtubules *in vivo*.

Chapter 5

Regulation of MAP65-1 protein through the cell cycle

5.1 Introduction

MAP65-1 expresses throughout the cell cycle, but the protein only binds subsets of the microtubule arrays in a cell cycle-dependent manner, indicating that regulated activation and inactivation, instead of periodic proteolysis, is the dominant mode of MAP65-1 regulation. However, the MAP65-1 gene contains a destruction box (D-box) motif in the C-terminus. The D-box consensus sequence is R-XX-L-XXXX-N where X can be any residue (Hussey *et al.*, 2002). It has been found that mutation of the two D-box conserved residues, arginine and leucine, results in the production of proteins resistant to degradation (Juang *et al.*, 1997). To knock out the D-box of MAP65-1, arginine-529 and leucine-532 were substituted by mutation to alanine. A BY2 cell line over-expressing NtMAP65-1a with a knocked out D-box was established and analyzed in this chapter. In addition, NtMAP65-1a R529A/L532A was cloned downstream of green fluorescent protein (GFP) in the pGreenII plant transformation vector and expressed in tobacco BY-2 cells. The localization of GFP: NtMAP65-1a R529A/L532A was observed throughout the cell cycle.

Phophorylation/dephosphorylation is an important mechanism which regulates

protein activities in cells. In animal cells, for example, the phosphorylation of microtubule associated proteins, MAP2, MAP4, and Tau affects their binding to microtubules (Alexa *et al.*, 2002; Shiina *et al.*, 1998). The MAP65 homologue PRC1 in mammalian cells has two Cdk phosphorylation motifs; mutation of these two sites causes extensive bundling of the metaphase spindle microtubules (Mollinari *et al.*, 2002). In this chapter, the level of MAP65 phosphorylation was analyzed during the cell cycle and was found to be dependent on the cell cycle stage. Several protein kinases, including CDKs and MAPKs, were found to be involved in the phosphorylation of MAP65-1 *in vitro* and *in vivo* (Smertenko *et al.*, 2006).

To identify phosphorylation motifs in AtMAP65-1, the protein was divided into four fragments (Fragment 1, amino acids 1-150; Fragment 2, amino acids 151-339; Fragment 3, amino acids 340-494; Fragment 4, 495-587). Only Fragment 4 could be phosphorylated *in vitro*. Bioinformatics predictions revealed nine potential phosphorylation motifs in Fragment 4 of AtMAP65-1. The mutation of Ser or Thr within the phosphorylation motifs to aspartic acid diminished the phosphorylation level of AtMAP65-1 to the interphase level *in vitro* and decreased its microtubule binding ability *in vivo*. It suggests that the microtubule bundling ability of MAP65-1 is regulated by phosphorylation. Subsequently, substitution of the phosphorylatable residues in MAP65-1 for alanine resulted in the excessive bundling of microtubules through cell division, a delayed mitotic progression, and increased numbers of pole-to-pole

microtubules in the metaphase spindles. Altogether, these data suggest that MAP65-1 is regulated by phosphorylation/dephosphorylation during the cell cycle and that MAP65-1 binds microtubules weaker when phosphorylated by different protein kinases.

5.2 Effect of D-box knockout on MAP65 function

From the bioinformatics search, it was predicted that MAP65-1 contains a D-box motif (Figure 5.2A). To knock out the D-box motif of NtMAP65-1 arginine-529 and leucine-532 were substituted for alanine (Figure 5.1). BY2 cell lines expressing NtMAP65-1a$^{R529A/L532A}$ mutant protein containing an HA-epitope on the C-terminus were established and the expression level of the transgene was analyzed by western blotting using anti-HA (Figure 5.2B). The level of mutant protein expression was about 2.3 times higher than the level of wild type NtMAP65-1a. The increased expression level of the mutant protein could result either from the fact that expression was driven by 35S promoter or from inhibition of MAP65-1 degradation via D-box dependent pathway or both. However, the growth rate of the cell line expressing mutant protein was normal (Figure 5.2C). The immunostaining data also showed that none of the microtubule arrays were affected by the overexpression of the D-box deficient NtMAP65-1a (Figure 5.3). Moreover, GFP-NtMAP65-1a also showed normal localization in BY2 cells (Figure 5.4). All these data suggested that mutations R529A/L532A in the D-box motif of NtMAP65-1a didn't affect either the microtubule arrays or cell division and that NtMAP65-1a is unlikely to be

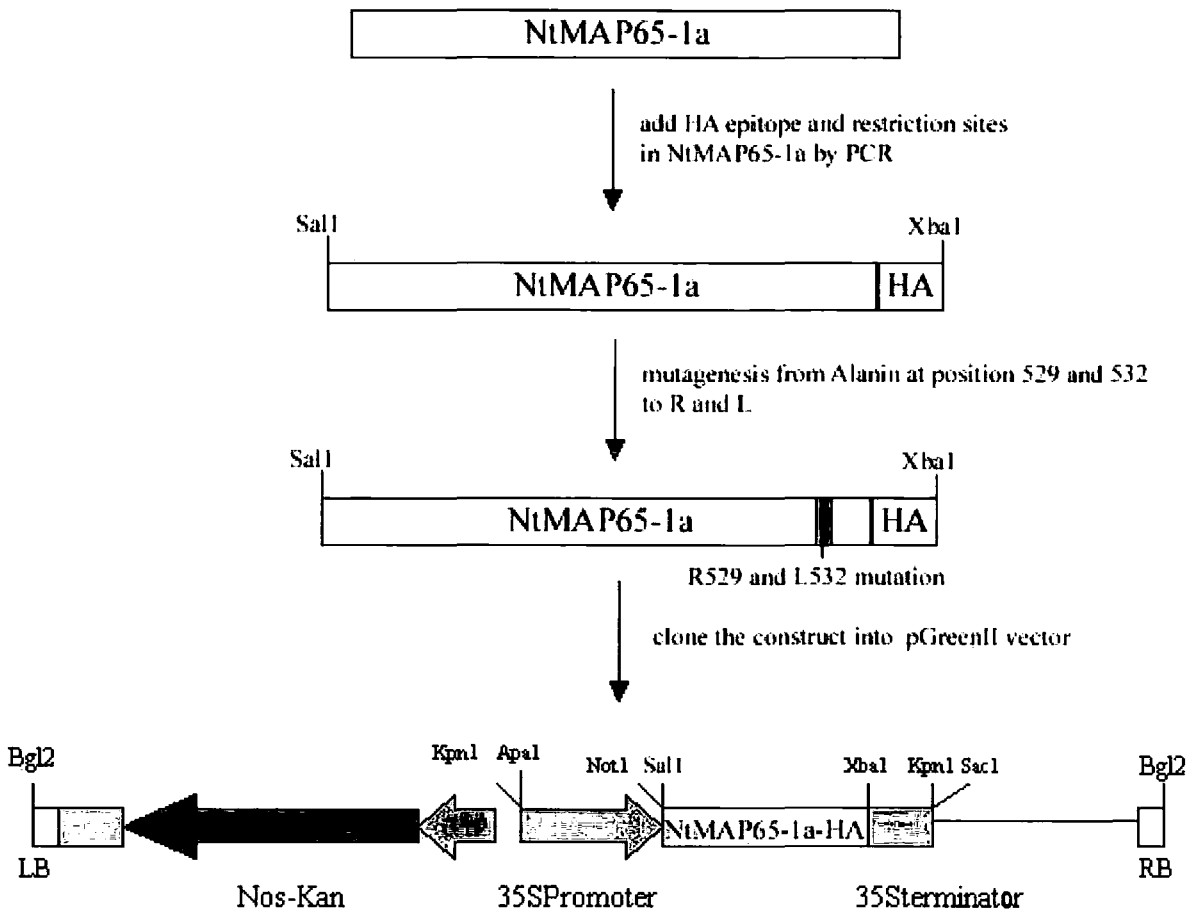

Figure 5.1 Schematic diagram of NtMAP65-1-HA D-box mutant construct.

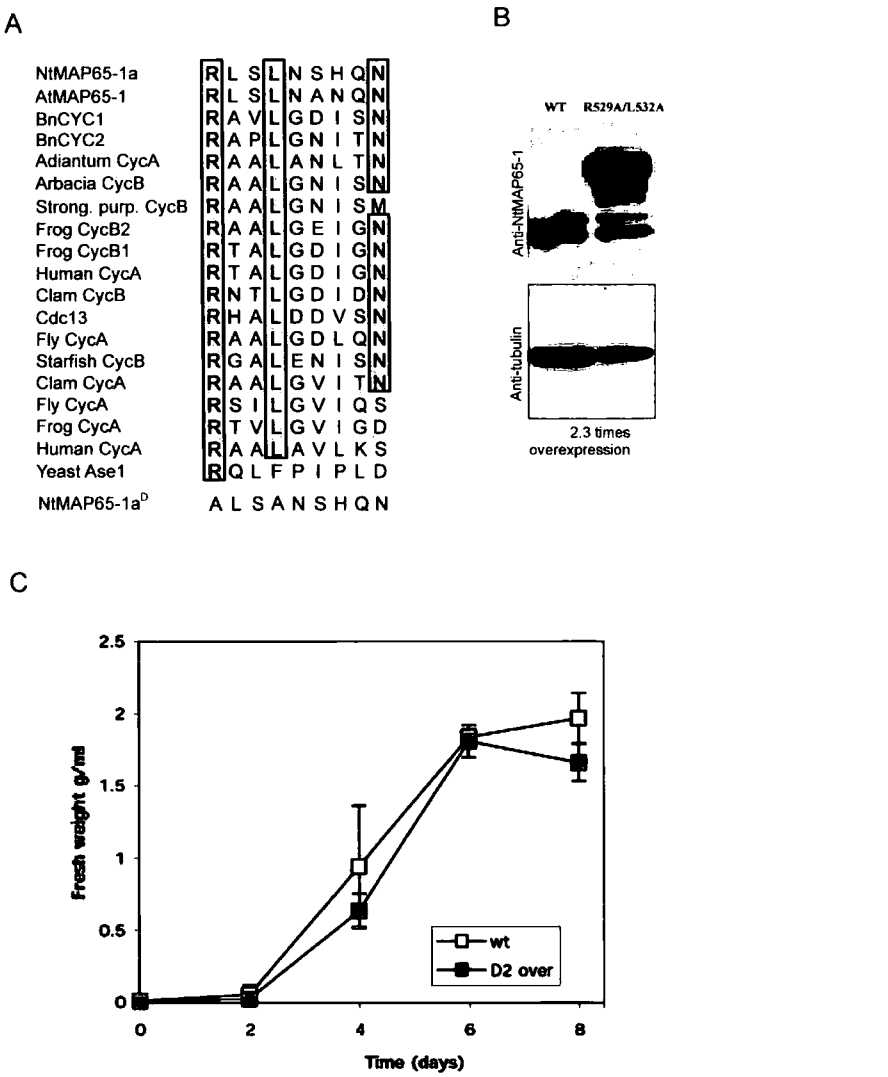

Figure 5.2 D-box mutant R529A/L532A BY2 lines shows normal growth curve.

(A) Alignment of several MAP65-like proteins from different organisms showed the conserved D-box motif (B) Western blotting membrane probed with anti-NtMAP65-1 (top) and anti-tubulin (bottom) antibody showed D-box mutant line expressed 2.3 times more protein than wild type BY2 cells. (C)The net weight of the BY2 cells from wild type and D-box mutant lines were measured for 8 days. The grow curve showed no differences between these two lines. Dark square represents R539A/L532A mutant. Light square represents the wild type.

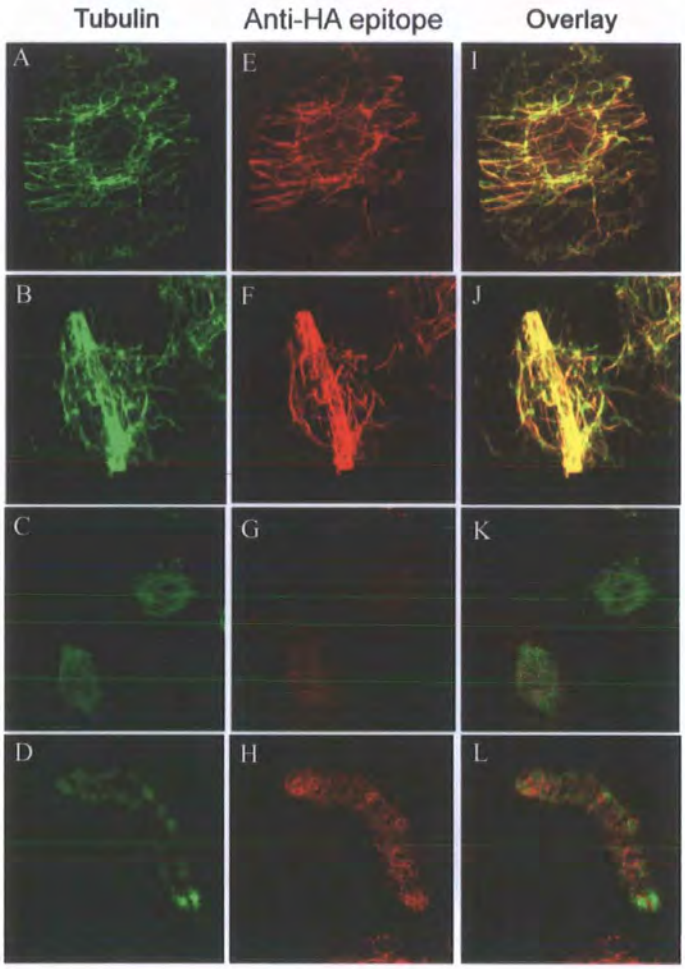

Figure 5.3 D-box mutation does not affect microtubule organization in BY2 cells. BY2 cell lines expressing NtMAP65-1a R529A/L532A mutant protein linked to HA-epitope on the C-terminus were stained with anti-HA- (red channel) and anti-tubulin (Green channel) (A,E,I) shows the cell is in the S/G2 transition preprophase band (B,F,J) metaphase spindle (C,G,K), and phragmoplast (D,H,L).

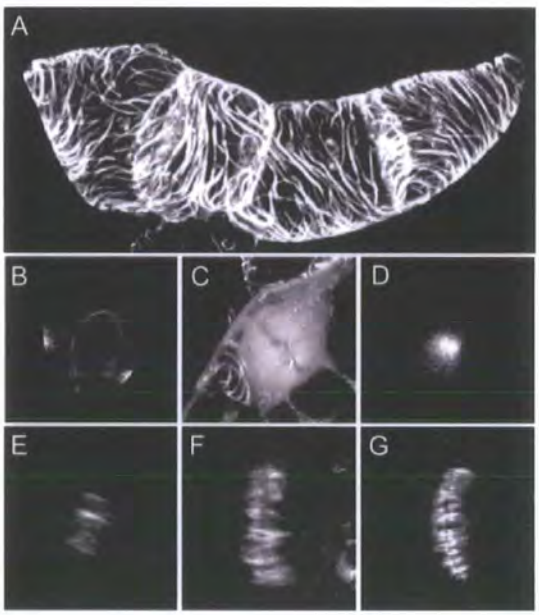

Figure 5.4 Localization of GFP: NtMAP65-1a R529A/L532A mutant protein in BY2 cells. Localization of GFP: NTMAP65-1a R529A/L532A protein was analyzed in tobacco BY2 cells throughout the cell cycle. R529A/L532A decorates the cortical microtubule array (A),the preprophase band (B), the anaphase spindle (D)(E), and the phragmoplast midzone (F)(G); but does not decorate the metaphase spindle (C).

regulated by cell cycle specific degradation.

5.3 MAP65-1 is regulated by phosphorylation/ dephosphorylation during the cell cycle

From section 5.2, the results suggested that MAP65-1 is not regulated through ubiquitin-mediated degradation. Therefore, MAP65-1 must be regulated by another mechanism. It is known that protein phosphorylation plays an important role in the execution and regulation of many cellular functions including the cell cycle. To check if MAP65 is regulated by phosphorylation, the phosphorylation of MAP65 was analyzed in a synchronized cell culture. BY2 cells were synchronized using aphidicoline and propyzamide treatment (Nagata T. and Kumagai F., 1999). Amphidicolin inhibit DNA synthesis; hence block the cells in the G1 phase of the cell cycle. Propyzamide is a microtubule depolymerizing agent which can be used to synchronize the cells in the M phase of the cell cycle. Sampling points 0-2 were collected after aphidicolin was washed off; points 3-5 were collected during propyzamide treatment and points 6-10 were collected after propyzamide was washed off (Figure 5.5A). Total protein extracts were prepared from sampling points 0-10 and used as a kinase in AtMAP65-1 phosphorylation assays. Phosphorylation assay was carried out by adding the protein samples intro the assay buffer (20 mM Hepes, PH7.5, 15mM $MgCl_2$, 5 mM EGTA, 1 mM DTT, 0.5 mg/ml histoneH1 (SIGMA type III), and 2 μCi of [γ^{-32}P]ATP) and incubated at room temperature for 30 min. The reaction was terminated by the addition of 5μl of 4x SDS sample buffer. The samples were

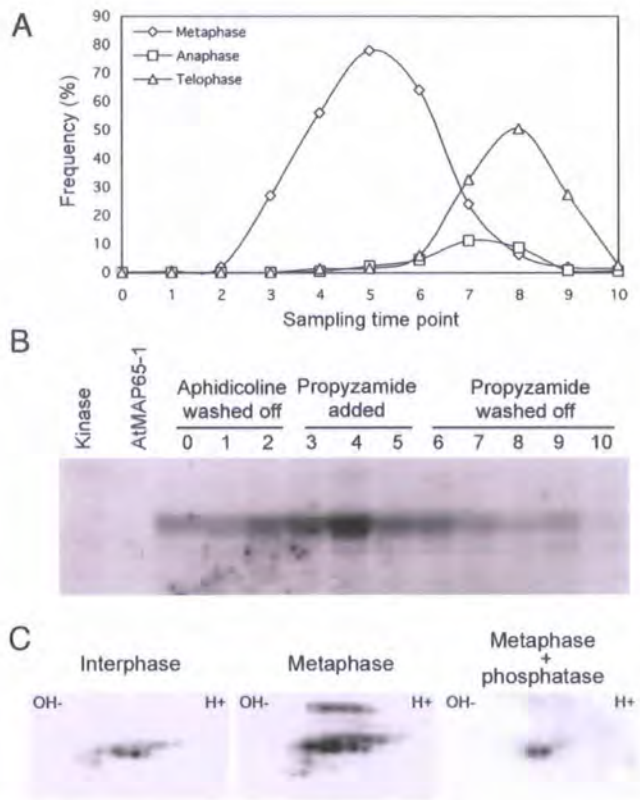

Figure 5.5 MAP-65 is phosphorylated in a cell cycle dependent manner.
A. Frequency of metaphases, anaphases and telophases in cell cycle synchronised cell population. Sampling points 0-2 were collected after aphidicolin was washed off, points 3-5 were collected during propyzamide treatment and points 6-10 were collected after propyzamide was washed off. B. Autoradiogram showing phosphorylation of AtMAP65-1 by the total protein extract from cells collected at sampling points 0-10 described in A. Extract from the sampling point 4 or AtMAP65-1 alone were used as negative controls (labeled as Kinase and AtMAP65-1). C. Western blotting with anti MAP-65 of total protein extract from interphase cells (sampling point 0), metaphase cells (sampling point 4) and metaphase cell protein extract treated with phosphatase. Proteins were separated by two dimensional SDS-PAGE, only MAP-65 area of the membrane is shown.

then analyzed by SDS-PAGE and subsequent autoradiography. The autoradiogram shows the different phosphorylation levels of AtMAP65-1 through the cell cycle (Figure 5.5B). The signal increased from point 0 to 4 as cells entered into mitosis as confirmed from the mitotic index and then decreased from 4 to 10, which suggests that AtMAP65-1 is phosphorylated through all stages of the cell cycle and highly phosphorylated during metaphase. Protein extracts from interphase (sampling point 0) and metaphase (sampling point 4) BY-2 cells were fractionated using two-dimensional SDS-PAGE and probed with anti-AtMAP65-1. Figure 5.5C shows that the heterogeneity of AtMAP65-1 increases during metaphase. When the metaphase protein extract was treated with phosphatase, the number of AtMAP65-1 isoforms dramatically decreased, suggesting that the increase in AtMAP65-1 heterogeneity resulted from extensive phosphorylation.

5.3.1 Phosphorylation regulates the interaction of MAP-65 with microtubules

As AtMAP65-1 recombinant protein was found to be hyper-phosphorylated during prometaphase/metaphase, it was important to check if phosphorylation can be responsible for the regulation of the MAP65 interaction with microtubules. To identify the kinase pathways responsible for the phosphorylation of MAP65, protein kinase inhibitors were used in the phosphorylation assays. General kinase inhibitors used in the phorphorylatoin assay includes K252-a and Staurosporine. K252a, an indrocarbazole

derivative, inhibits PKA (Protein kinase-A), PKG (protein kinase G), MLCK (myosin light-chain kinase), PKC (protein kinase C), CaMK (Ca2+/calmodulin-dependent protein kinase), phosphorylase kinase, MAP kinase, the trk family of receptor tyrosine kinases, and numerous other kinases by acting as a competitive inhibitor with respect to ATP (Angeles *et al.*, 1998). Staurosporine inhibits PKA, PKG, MLCK, PKC, CaMK, tyrosine kinases and phosphorylase kinase. Inhibition is via interaction with the ATP binding site (Meggio *et al.*, 1995). Specific protein inhibitor used includes Olomoucine and DMAP. Olomoucine, a purine derivative, found to be a highly specific inhibitor of cyclin-dependent kinases. Olomoucine behaves as a competitive inhibitor for ATP and as a non-competitive inhibitor for histone H1 binding in CDKs kinases (Havlicek *et al.*, 1997). 6-dimethylaminopurine (6-DMAP) inhibits protein kinase by rephosphorylation on tyrosine of the p34cdc2 homolog, the M-phase promoting factor (MPF) catalytic subunit (Neant *et al.*, 1988).

In the control reaction, recombinant AtMAP65-1 was phophorylated by the protein extracted from metaphase BY2 cell (Figure 5.6A, lane 1). General kinase inhibitors, K252-a and Staurosporine, abolished AtMAP65-1 phosphorylation. Whereas DMAP and Olomoucine only partially inhibited kinase activity (Figure 5.6A). These data confirm that several kinases can phosphorylate AtMAP65-1. Furthermore, immunoprecipitated protein kinases of different classes were able to phosphorylate AtMAP65-1 *in vitro*. The radiograph

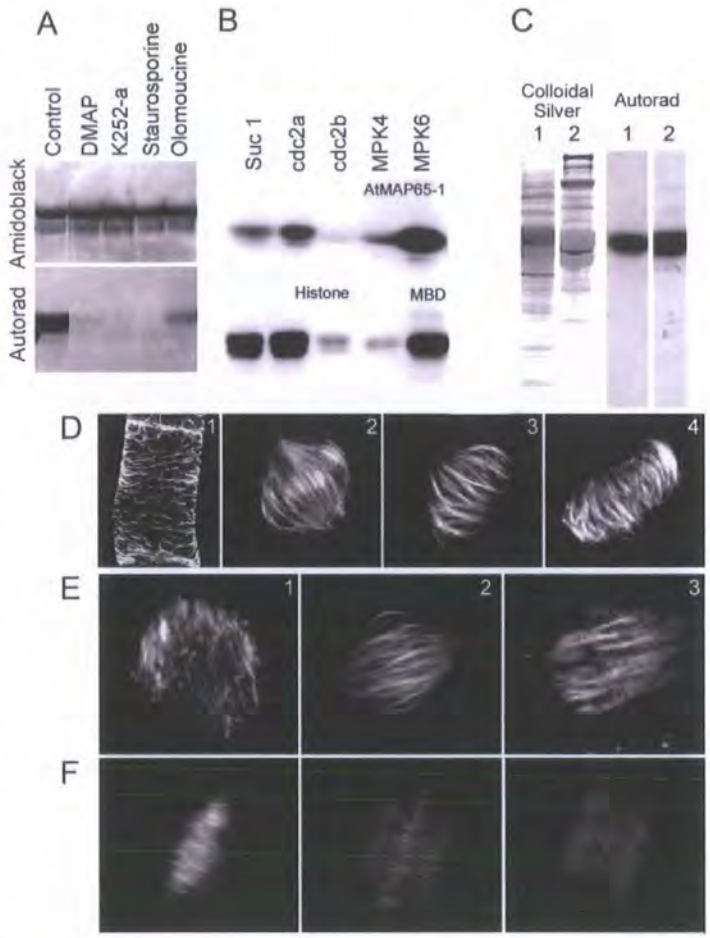

Figure 5.6 Phosphorylation regulates interaction of MAP-65 with microtubules. A. Effect of protein kinase inhibitors on MAP-65 phsophorylation. Recombinant AtMAP65-1 was phosphorylated by metaphase protein extract (sampling point 4 as in Figure 1) without inhibitor (lane Control) or in the presence of DMAP, K252-a, Staurosporine, and OlomoucineB. Phosphorylation of AtMAP65-1 by cyclin dependent kinases precipitated by pSuc1 bound beads, anti-cdc2a and anti-cdc2b antibodies; and by MAP kinases precipitated with anti-MPK4 and anti-MPK6. The activity of precipitated protein kinases was checked with their know substrates (Histone for cycling dependent kinases and MBD for MAP kinases) .C. MAP-65 can be phosphorylated by a kinase that interacts with microtubules. \Colloidal silver staining of metaphase protein extract from BY2 cells (lane 1) and microtubule proteins (lane 2). Autoradiogram shows MAP65-1 kinase activity of both extracts D. Localisation pattern of GFP:AtMAP65-1 chimera after treatment with DMAP protein kinase inhibitor ininterphase cells (panel 1),metaphase or anaphase spindles (panels 2 and 3) and phragmoplast (panel 4).E. Effect of olomoucine on GFP:AtMAP65-1 chimera localisation in prometaphase cells (panel1), metaphase cells (panels 2 and 3).F. Time laps series of two cells treated with okadeic acid. The frames were collected 5, 16 and 22 minutes after the drug application as indicated on each frame.

in Figure 5.6B, shows that AtMAP65-1 can be phosphorylated by CDKs precipitated by pSuc1 beads and by anti cdc1a, cdc2a and MPKs precipitated with anti MPK4/MPK6 antibodies. Interestingly, a microtubule protein preparation (the details of microtubule protein preparation procedure described in 2.2.10) from BY2 cells can also phosphorylate AtMAP65-1. This result indicates that kinases regulating MAP65 can be associated with microtubules (Figure 5.6C). It has been reported that both CDKs and MAP kinases can be associated with microtubules (Weingartner *et al.*, 2001; Nishihama and Machida, 2001).

Moreover, protein kinase inhibitors (DMAP and Olomoucine) and phosphatase inhibitor (Okadeic acid) were applied to the BY2 cell line expressing GFP: AtMAP65-1. Okadeic acid inhibits the serine/threonine phosphatase by binding to its catalytic subunit and inhibiting its enzymatic activity. Treatment with protein kinase inhibitors induced binding of the GFP: AtMAP65-1 to the microtubules of the prophase and metaphase spindles after 15 min application (Figure 5.6D). AtMAP65-1 bound microtubules in the metaphase spindle and appeared there as thick bundles. The microtubules of the anaphase spindle and phragmoplast were curved and extremely bundled. Treatment with olomoucine, also induced binding of AtMAP65-1 to microtubules during prophase and metaphase, but the effect was less dramatic compared to DMAP (Figure 5.6 E). Moreover, treatment of the BY2 line expressing GFP: AtMAP65-1 with okadeic acid caused a fading of the phragmoplast midzone signal (Figure 5.6F).

Therefore, phosphorylation inhibitors affect the binding of AtMAP65-1 to microtubules during prophase and metaphase.

5.3.2 MAP-65 phosphorylation sites are located within C-terminal coiled coil domain

To identify phosphorylation sites in AtMAP65-1, the protein was divided into four fragments. These fragments (Fragment 1, amino acids 1-150; Fragment 2, amino acids 151-339; Fragment 3, amino acids 340-494; Fragment 4, 495-587) of AtMAP65-1 were expressed in E.coli as recombinant proteins and purified by Ni^{2+} affinity chromatography. Metaphase protein extract from metaphase BY2 cell (sampling point 4 showed in figure 5.5A) was mixed with each of these four fragments of AtMAP65-1 in phosphorylation assays. Figure 5.7A lanes 1-5 shows that out of four fragments, only fragment 4 was phosphorylated. Olomoucine inhibited phosphorylation of Fragment 4 by the metaphase protein extract (lane 10. figure 5.7A). Moreover, both purified cdc2a and a microtubule protein preparation (2.2.10) only caused phosphorylation of Fragment 4 (Figure 5.7B C). These data suggest that all residues that are phosphorylated in AtMAP65-1during metaphase are located within the C-terminal region conresponding to Fragment 4. Several synthetic peptides were made corresponding to the regions of Fragment 4 that contain putative phosphorylation motives. These peptides were phosphorylated by metaphase protein extract, transferred onto phosphocellulose p81 paper and the efficiency

Therefore, phosphorylation inhibitors affect the binding of AtMAP65-1 to microtubules during prophase and metaphase.

5.3.2 MAP-65 phosphorylation sites are located within C-terminal coiled coil domain

To identify phosphorylation sites in AtMAP65-1, the protein was divided into four fragments. These fragments (Fragment 1, amino acids 1-150; Fragment 2, amino acids 151-339; Fragment 3, amino acids 340-494; Fragment 4, 495-587) of AtMAP65-1 were expressed in E.coli as recombinant proteins and purified by Ni^{2+} affinity chromatography. Metaphase protein extract from metaphase BY2 cell (sampling point 4 showed in figure 5.5A) was mixed with each of these four fragments of AtMAP65-1 in phosphorylation assays. Figure 5.7A lanes 1-5 shows that out of four fragments, only fragment 4 was phosphorylated. Olomoucine inhibited phosphorylation of Fragment 4 by the metaphase protein extract (lane 10. figure 5.7A). Moreover, both purified cdc2a and a microtubule protein preparation (2.2.10) only caused phosphorylation of Fragment 4 (Figure 5.7B C). These data suggest that all residues that are phosphorylated in AtMAP65-1during metaphase are located within the C-terminal region conresponding to Fragment 4. Several synthetic peptides were made corresponding to the regions of Fragment 4 that contain putative phosphorylation motives. These peptides were phosphorylated by metaphase protein extract, transferred onto phosphocellulose p81 paper and the efficiency

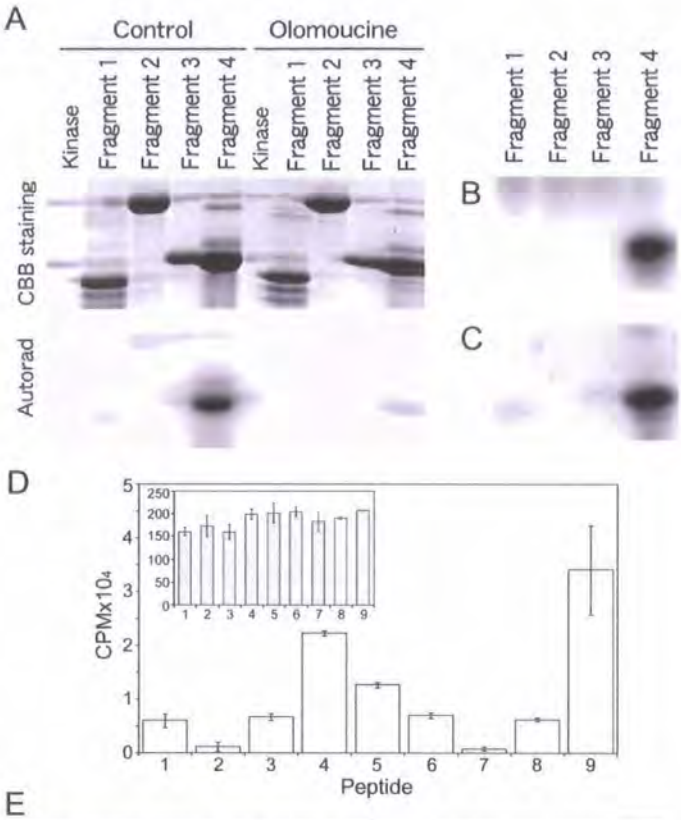

Peptide	Sequence	Residue	Protein kinase	Reference
1	QESAFSTRPSPA	S503	CDK,PKA,PKC	1, Scansite
3	ANGTHN	T526	CDK	Scansite
4	NRRLSLNA	S532	PKA,AuroraB, cAMK,cGMK	Scansite, Prosite
5	NGSRSTA	S539	CK1	Prosite
		T543	CK2,PKC	Prosite
6	RRETLNR	T552	cAMK,cGMK,PKA, PKC, AuroraB	Prosite,Scansite
8	AASSPVSGA	S543	CDK, Erk1	2, Disphos, PhosphoELM
		S576	CK1	1
9	QVPASP	S586	CDK	2, Disphos, PhosphoELM

Figure 5.7 MAP-65 phosphorylation sites are located within C-terminal coiled coil domain.

A. Phosphorylation of four AtMAP65-1 fragments with metaphase protein extract alone or with mitotic protein extract supplemented with olomoucine. Metaphase protein extract without substrate was used as negative control (lane Kinase). B. Phosphorylation of AtMAP65-1 fragments with cdc2a.C. Phosphorylation of AtMAP65-1 fragments with microtubule proteins preparation.D. Phosphorylation of peptides designed for putative phosphorylation sites in Fragment 4 by metaphase protein extract. The inset shows total counts per minute (CPM) in the reaction mixture.E. Bioinfomatics analysis of putative phosphorylation sites within phosphorylated peptides. The phosphorylating S/T residue is highlited in bold within each peptide sequence. CDK – cyclin dependent protein kinase; PKA – protein kinase A; PKC – protein kinase C; cAMK – cAMP dependent protein kinase; cGMK – cGMP dependent protein kinase; CK1 – casein kinase 1; CK2 - casein kinase 2; Erk1 - Extracellular signal-regulated kinase 1. Prosite - http://www.expasy.org/prosite/; Scansite - http://scansite.mit.edu/; Disphos - http://core.ist.temple.edu/pred/; PhosphoELM - http://phospho.elm.eu.org/pictures/phospho.logo.png.

of phosphorylation was measured using counts for each of the peptides (figure 5.7D). Peptides nine, four and five showed high phosphorylation levels, while peptides one, three, six and eight showed medium phosphorylation levels. However, peptides two and seven showed low phosphorylation levels. Combining these data together with the prediction of phosphorylation sites using a bioinformatics search, several phosphorylation motives for known protein kinases were predicted (Figure 5.7 E). Several different kinases including CDK, CK1, CK2, PKA, PKC, Aurora B, cAMK, cGMK, Erk1 had phosphorylation activities within these peptides. (Kennelly and Krebs, 1991; Chang *et al.*, 2003; Prosite- http://www.expasy.org/prosite/;

Scansite -.http://scansite.mit.edu/; Disphos-http://core.ist.temple.edu/pred/;

PhosphoELM– http://phospho.elm.eu.org/pictures/phospho.logo.png;).

5.3.3 Phosphorylation regulates interaction between AtMAP65-1 and microtubules

5.3.3.1 Effect of AtMAP65-1 phoshporylation on the protein activity *in vitro*

From section 5.3.1, it has been shown that CDK specific inhibitors can only partially inhibit MAP65 phosphorylation. Together with the bioinformatics predictions of AtMAP65-1a phophorylation sites from section 5.3.2, it is more

likely that the regulation of MAP65 is through several phosphorylation sites instead of one single site. To knock out all the possible sites, four mutants were generated where 2, 4, 7 or 9 phosphorylation residues were substituted for aspartic acid, a known mimic of phosphorylation: AtMAP65-$1^{2D, 4D, 7D, 9D}$ (table 5.1). The recombinant proteins were expressed in E.coli and used in the tubulin turbidimetric assay and the microtubule co-sedimentation assay. All phosphorylation sites of AtMAP65-1 which control its activity were therefore knocked out in AtMAP65-1^{9D}. Figure 5.8A shows the autoradiogram of wild type AtMAP65-1 and AtMAP65-1^{9D} mutant recombinant proteins phosphorylated by the metaphase or interphase protein extract. These results showed that during S phase the phosphorylation levels were the same between the wild type and mutant protein, whereas during metaphase the phosphorylation level of AtMAP65-1^{9D} mutant was obviously lower than wild type protein. The results of co-sedimentation assay showed that there were less AtMAP65-1^{9D} proteins binding with polymerized microtubule (Figure 5.8 B, C). The turbidimetric assay results showed that lower signals and therefore less microtubule bundling occurred when AtMAP65-1^{9D} protein was added to the reaction comparing to the wild type protein (figure 5.8D). All together, these data suggest that phosphorylation inhibits the microtubule binding and bundling ability of AtMAP65-1 *in vitro*.

A

Peptide	Sequence	Residue	Protein kinase	Reference
1	QESAFSTRP**S**PA	S503	CDK,PKA,PKC	1, Scansite
3	ANG**T**HN	T526	CDK	Scansite
4	NRRL**S**LNA	S532	PKA,AuroraB, cAMK,cGMK	Scansite, Prosite
5	NG**S**RS**T**A	S540	CK1	Prosite
		T543	CK2,PKC	Prosite
6	RRE**T**LNR	T552	cAMK,cGMK,PKA, PKC, AuroraB	Prosite,Scansite
8	AAS**S**PV**S**GA	S573	CDK, Erk1	2, Disphos, PhosphoELM
		S576	CK1	1
9	QVPA**S**P	S586	CDK	2, Disphos, PhosphoELM

B

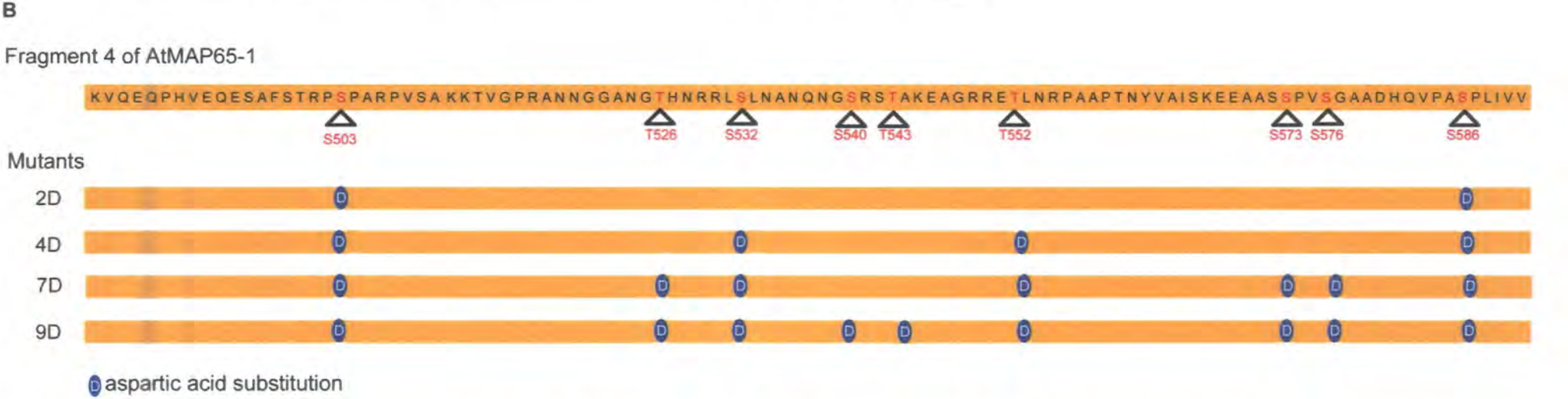

Table 5.1 Prediction of phosphorylation sites in the peptides of Fragment 4 which were phosphorylated by metaphase cell extract and description of AtMAP65-1 phosphomimetics AtMAP65-12D (2D), AtMAP65-14D (4D), AtMAP65-17D (7D), AtMAP65-19D(9D).(A)The phosphorylating S/T residue is highlighted in bold within each peptide sequence.Abbreviations: CDK – cyclin dependent protein kinase; PKA – protein kinase A; PKC – protein kinase C; cAMK – cAMP dependent protein kinase; cGMK – cGMP dependent protein kinase; CK1 – casein kinase 1; CK2 - casein kinase 2; Erk1 - Extracellular signal-regulated kinase 1.
References: Prosite - http://www.expasy.org/prosite/; Scansite - http://scansite.mit.edu/; Disphos - http://core.ist.temple.edu/pred/; PhosphoELM - http://phospho.elm.eu.org/pictures/phospho.logo.png.1Kennelly&Krebs, 1991; 2Chang et al., 2003.
(B)Sheme presenting AtMAP65-1 phosphomimetics AtMAP65-12D (2D), AtMAP65-14D (4D), AtMAP65-17D (7D), AtMAP65-19D(9D) mutants.

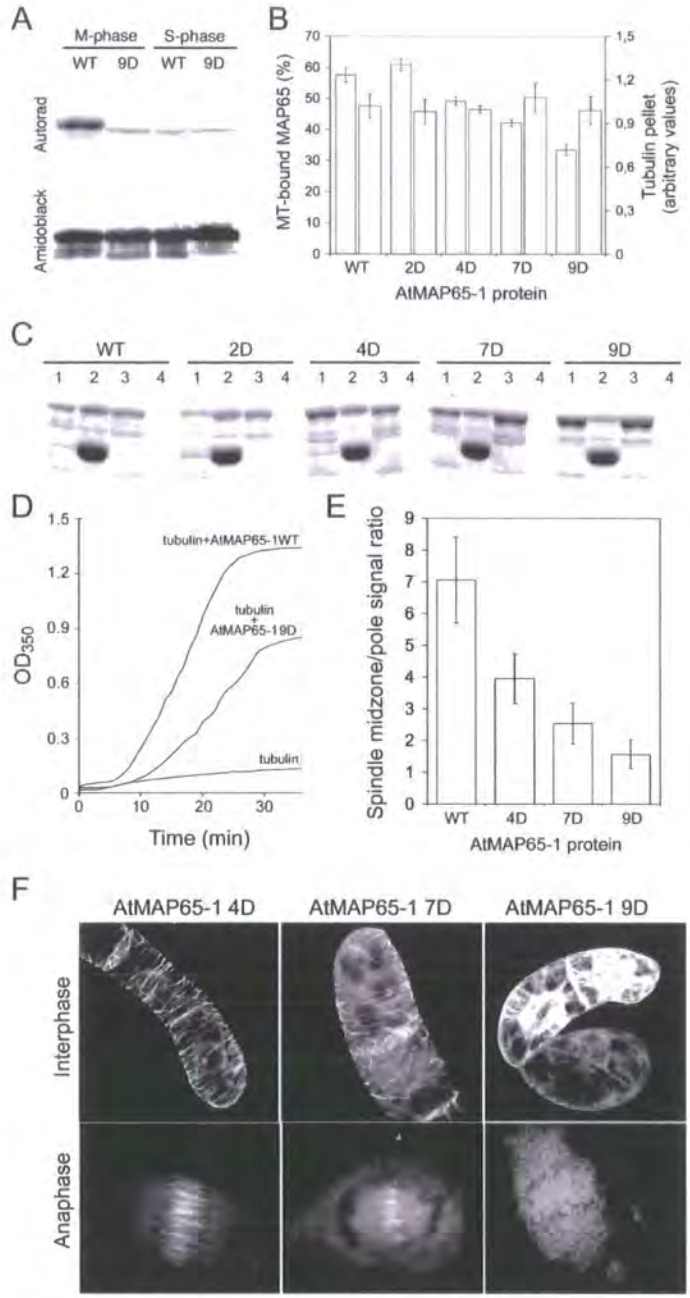

Figure 5.8 Phosphorylation regulates interaction between MAP-65 and microtubules.

A. Autoradiogram (Autorad) of wild type AtMAP65-1 (WT) and AtMAP65-19D mutant (9D) recombinant proteins phosphorylated with metaphase (M-phase) or interphase (S-phase, sampling point 0) protein extract. Corresponding nitrocellulose membrane was stained with Amido Black die (Amidoblack).B,C, Cosedimentation assay of AtMAP65-1 wild type (WT), AtMAP65-12D (2D), AtMAP65-14D(4D), AtMAP65-17D(7D), AtMAP65-19D(9D) recombinant proteins with microtubules . Quantification of recombinant MAP-65 protein (grey bars) and tubulin (white bars) in the pellet is shown in B. Coomassie Brilliant Blue stained SDS-PAGE gel of supernatants (lanes 1 and 3) and pellets (lanes 2 and 4) of recombinant MAP-65 proteins mixed with microtubules (lanes 1 and 2) or on their own (lane s 3 and 4) is shown in C.D. Turbidimetric analysis of 1.4 mg/ml tubulin solution and tubulin solution mixed at equimolar ratio with wild type AtMAP65-1 or AtMAP65-19D mutant.E. Ratio between midzone and cytoplasmic signal of AtMAP65-1 wild type (WT), AtMAP65-14D(4D), AtMAP65-17D(7D) and AtMAP65-19D(9D) GFP fusion proteins.F. A typical localisation pattern of AtMAP65-14D(4D), AtMAP65-17D(7D), AtMAP65-19D(9D) GFP fusion proteins in interphase and anaphase cells.

5.3.3.2 Effect of phosphorylationon on the activity of AtMAP65-1 *in vivo*

Next, the phosphorylation mutant proteins of AtMAP65-1 were linked to GFP and the localization of GFP fusion proteins was analyzed through the cell cycle. Figure 5.8 F shows the localization of 4D, 7D, 9D proteins in the interphase cortical microtubule array and anaphase spindles. The binding of AtMAP65-1 to microtubules in both arrays decreased according to the number of mutated amino acids. The anaphase spindle midzone decoration was absent in the 9D mutant, 7D had weak decoration, and 4D had stronger decoration. The measurement of the ratio between GFP signal in the midzone and the anaphase spindle showed a gradual decrease of GFP: AtMAP65-1 localization in the midzone according to the number of mutated phosphorylation sites (Figure 5.8E).

To knock out phosphorylation sites and create non-phosphorylatable constantly active protein, all phosphorylation sites in AtMAP65-1 were changed to alanine. This protein (GFP: AtMAP65-1^{9A}) was linked to GFP and transformed into BY2 cells. The localization of GFP: AtMAP65-1^{9A} mutant protein was different to GFP: AtMAP65-1^{9D}. The decoration of microtubules did not disappear during PPB disassembly, but persisted during prophase and metaphase (supplementary information movie 2, Figure5.10A). The microtubules decorated with GFP: AtMAP65-1^{9A} appeared as thick bundles. Immunostaining showed that the 9A mutant protein indeed induced excessive bundling of prometaphase

and metaphase spindle microtubules (Figure 5.9 A, C, E), which is not the case in the cells expressing wild type GFP: AtMAP65-1 (Figure 5.9 B, D, F). Although the total number of microtubule bundles in the metaphase spindle was similar to the control, the number of pole-to-pole microtubules increased significantly (Figure 5.9G). The time required for the cell to proceed from prophase to telophase was about two times longer in the cells expressing AtMAP65-1^{9A} (70 minutes compared to 37 minutes) (Figure 5.10A). Quantification of the signal in the cell division midzone in both wild type and GFP: AtMAP65-1^{9A} showed that GFP: AtMAP65-1^{9A} persists in the cell division midzone and delayed the progression of the cell division (Figure 5.10B) comparing to the wild type. Therefore, inhibition of AtMAP65-1 phosphorylation results in constant association of AtMAP65-1 and microtubules, inducing extra bundling of microtubules. The extra bundling of microtubule in GFP: AtMAP65-1^{9A} cell line delays cell division.

5.3.3.3 Interaction between microtubules and AtMAP65-1 phosphorylation site mutants *in vivo*

Substitution of phosphorylation residues for aspartic acid or alanine had the opposite affect on the dynamics of the AtMAP65-1 microtubule interaction *in vivo* as determined using FRAP. While turnover of GFP: AtMAP65-1^{9D} was faster than turnover of wild-type protein and the binding to phragmoplast microtubules was reduced by 40% (Table 5.2), the turnover of GFP: AtMAP65-1^{9A} was slightly slower than wild-type in all arrays, except the

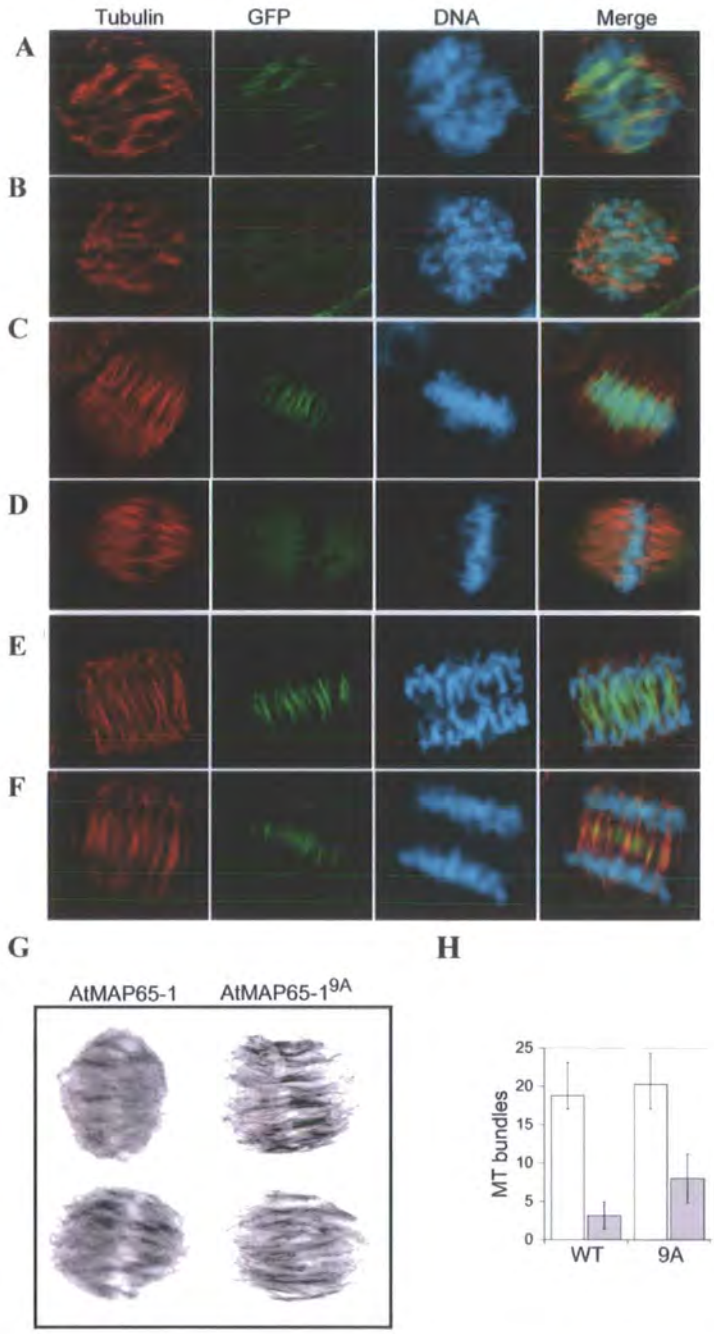

Figure 5.9 Disruption of phosphorylation de-regulates interaction between AtMAP65-1 and microtubules during metaphase.
Immunostaining of tubulin (red channel), AtMAP65-1^{9A} (A,C,E) or GFP:AtMAP65-1 (B,D,F; green channel) and DNA (blue channel) in prometaphase (A,B), metaphase (C,D) and anaphase (E,F) cells. (G)Immunostaining of tubulin shows increase in the number of pole to pole microtubule bundles in the AtMAP65-1^{9A} mutant comparing to the wild type. (H) The number of all microtubules bundles (blank bar) and the number of pole to pole bundles in metaphase spindles (grey bar) in cells expressing wild type AtMAP65-1 or AtMAP65-1 ^{9A} mutant.

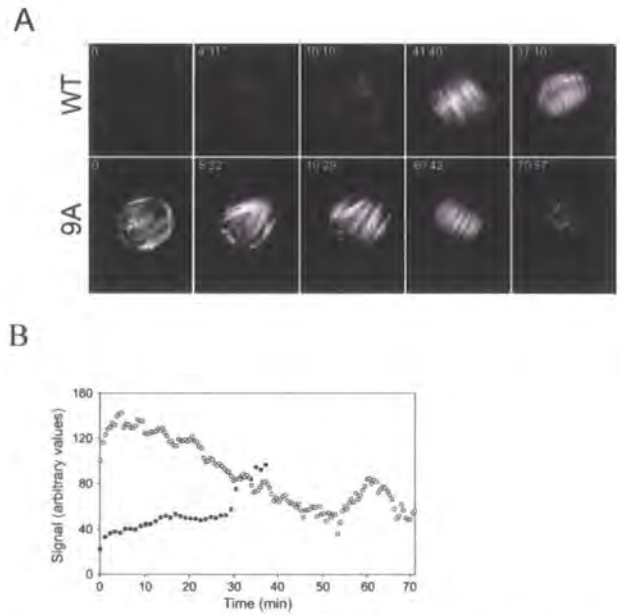

Figure 5.10 Non-phosphorylatable AtMAP65-1 affects metaphase spindle organisation and cell division. A. Localisation of wild type AtMAP65-1 (WT) and AtMAP65-19A (9A) GFP fusions during mitosis. The wild type protein becomes associated with microtubules only in anaphase, while the mutant bins to microtubules at every stage of mitosis. Numbers in the top right corner indicate timing of each frame. B. Quantification of the signal in the cell division midzone of AtMAP65-1 wild type (closed circles) and AtMAP65-19A (open circles).

Table 5.2 Analysis of the MAP65:GFP FRAP data in BY-2 cells.
The dissociation constants k_{off} and $t_{1/2}$ were estimated for GFP fusions in various cell types and at various cell cycle stages. 'N' column shows the number of cells analysed in each experiment and the 'Bound' column shows the fraction of MAP65:GFP initially bound to the microtubules, expressed as percentages of total fusion protein.

	k_{off}[1]	$t_{1/2}$ (s)	N	k_{off}[2]	Bound (%)
NtMAP65-1a					
Interphase[3]	0.100	6.95±0.91	23	0.094	80.7
PPB[3]	0.117	5.92±0.64	19	0.083	85.8
Metaphase[3]	0.960	0.72±0.21	23	Nd[6]	Nd[4]
Phragmoplast[3]	0.146	4.83±0.64	20	0.117	75.0
Oryzalin[3]	0.402	1.71±0.24	23		
AtMAP65-1					
Interphase[3]	0.117	5.93±0.86	20	0.081	67.4
AtMAP65-1^{9D}					
Phragmoplast	0.195	3.55	18	0.081	44.6
AtMAP65-1^{9A}					
Interphase	0.082	8.45±0.83	14	0.065	78.5
PPB	0.069	10.05±0.42	17	0.073	100.0
Metaphase	0.179	3.87±0.53	15	0.147	73.8
Phragmoplast	0.085	8.16±0.76	17	0.069	80.1

[1]k_{off} estimated by single exponential fit; [2]k_{off} estimated by double exponential fit; [3]Chang et al., 2005; [4]Not determined due to values being below the threshold for diffusion seen in the oryzalin treated control cells.

metaphase spindle where K_{off} decreased by 5 times. The proportion of GFP: AtMAP65-1^{9A} bound to microtubules in metaphase was about 73.8% compared to 0% in wild type. These data indicate that interaction of AtMAP65-1 with microtubules through the cell cycle is regulated by phosphorylation.

5.4 Discussion

MAP65 contains a conserved destruction box motif in the C terminus (Hussey *et al.*, 2002). To knock out this motif, arginine-529 and leucine-532 were substituted for alanine. Both immunostaining and GFP localization data show normal localization of the AtMAP65-1 D-box mutant and cell division is unaffected. These results suggest that MAP65-1 is not regulated through the cyclin D-box dependent degradation pathway.

Analysis of the AtMAP65-1 phosphorylation status during the cell cycle shows that the protein is phosphorylated at all stages of the cell cycle but hyperphosphorylated at prophase and metaphase. When a BY2 cell line expressing GFP: AtMAP65-1 was treated with the general protein kinase inhibitor, DMAP and the CDK specific inhibitor-olomoucine, GFP: AtMAP65-1 was bound to the metaphase spindle. Treatment with the phosphatase inhibitor okadeic acid caused progressive loss of the GFP signal in the phragmoplast midzone. These results suggest that the microtubule binding activity of MAP65-1 is regulated by phosphorylation. Kinase activity was found in the microtubule protein preparation, indicating that these kinases are associated

with microtubules. Interestingly, both CDK and MAP kinase have been found to associate with microtubules (Weingartner *et al.*, 2001; Nishihama and Machida, 2001), and both kinases can phosphorylate AtMAP65-1 *in vitro*. These data indicate that several protein kinase pathways are involved in the control of MAP65-1 binding to microtubules and their cooperative activity is required for this control.

Nine potential phosphorylation motifs were predicted in AtMAP65-1 Fragment 4: CDKs (S503, T526, S586), MAPK Erk1 (S543), Aurora B/cyclic nucleotide dependant kinase (S532, T552) and casein kinase 1 and II/PKC (S539, T573, S576). Mutation of these residues for non-phosphorylatable residues diminished the phosphorylation level of AtMAP65-1 to the interphase level, suggesting that these nine sites control activity of MAP65 during mitosis.

Phosphomimetics of AtMAP65-1 were produced in which potential phosphorylation residues were substituted for aspartic acid. These substitutions caused the decrease of microtubule binding activity. The FRAP data showed that the turnover of GFP: AtMAP65-1^{9D} is faster than wild-type and the amount of protein bound to microtubules *in vivo* was reduced by 40%, while decoration of the anaphase spindle midzone was almost abolished. It suggests that dephosphorylation of MAP65-1 is necessary for its activity. Moreover, these nine potential phosphorylation residues were then substituted for non-phosphorylatable alanine. GFP: AtMAP65-1^{9A} was found to be bound to the

midzone of the metaphase spindle, causing an increase in pole-to-pole microtubule bundles and delayed mitosis. Altogether, the data suggest that AtMAP65-1 is regulated by phosphorylation/dephosphorylation through the cell cycle.

Chapter 6

Discussion

6.1 The interaction of MAP65 with microtubules *in vivo*

MAP65 only interacts with polymerized microtubules and not with tubulin. GFP: MAP65-1 decorates microtubules in the cortical array, the PPB, the anaphase spindle, and the phragmoplast. The turnover rate of MAP65 as assessed by FRAP is high *in vivo* and MAP65 can associate/disassociate randomly along the microtubule length. Moreover, the MAP65 / microtubule interaction is regulated in a cell-cycle dependent manner.

6.1.1 Localisation of MAP65-1 *in vivo*

GFP: MAP65-1 decorated microtubules arrays through the cell cycle, confirming the previously published immunostaining data (Smertenko *et al.*, 2000). Interestingly, MAP65-1 did not decorate the metaphase spindle but was scattered around in the nuclear area. After metaphase, the GFP: MAP65-1 signal dramatically concentrated and decorated the anaphase spindle midzone. During the anaphase spindle to phragmoplast transition, GFP: MAP65-1 decorated the phragmoplast microtubules concentrating at the midline. The midline decoration of the phragmoplast then disappeared gradually. Following phragmoplast expansion and cell plate formation, the interphase cortical

microtubule array started to form. In cortical microtubule arrays, the MAP65-1 signal was associated with thick bundles of microtubules.

The metaphase spindle is a very dynamic structure and relies on microtubules for its normal function. Two types of microtubule in the mitotic spindle are known: polar microtubules, which are associated with spindle pole and kinetochore; kinetochore microtubules, which are associated with kinetochore of the chromosome. The chromosomes are connected with the kinetochore microtubules. Each set of chromosomes will segregate after passing metaphase. Therefore, the correct spindle structure is very important for chromosome segregation and cell division. The maintenance of the dynamic spindle structure requires tight control of microtubule dynamics and bundling. Excessive microtubule bundles might disturb the progress of cell division. This could be why MAP65-1, which bundles microtubules, has to be inactivated during metaphase. The other interesting observation is the midzone decoration of MAP65-1 in anaphase spindle and phragmoplast. The localization of MAP65-1 suggests that it could cross-link anti-parallel microtubules in these structures and stabilise them. Recently, there is some debate about whether or not anti-parallel microtubules can be observed in the cell-plate assembly matrix. From electron tomography observations, the phragmoplast microtubules do not interdigitate at the cell-plate midline during somatic-type cytokinesis (Austin *et al.*, 2005). However, from our observations of tobacco BY2 cells, GFP-MAP65 concentrates in the midline of the newly formed phragmoplast and the edge of

the expended phragmoplast. This midline decoration then disappears when the phragmoplast reaches the mother cell wall. It is possible that the anti-parallel microtubules formation in the phragmoplast is transient and only on the edge, where the cell-plate assembly matrix has not fully formed. This might explain why the anti-parallel microtubules in the phragmoplast might not easily be observed by electron tomography. MAP65, in the phragmoplast midline, holds the two halves of the phragmoplast together by cross-bridging these anti-parallel microtubules transiently. However, once the cell-plate assembly matrix is formed, MAP65 retreats from the midline of the phragmoplast and leaves a gap between the two halves of the phragmoplast.

The cell plate materials are transported to the midline of the phragmoplast by kinesin and other associated proteins. Therefore, keeping the intact phragmoplast structure is important for cell plate formation. It has been reported that mutation of MAP65 protein AtMAP65-3 results in abnormal cytokinesis causing the formation of multinucleating root cells with incomplete cell walls. The phragmoplast in the mutant has an abnormally expanded midzone. MAP65-1, although it has different localization from MAP65-3 is also located in the phragmopalst midline. The midline localization implies that both proteins might play a similar role in this area. However, the real function of this midline localization of MAP65-1 still needs to be clarified.

There was no phenotype found in *Arabidopsis* seedlings expressing GFP: AtMAP65-1, and the GFP signal can be detected on cytoplasmic microtubules in most of the tissues. In some tissues (e.g. petals, stigmas and stamens) the GFP signal was not detectable due to the auto-fluorescence of these tissues. Interestingly, GFP: AtMAP65-1 does not decorate microtubules in the cells of the root extension zone, suggesting that the interaction of AtMAP65-1 with microtubules is regulated in a tissue specific manner. However, GFP: AtMAP65-1 decorates microtubule arrays in the dividing cells of the root tips, including the cortical microtubule, the PPB, and the phragmoplast. Furthermore, the decoration in trichomes and root hairs makes this cell line an interesting model for investigating the microtubules' organisation *in vivo*.

6.1.2 MAP65 is ideal for bundling and crossbridging plant microtubules during microtubule array formation and reorganisation

The rate of GFP: NtMAP65-1a turnover on interphase cortical microtubules was found to be similar in *Arabidopsis* hypocotyl epidermal cells and in rapidly proliferating tobacco suspension culture cells, indicating that the interaction of NtMAP65-1a is the same in both homologous and heterologous plant cells, and that the interaction is similar in differentiated and rapidly dividing tissues. The turnover of the GFP: AtMAP65-1 chimeric protein, the *Arabidopsis* homologue of NtMAP65-1a, was found to be very similar to that of GFP: NtMAP65-1a suggesting that they share the same mechanism of microtubule interaction. The recombinant AtMAP65-1 and NtMAP65-1b bundle, but neither promote

polymerisation nor prevent catastrophes of microtubules *in vitro* (Smertenko *et al.*, 2004: Wicker-Planquart *et al.*, 2004). Also, the turnover of GFP: NtMAP65-1a in all cell types and microtubule arrays examined was found to be at least four -fold greater than plant tubulin itself. The high rate of microtubule association /dissociation for this MAP65 isotype correlates with it having no impact on microtubule dynamics *in vitro*. Therefore, this MAP will not significantly affect the dynamics of microtubule *in vivo* and is ideally suited for bundling and crossbridging of plant microtubules during microtubule array formation and reorganisation. So far, nothing is known about the dynamics of interaction between other plant MAPs and microtubules. Thus, it will be very interesting to investigate if other plant MAPs will have a different turnover on microtubules and how this will correlate with their functions.

6.1.3 Dynamics of the MAP65 microtubule interaction during the cell cycle

Microtubules have an increased growth and catastrophe rate in the transition from interphase to preprophase band formation. However, the shrinkage rate and the rescue frequency are not affected. The net result is that during this transition microtubules become shorter and more dynamic (Dhonukshe and Gadella, 2003). However, in the observation of MAP65 turnover, the turnover rate in the preprophase band is similar to that in the interphase cortical array. It suggests that changes in microtubule dynamics do not affect the dynamics of the MAP65 microtubule interaction. Also, if binding of MAP65 is a prerequisite for

microtubule bundling, which is the case in vitro studies, then the same bundling mechanism is likely to occur in the two cortical arrays.

In the metaphase spindle a significant increase in the turnover of GFP: NtMAP65-1a was observed: the $t_{1/2}$ value decreased sevenfold. As we have shown that NtMAP65-1a does not interact with tubulin dimers, depolymerisation of microtubules with oryzalin will remove the major binding site for this MAP-65 in the cell. In the absence of microtubules the $t_{1/2}$ value was greater than in metaphase, indicating that in the metaphase spindle GFP: NtMAP65-1a does not bind to any structure and nor does it make any complexes. Its diffusion is presumably increased due to the dynamic cytoplasmic flow within mitotic spindles. However, there must be some interaction with as yet unknown factors that inhibit the ability of NtMAP65-1a to bind microtubules. This could be, for example, the presence of proteins that compete for the same binding site or post-translational modification of NtMAP65-1a that can alter its structure.

In anaphase and telophase GFP: NtMAP65-1a is observed to concentrate mainly in the midzone of the spindle and the phragmoplast as was previously shown by antibody staining in tobacco and *Arabidopsis* tissue culture cells (Smertenko *et al.*, 2000; Smertenko *et al.*, 2004). However, the video of the GFP fluorescence (see supplementary information Movie 3) shows how dramatic this concentration proceeding poleward movement of the chromosomes actually is. FRAP data shows no significant differences in the turnover of NtMAP65-1a on

microtubules in the phragmoplast, the interphase cortical microtubules and the preprophase band. These data indicate that either the exchange rate of the NtMAP65-1a or the lifetime of the bridges between microtubules does not depend on the stage of the cell cycle. It would appear that the interaction of NtMAP65-1a with microtubules is regulated on an "on or off" principle and wherever bundling occurs the dynamics are the same. Other proteins known to be involved in the control of plant microtubule organisation *in vivo* such as katanin (e.g. Stoppin-Mellet *et al.*, 2002), MOR1/GEM1 (e.g. Twell *et al.*, 2002) or EB1 (e.g. Chan *et al.*, 2003) must be able to work in concert with MAP65 to regulate the dynamics and spatial pattern of microtubules bundled by MAP-65. Interestingly, the turnover of the yeast homologue of MAP-65, Ase1p, was found to be 7.5 minutes (Schuyler *et al.*, 2003), which is almost 100 times slower than NtMAP65-1a and AtMAP65-1. It is known that Ase1p is an important component of the spindle midzone matrix, responsible for the stabilisation and the maintenance of the spindle midzone. In *Arabidopsis* there are nine MAP65 genes, and they form a divergent gene family (Hussey *et al.*, 2002). Moreover, the two isoforms AtMAP65-1 (Smertenko *et al.*, 2004) and AtMAP65-3 (Muller *et al.*, 2004) show differential localisation in the four microtubule arrays, with AtMAP65-3 being restricted to only the mitotic arrays. AtMAP65-3 is essential for the maintenance of phragmoplast structure (Muller *et al.*, 2004) and it's tempting to speculate that this isoform is more closely related in function to Ase1p than to NtMAP65-1a. Perhaps it is the case that AtMAP65-3 stabilizes the subsets of microtubules responsible for anchoring and maintaining the integrity of the

spindle and phragmoplast midzone but that AtMAP65-1 plays a more active role in the bundling of dynamic microtubules, helping them retain spatial organisation in dynamic microtubule arrays.

6.1.4 NtMAP65-1 associates and dissociates randomly along microtubules

Recently, it has been shown that PRC1, the mammalian homologue of MAP65, binds several kinesin motor proteins: KIF4, MKLP and CENP-E. In KIF-4 deficient cells, the localization of proteins normally residing in the spindle midzone, including PRC1, was affected (Kurasawa *et al.*, 2004). In PRC-1 deficient cells no midzone appears and both KIF4 and CENP-E failed to concentrate in the spindle midzone. These results suggest that KIF 4 and PRC1 are essential for the organisation of the spindle midzone and possibly that KIF4 translocates PRC1 to the midzone. The *A. thaliana* genome has homologues of KIF4 and MKLP. However, it is not known whether they interact with MAP65. Moreover, from the FRAP analysis, it is obvious that NtMAP65-1 associates and dissociates randomly along microtubules rather than being translocated. Therefore, plants may have a different mechanism for MAP65 midzone localization during cell division.

In summary, these data show that the interaction of the MAP-65 with microtubules is very dynamic, that it occurs randomly along the length of microtubules and that it is cell-cycle stage dependent. Taken together with the finding that NtMAP65-1 and AtMAP65-1 proteins form crossbridges but have no

effect on microtubule dynamics in vitro (Chan *et al.*1999: Wicker-Planquart *et al.*, 2004: Smertenko *et al.*,2004), it appears that NtMAP65-1a and AtMAP65-1 are ideally suited to a role in forming crossbridges between microtubules and maintaining spatial organisation in rapidly reorganizing microtubule arrays.

6.2 The *Arabidopsis* microtubule associated protein AtMAP65-1: molecular analysis of its microtubule bundling activity

6.2.1 AtMAP65-1 cross-bridges microtubules

Recombinant AtMAP65-1 bundles microtubules forming crossbridges of 25 nm in length but does not increase the total amount of tubulin polymer, suggesting that bundling of microtubules does not directly affect the frequency of catastrophes or rescues. One can imagine a condition when either the frequency of catastrophe and rescue might increase or decrease similarly or that tubulin turnover might change for the microtubules bundled by AtMAP65-1. In either case the microtubule dynamics might be different but the total amount of tubulin polymer under steady state conditions of microtubule polymerization will remain the same. Nonetheless, this equilibrium will change when the steady state conditions are affected. An increase in the dynamics of microtubules resulting from either high rescue and catastrophe frequencies or a rapid tubulin turnover will cause a faster rate of microtubule de-polymerization and a decrease in the total amount of tubulin polymer when the concentration of tubulin is below the critical assembly point. If the dynamics of microtubules are decreased either

because of low frequencies of rescue and catastrophe or slow tubulin turnover, the total amount of tubulin polymer will be less vulnerable to the decrease of tubulin concentration. During the isothermal dilution of microtubules, the total amount of tubulin polymer was not affected by bundling with AtMAP65-1 producing identical curves for samples containing tubulin with or without AtMAP65-1. In contrast, when taxol, which promotes microtubule polymerization and decreases tubulin turnover, was added we observed a significant increase in the amount of tubulin polymer and a decrease in the microtubule de-polymerization when the tubulin concentration was below the critical assembly point. These data suggest that AtMAP65-1 is unlikely to have a significant effect on microtubule dynamics *in vitro.*

The fact that bundling does not decrease microtubule dynamics is consistent with the rapid recovery by treadmilling of bundled GFP-tubulin-tagged microtubules following photobleaching (Shaw *et al.*, 2003) and the movement of AtEB1a:GFP–tagged microtubules within bundles (Chan *et al.*, 2003a). It would therefore seem that the principal role of AtMAP65-1 would be to form a lattice network rather than to stabilize the microtubules *per se*. Of the nine AtMAP65 proteins AtMAP65-1 has the greatest sequence identity to NtMAP65-1, and falls in the same phylogenetic clade (Hussey *et al.*, 2002). The biochemical activity of AtMAP65-1 corresponds to the *in vivo* experimental data on NtMAP65-1 where the effect of cold on BY-2 cell microtubules was examined. In these experiments, microtubules in BY-2 cells were de-polymerized by cold and

their reformation was followed as the temperature was increased to 25°C (Smertenko *et al.*, 2000). The recovery of the microtubules occurred independently of MAP-65 binding, and MAP65 binding was only observed after the microtubules were polymerized, suggesting that NtMAP65-1 was not involved in the promotion of microtubule polymerization but in the crossbridging of microtubules once formed. These *in vivo* data from tobacco NtMAP65-1a protein correspond with the *in vitro* data for AtMAP65-1.

The crossbridging of microtubules by AtMAP65-1 is similar to that observed using carrot MAP65 enriched preparations (Chan *et al.*, 1999). The carrot MAP65 preparation contained 3 electrophretically separable bands, minor 60kDa and 68kDa bands and a predominant (85%) 62kDa band (Chan *et al.*, 1999). These protein bands were subsequently analysed by mass spectral analysis: the 68kDa and 60kDa were shown to disappear when the carrot suspension culture stopped dividing, leaving the 62kDa species as the sole detectable MAP65 in elongating cells containing only cortical microtubules (Chan *et al.*, 2003b). Peptide sequencing and sequencing of the cDNA (DcMAP65-1) established that carrot MAP62 was more similar to AtMAP65-1 and NtMAP65-1 than to any other known MAP65 (Chan *et al.*, 2003b). As MAP-62 was biochemically purified it is not known whether it is post-translationally modified. From the data presented in this study we can conclude that mixtures of MAP65 isoforms are not required to promote bundling,

and that the single unmodified gene product of AtMAP65-1 is capable of forming the 25nm cross-bridges.

6.2.2 Microtubule binding and dimerisation regions of AtMAP65-1

The AtMAP65-1 microtubule binding region is in the C-terminal half of the protein and the two amino acids Ala420 and Ala409 are essential structural elements in the microtubule: AtMAP65-1 interaction. The C-terminal half of the protein was divided into fragments 3 and 4. Fragment 3 harbours the sequence that was most conserved in all nine AtMAP65 genes. Fragment 4 contains the most divergent sequences across the MAP65 family and is highly charged (pI of 10.47). Both fragments 3 and 4 bound microtubules although it cannot be discounted that the high charge of fragment 4 might be responsible for non-specific binding. Fragment 3 is not only conserved between plant MAP65 proteins, but the sequence within this fragment also exhibits strong similarity with mammalian PRC1 and yeast Ase1p, especially within a 25 amino acid region (37.5%; Schuyler *et al.*, 2003). Mutation of a conserved amino acid within this short sequence, Ala 420 Val, diminished MAP-65 microtubule binding. This mutation was mimicked in AtMAP65-1 based on the sequence of the cytokinesis defective *ple-4* allele. Changing the conserved Alanine to a more hydrophobic amino acid disturbs the structure to such an extent that microtubule binding is greatly reduced. Mutating a second Alanine, at residue 409, in the conserved 25 amino acid sequence also diminished microtubule binding. By synthesising a peptide covering the whole 25 amino acid conserved motif, competition studies

were performed where AtMAP65-1 and the synthetic peptide were allowed to compete for the microtubule binding site. These studies demonstrated that the AtMAP65-1 microtubule interaction could not be inhibited in this way, which strongly suggests that sequences other than this 25 amino acid conserved motif, within fragment 3, are structurally important for microtubule binding. It is possible that the microtubule binding site depends on several points of contact and requires a specific tertiary structure as is known for MAP2/tau.

The amino terminal half of AtMAP65-1 harbours a dimerisation region and dimerisation may be important for 25 nm crossbridge formation. The N-terminal half of AtMAP65-1 was divided into two sections and the fragment encompassing residues 151 to 339 was found to bind another MAP65. Consideration of the structure of the crossbridges between microtubules created by carrot MAP65s, and the size of MAP65, led to the suggestion that MAP65 is unlikely to crossbridge as a single molecule (Chan *et al.*, 1999). The fact that neither the microtubule-binding region, nor the dimerisation region alone was capable of microtubule-bundling strongly suggests that these crossbridges are formed by MAP65 dimers with the C-terminal halves binding adjacent microtubules and the N-terminal halves being responsible for MAP65: MAP65 interaction.

6.2.3 Interaction of MAP65 with microtubules is cell cycle specific

AtMAP65-1 is expressed constitutively through the cell cycle, but the protein

binds only subsets of microtubules in a cell cycle dependent manner. The main difference in the localization of AtMAP65-1 in cells compared to AtMAP65-3/PLE (Muller *et al.*, 2004) and its homologues in animals and fungi, is that AtMAP65-1 (like NtMAP65-1; Smertenko *et al.*, 2000) also binds interphase cortical microtubules (Jiang *et al.*, 1998, Pellman *et al.*, 1995). However, mammalian PRC1 is capable of binding and bundling microtubules in interphase as overexpression causes the disruption of normal microtubule organisation and the appearance of circular filaments around the nuclei (Mollinari *et al.*, 2002). Bundling of microtubules in the interphase plant cells is thought to be important for the formation of the interphase cortical array (Smith *et al*, 2003). As the cells enter M-phase AtMAP65-1 does decorate the preprophase band but not the metaphase spindle. Thus, it binds microtubules at the midzone of the anaphase spindle and in the phragmoplast midzone. In both structures, MAP65 concentrates in the area where microtubules overlap.

6.3 Regulation of MAP65 activity through the cell cycle

6.3.1 Microtubule binding activity of MAP65-1 is regulated by phosphorylation/dephosphorylation

The binding of AtMAP65-1 to microtubules is down regulated during prometaphase/meptaphase. The activity of MAP65 homologues SPD-1(*C. elegans*), and FEO (Drosophila) is also downregulated during metaphase, while PRC1 (mammalian) decorates metaphase spindle microtubules (Verbrugghe

and White, 2004; Verni *et al.*, 2004; Jiang *et al.*, 1998). Two mechanisms have been suggested to be involved in the regulation of MAP65-like protein: through APC degradation pathway, or phosphorylation/dephosphorylation. PRC1 and Ase1 share two notable sequences features: a consensus cyclin-dependent kinase phosphorylation site and a sequence that is similar to a mitotic cyclin destruction box. It has been proven that PRC1 is phosphorylated at the consensus CDK phosphorylation site by CDK2 (Mollinari *et al.*, 2002) and that Ase1 is targeted to proteolysis by the anaphase-promoting complex (Juang *et al.*, 1997). AtMAP65-1 sequences also contain a destruction box and several predicted phsophorylation sites (Hussey *et al.*, 2002). However, the expression of D-box knocking out AtMAP65-1 protein in BY-2 cells did not affect the cell growth and cell division, indicating that AtMAP65-1 is not regulated by cell cycle specific degradation. Instead, phosphorylation/dephosphorylation is involved in the control of MAP65 binding to microtubules during the cell cycle. Phosphorylation is a common mechanism to control protein activity in a cell cycle dependent manner. AtMAP65-1 is phosphorylated at all stages of the cell cycle but hyperphosphorylated at prophase and metaphase. When a BY2 cell line expressing GFP: AtMAP65-1 was treated with the general protein kinase inhibitor, DMAP and the CDK specific inhibitor-olomoucine, GFP: AtMAP65-1 was bound to the metaphase spindle. Treatment with the phosphotase inhibitor, okadeic acid, caused progressive loss of the GFP signal in the phragmoplast midzone. These results suggest that the microtubule binding activity of MAP65-1 is regulated by phosphorylation. Kinase activity was found in the microtubule

protein preparation, indicating that these kinases are associated with microtubules. Interestingly, both CDK and MAP kinase have been found to associate with microtubules (Fellous *et al.*, 1994; Reszka *et al.*, 1995), and both kinases can phosphorylate AtMAP65-1 in vitro. Thus, several protein kinase pathways are involved in the control of MAP65-1 binding to microtubules and their cooperative activity is required for this control.

It has been suggested that the regulation of other plant MAPs activity affects the dynamics of microtubules through the cell cycle (Sedbrook., 2004) and several of these MAPs also show a cell cycle specific pattern of interaction with microtubules. For example a component of the MTOC, AtSpc98p, which is involved in the nucleation of microtubules, localizes at the nuclear surface and at the cell cortex (Erhardt *et al.*, 2002), but not on the mitotic microtubule arrays (Erhardt *et al.*, 2002). EB1 binds microtubule at the poles of the mitotic spindle, but not to the rest of the spindle microtubules (Chan *et al.*, 2003; Van *et al.*, 2004). MOR1/GEM1 localizes along the cortical microtubules and the phragmoplast midline (Twell *et al.*, 2002) where it might stabilize microtubules (Twell *et al.*, 2002). Moreover, it has been suggested that MOR1/GEM1 may interact with a microtubule destabilising kinesin-13 and compete for its binding site on the microtubule, preventing depolymerisation of microtubules induced by kinesin-13 (Hussey and Hawkins., 2001).

Besides MAP65 regulation mechanism discussed in this thesis, nothing is known

about regulation of other plant MAPs. In animal cells, the phosphorylation of MOR1/GEM1 homologue, *Xenopus* XMAP215, by CDK1 reduces its binding ability to microtubules. Although MOR1/GEM1 has several putative CDK phosphorylation sites (Hussey and Hawkins., 2001), it's still not clear whether phosphorylation controls MOR1/GEM1 functions (Whittington *et al.*, 2001). Animal EB1 has been found to interact with the carboxyl terminus of another MAP, adenomatous polyposis coli (APC) tumor suppressor protein (Su *et al.*, 1995; Wen *et al.*, 2004). The interaction between EB1 and APC controls functions of both proteins and has been implicated in the capturing and stabilization of microtubules *in vivo* (Wen *et al.*, 2004). Plants also have microtubule associated protein which is homologues to APC, TANGLED 1 (Smith *et al.*, 1996), and therefore might have a similar mechanism for the regulation of microtubule functions.

6.3.2 Identification of phosphorylation sites in AtMAP65-1

AtMAP65-1 was subdivided into four fragments (Fragment 1, amino acids 1-150; Fragment 2, amino acids 151-339; Fragment 3, amino acids 340-494; Fragment 4, 495-587). However, only Fragment 4 (residues 494-587) was phosphorylated by the mitotic protein extract or by the microtubule protein preparation. Therefore, all phosphorylation sites are localized in the C-terminal region of AtMAP65-1.

The phosphorylation motifs were predicted within Fragment 4 using bioinformatics. All together, nine potential phosphorylation motifs were found:

CDKs (S503, T526, S586), MAPK Erk1 (S543), Aurora B/cyclic nucleotide dependant kinase (S532, T552) and casein kinase 1 and II/PKC (S539, T573, S576). Mutation of these residues for non-phosphorylatable residues diminished the phosphorylation level of AtMAP65-1 to the interphase level, suggesting that these nine sites control activity of MAP65 during mitosis.

6.3.3 Dephosphorylation of MAP65-1 is necessary for microtubule binding/bundling

Phosphomimetics of AtMAP65-1 were produced in which potential phosphorylation residues were substituted for aspartic acid. All phosphor-mimetics except AtMAP65-1^{2D} had decreased microtubule binding activity, but the strongest effect was observed in AtMAP65-1^{9D} , where microtubule binding and bundling activity was decreased by 40% compared to the wild type. The FRAP data showed that the turnover of GFP: AtMAP65-1^{9D} is faster than wild-type and the amount of protein bound to microtubules *in vivo* was reduced by 40%, while decoration of the anaphase spindle midzone was almost abolished. All together, it suggests that dephosphorylation of MAP65-1 is necessary for its activity.

The phenotype of the GFP: AtMAP65-1^{9A} mutant also emphasizes the role of phosphorylation in the regulation of AtMAP65-1 activity. Live cell imaging revealed that microtubules in prophase and metaphase were decorated by GFP: AtMAP65-1^{9A} , alike in cells expressing GFP: AtMAP65-1 after treatment with

protein kinase inhibitors. Interestingly, GFP: AtMAP65-1^{9A} was bound just to the midzone of the metaphase spindle, causing an increase in pole to pole microtubule bundles and delayed mitosis.

6.4 Summary

The results of the work presented in this thesis demonstrate that MAP65 bundles microtubules *in vitro* and *in vivo.* It forms homodimers through the N-terminal domain and binds to microtubules through the C-terminal domain. Full length AtMAP65-1 is essential for efficient microtubule binding *in vivo*, while *in vitro* two distinct parts (Fragment 3: amino acids 340-494,and Fragment 4: 495-587) of AtMAP65-1 are able to bind microtubules. The GFP: AtMAP65-1 fusion protein expressed in tobacco BY 2 cells localizes to the interphase cortical microtubules, the PPB, the anaphase spindle, and the phragmoplast, whereas there is no metaphase spindle decoration. Live cell images traced AtMAP65-1 localization through the cell cycle and demonstrated a dynamic redistribution of AtMAP65-1 during the metaphase/anaphase formation and during cytokinesis. The midzone decoration of the anaphase spindle and the phragmoplast indicates that AtMAP65-1 might play an important role in these areas and that its function is to maintain phragmoplast structure. The interaction of AtMAP65-1 with microtubules is highly dynamic and is faster than tubulin turnover. Moreover, AtMAP65-1 is not translocated along microtubules, but can associate/disassociate randomly at any site along microtubules. The dynamics of AtMAP65-1 binding to microtubules do not change dramatically during the cell

cycle. Except for in metaphase, AtMAP65-1 does not bind to spindle microtubules, but diffuses around chromosomes. The highly dynamic binding of AtMAP65-1 to microtubules also proves that it is a good candidate for cross bridging microtubules as it organizes microtubules without affecting their dynamics. The cell cycle specific activity of AtMAP65-1 is not regulated by a destruction box, but is controlled by phosphorylation. Phosphorylation of AtMAP65-1 reduces binding and bundling of microtubules *in vitro* and *in vivo*, while expression of a non-phosphorylatable form of AtMAP65-1 induces excessive bundling of spindle microtubules and delays mitosis. Moreover, several protein kinase pathways including CDK and MAPK have been found to control the level of AtMAP65-1 phosphorylation and the combined activity of all these kinases is required for regulation of MAP65 activity.

To conclude, MAP65 cross-bridges microtubules and plays an important role in stabilizing the anaphase spindle and phragmoplast structure. In this way, MAP65 can provide a matrix for other proteins to localize to the division midzone and enable successive cytokinesis.

6.5 Future work

During the course of this work, a number of constructs containing GFP fusions with wild type AtMAP65-1 and its fragments and mutants were generated. First of all, wild type AtMAP65-1 and NtMAP65-1a are good markers of the cell division midzone and can be used to study dynamics of the cell plate formation

under normal conditions or after drug treatments. *Arabidopsis thaliana* plants expressing GFP: MAP65 fusion proteins can also be crossed with cell division mutants in order to analyze cell plate formation in the mutants. AtMAP65-1 phosphomimetics and AtMAP65-1^{9A} can be expressed in plants under constitutive or inducible promoter to analyze their effect on plant development.

Another prospect is the determination of what other proteins MAP65 interacts with. It has been shown that MAP65 homologue mammalian PRC1 interacts with a kinesin-4 family member-KIF4 (Kurasawa *et al.*, 2004). If interactions between MAP65 and some other proteins can also be found, this will help to establish which protein MAP65 cooperates with in mitosis.

Primers for the GFP: AtMAP65-1 construct

>AtMAP65-1
ATGGCGGTGACAGATACTGAAAGTCCTCATCTTGGGGAAATTACTTGTGGTACCTTACTTGAGAAGTTGCAGGAAATCTGGGA
TGAAGTTGGTGAGAGTGATGATGAACGAGACAAACTGCTTCTTCAGATAGAGCAAGAGTGTCTTGACGTTTACAAGAGAAAAG
TCGAGCAGGCTGCGAAATCCCGAGCTGAGCTTCTTCAAACCTTGTCAGATGCTAATGCTGAACTCTCCAGCCTCACAATGTCT
CTTGGAGACAAAAGCTTAGTTGGCATTCCGGATAAGTCTTCAGGAACGATTAAAGAACAACTTGCTGCAATAGCACCGGCTCT
TGAACAACTGTGGCAACAGAAAGAGGAGAGAGTCCGAGAGTTCTCTGATGTACAATCACAGATTCAGAAGATATGTGGAGAGA
TTGCTGGAGGTTTGAGCAATGAGGTTCCTATAGTCGATGAGTCTGATTTGTCACTGAAGAAATTAGACGATTTCCAGAGCCAA
CTCCAAGAGCTCCAGAAAGAAAAGAGTGACAGGCTGCGCAAGGTGTTAGAGTTTGTGAGTACTGTTCATGATCTATGTGCTGT
TCTTGGTTTGGATTTCTTAAGCACCGTCACCGAAGTTCATCCGAGCTTAGATGAAGATACCAGTGTCCAGTCTAAGAGCATTA
GCAATGAGACTCTTTCAAGGTTGGCTAAAACCGTCTTGACTCTTAAAGATGATAAGAAGCAAAGACTTCAAAAGCTTCAAGAG
CTGGCTACTCAGCTAATTGACCTGTGGAATCTGATGGATACTCCTGATGAGGAAAGAGAGCTTTTTGATCATGTTACCTGTAA
CATTTCATCTTCAGTCGATGAGGTCACTGTGCCAGGTGCTCTTGCACGTGATTTGATTGAGCAGGCTGAGGTGGAAGTTGATA
GGCTTGACCAGCTGAAAGCTAGCCGAATGAAAGAAATTGCGTTCAAGAAGCAATCTGAGCTTGAAGAGATATATGCTCGTGCC
CATGTAGAAGTTAACCCGGAATCTGCTCGTGAGAGAATCATGTCGCTGATTGATTCTGGAAACGTTGAGCCTACTGAATTATT
GGCAGACATGGATAGCCAGATATCAAAGGCTAAGGAAGAAGCATTTAGTAGAAAAGATATATTGGACCGAGTCGAGAAATGGA
TGTCAGCTTGTGAGGAAGAGAGCTGGCTAGAAGACTACAATCGGGATCAGAACAGGTACAGCGCAAGCAGAGGTGCACACTTG
AATCTCAAGAGAGCTGAGAAAGCTCGGATTCTGGTTAGCAAGATTCCTGCCATGGTTGACACATTAGTTGCCAAGACCCGGGC
TTGGGAAGAAGAACACAGCATGTCCTTTGCCTACGATGGTGTTCCTCTGCTAGCTATGCTAGACGAGTACGGTATGCTTAGGC
AAGAACGAGAAGAGGAGAAACGGAGGCTGAGGGAACAAAAGAAGGTTCAAGAACAGCCACATGTAGAGCAAGAATCTGCCTTT
AGCACCAGGCCAAGCCCTGCAAGACCGGTCAGTGCTAAGAAAACGGTGGGGCCACGAGCTAACAACGGAGGAGCCAATGGAAC
ACATAACCGGCGTTTATCTTTGAATGCAAACCAGAATGGAAGCAGGTCTACTGCAAAAGAAGCAGGGAGAAGGGAGACTCTCA
ACAGGCCGGCTGCTCCTACAAACTACGTTGCCATTTCGAAAGAGGAAGCTGCTTCATCTCCAGTTTCTGGTGCTGCAGATCAT
CAAGTTCCAGCTTCACCATGATTGATAGTTGTA

Forward primer (At651GFPf): AA CTCGAG ATGGCGGTGACAG
XhoI

Reverse primer (At651GFPTermR): T GAATTC TCATGGTGAAGCTGG
EcoRI

Primers for AtMAP65-1 protein fragments

Forward primer 1(TR1): A CATATG GCG GTGACAGATACTGA

Reverse primer 1(TR1r): TCTCGAGTCAGACTATAGGAACCTCATTGCT

Forward primer 2 (TR2F): ACATATGAGCAATGAGGTTCCTATAGTC

Reverse primer 2 (TR2R): TCTCGAGTCACATGATTCTCTCACGAGCAG

Forward primer 3 (TR3F): ACATATGTCTGCTCGTGAGAGAATCATG

Reverse primer 3 (TR3R): TCTCGAGTCATTGCTCTACATGTGGCTGTTC

Forward primer 4 (TR4F): ACATATGGAACAGCCACATGTAGAGCAA

Reverse primer 4 (TR4R): TCTCGAGTCATGGTGAAGCTGGAACTTG

Primers for the AtMAP65-1 mutagenesis PCR

Original sequences: CAG AAC AGG TAC AGC GCA AGC AGA GGT GCA CAC TTG (underline shows the mutation position)

*Ala 409 to Asp

Forward primer (At409Af): CAG AAC AGG TAC AGC GAT AGC AGA GGT GCA CAC TTG

Reverse primer (At409Ar): CAA GTG TGC ACC TCT GCT ATC GCT GTA CCT GTT CTG

*Ala 420 to Val

Original sequences: CAC TTG AAT CTC AAG AGA GCT GAG AAA GCT CGG ATT CTG

Forward primer (At420Vf):CAC TTG AAT CTC AAG AGA GTT GAG AAA GCT CGG ATT CTG

Reverse primer (At420Vr): CAG AAT CCG AGC TTT CTC AAC TCT CTT GAG ATT CAA GTG

Primers for the GFP: AtMAP65-1 fragments

*At651GFPf: AA CTCGAG ATGGCGGTGACAG
XhoI

*TR2f-NGFP: A CTCGAG ATG AGCAATGAGGTTCCTATAGTC
Xho1

*TR3r-NGFP: T GAATTCTCATTGCTCTACATGTGGCTG
EcoRI

* At651GFPTermR: T GAATTC TCATGGTGAAGCTGG
EcoRI

Primers for GFP: AtMAP65-1 phosphorylation site multi-mutagenesis PCR

S503D: AGCACCAGGCCAGACCCTGCAAGACCG

S542D: AACCGGCGTTTAGATTTGAATGCAAAC

S586D: CAAGTTCCAGCTGATCCATGAGAATTC

T528D: CGGAGGAGCCAATGGAGATCATAACCGGCGTTTAGATTTG

T552D: AAAGAAGCAGGGAGAAGGGAGGATCTCAACAGGC

D539/543: TGCAAACCAGAATGGAGACAGGTCTGATGCAAAAGAAGCAGGGA

D573/576: AAGAGGAAGCTGCTTCAGATCCAGTTGATGGTGCTGCAGATCATC

S503A: AGCACCAGGCCAGCCCCTGCAAGACCG

S542A: AACCGGCGTTTAGCTTTGAATGCAAAC

S586A: CAAGTTCCAGCTGCACCATGAGAATTC

T526A: GGAGCCAATGGAGCACATAACCGGCGTTTATCTTTG

T552A: AAAGAAGCAGGGAGAAGGGAGGCTCTCAACAGG

A573/576: AAGCTGCTTCAGCTCCAGTTGCTGGTGCTGCAGATC

A539/543: TGCAAACCAGAATGGAGCCAGGTCTGCTGCAAAAGAAGCAGGG

Primers for the GFP: NtMAP65-1 construct

>NtMP651 coding sequence only
ATGGCAGAAGCAGATGCTCAAGCTCCTGTTCTTGACGAAACAACTTGCGGTTCCCTACTACAAAAGCTGCAG
CAAATTTGGGATGAGGTCGGTGAAACTGATGATGAGCGGGACAATATGCTTCTTCAGATAGACCAAGAGTGC
CTGGATGTCTACAAGAGAAAGGTTGACCAGGCTGTGAAGTCACGGGCTCACCTTCTTCAGGCATTGGCAGAT
GCCAAAGTTGAACTCTCCAGGCTGCTATCAGCCCTGGGAGAGAAGACATATGTTGGAATTCCTGAGAAGACT
TCAGGTACAATCAAGGAACAGCTTGCAGCTATAGCACCAGCACTGGAAAAACTGTGGGAGCAGAAAGATGAT
AGGATAAAAGAGTTTTTTGATGTGCAATCACAAATTCAGAAGATAAGCAGTGAGATTGCAGGAACTCGCGAG
CAAGTTGAGAGTCTTACAGTGGACGAATCTGATTTATCTCTTAAAAAGTTGGATGAGTTTCAGGCACAGCTT
CAAGAGCTCCAAAAAGAGAAGAGTGAGAGACTACAGAAGGTCCTTGAACTTGTGAGTACCGTGCATGACCTT
TGTGCTGTTCTTGGCATGGACTTCTTCAGTACTGTCACAGAAGTTCACCCAAGCCTGAATGATTCAACTGGT
GTACAGTCAAAAAGTATTAGCAATGATACTCTGTCAAGTCTGGCTAAAACTGTCTTAGTATTAAAGGAGGAT
AAGAAGCAGAGATTGCATAAGCTTCAAGAGTTAGCAACTCAGCTAATCGATTTATGGAATTTGATGGATACC
CCAGAAGAAGAAAGGAGCTTGTTTGACCATGTTACCTGCAACATATCAGCTTCAGTAGATGAAGTGGCCATT
CCAGGGGCTCTTGCTCTTGATCTGATTGAACAGGCTGAAGTAGAAGTTGAAAGGCTTGATCAACTAAAAGCT
AGCAAGATGAAGGAGATTGCTTTCAAAAGGCAGGCTGAACTGGAAGACATTTATGCTCGTGCCCACGTAGAG
ATTGATACGGAGGCTGCTCGAGAAAAAATTATGGCACTGATCGATTCTGGGAATGTTGATCCTGCAGAGTTA
CTAGCTGACATGGACAATCAGATTGTAAATGCAAAAGAAGAGGCTCATAGCAGGAAAGAAATATTGGATAAA
GTTGAGAAATGGATGGCAGCTTGTGAAGAAGAGAGCTGGCTTGAAGACTACAACAGGGACGACAACCGATAT
AATGCAAGTAGAGGAGCACACTTAAATTTGAAGAGGGCTGAAAAGGCTCGGATATTGGTCAACAAAATTCCA
GCTCTTGTGGACTCCTTGGTTGCAAAAACCAGAGCATGGGAGCAAGAGCGAGACACCACATTCACTTATGAT
GGCGTTCCACTACTTGCCATGCTAGATGAATATATGATGCTCAGGCACGACAGAGAAGAAGAGAAAAGAAGG
TTGAGGGACCAGAAGAAGTTCCATGAGCAGATAAGCAAAGAAGAAACAGTATTTGGATCAACGCCAAGCCCT
GCTCGACCACTTGGTCCAAAGAAGGTAACAGGCCCACGAGCAAATGGCAGTGCCAATGGGCCGACAAGCAGA
AGGCTGTCACTTAATTCCCACCAAAACGGTTCCAGGTCAACTAATAAAGATGGGAAGAGAGACACCAGACCA
ATTGCTCCTCTGAACTATGTTGCCATGACAAAGGATGATGCAGCCTCTCACATTTCTGGAAGTGAGCATAGT
CCTAGCACACCTTAG

Primers for NtMAP65-1a D-BOX mutagenesis

Original: CCGACAAGCAGAAGGCTGTCACTTAATTCCCACCAA

Forward primer (HSY5):
CCGACAAGCAGAGCGCTGTCAGCTAATTCCCACCAAAACGG

Reverse primer (HY6):
CCGTTTTGGTGGGAATTAGCTGACAGCGCTCTGCTTGTCGG

SM-GFP sequences

GGATCCAAGGAGATATAACAATGAGTAAAGGAGAAGAACTTTTCACTGGAGTTGTCCCAATTCTTGT
TGAATTAGATGGTGATGTTAATGGGCACAAATTTTCTGTCAGTGGAGAGGGTGAAGGTGATGCAACA
TACGGAAAACTTACCCTTAAATTTATTTGCACTACTGGAAAACTACCTGTTCCATGGCCAACACTTGT
CACTACTTTCTCTTATGGTGTTCAATGCTTTTCAAGATACCCAGATCATATGAAGCGGCACGACTTCT
TCAAGAGCGCCATGCCTGAGGGATACGTGCAGGAGAGGACCATCTCTTTCAAGGACGACGGGAACT
ACAAGACACGTGCTGAAGTCAAGTTTGAGGGAGACACCCTCGTCAACAGGATCGAGCTTAAGGGAA
TCGATTTCAAGGAGGACGGAAACATCCTCGGCCACAAGTTGGAATACAACTACAACTCCCACAACGT
ATACATCACGGCAGACAAACAAAAGAATGGAATCAAAGCTAACTTCAAAATTAGACACAACATTGA
AGATGGAAGCGTTCAACTAGCAGACCATTATCAACAAAATACTCCAATTGGCGATGGCCCTGTCCTT
TTACCAGACAACCATTACCTGTCCACACAATCTGCCCTTTCGAAAGATCCCAACGAAAAGAGAGACC
ACATGGTCCTTCTTGAGTTTGTAACAGCTGCTGGGATTACACATGGCATGGATGAACTATACAAATA
AGAGCTC

References

Angeles, T. S., Yang, S. X., Steffler, c., Dionne, C. A. (2002): Kinetics of trkA Tyrosine Kinase Activity and Inhibition by K-252a. Arch. Biochem. Biophys. 349(2):267-274.

Arioli, T., Peng, L., Betzner, A.S., Burn, J., Wittke, W., Herth, W., Camilleri, C., Hofte, H., Plazinski, J., Birch, R., Cork, A., Glover, J., Redmond, J., Williamson, R.E. (1998): Molecular analysis of cellulose biosynthesis in *Arabidopsis*. Science 279:717–720.

Asada, T. and Shibaoka, H. (1994): Isolation of polypeptides with microtubule translocating activity from phragmoplasts of tobacco by-2 cells. Journal of Cell Science **107**, 2249-2257.

Austin, J.R. 2nd, Segui-Simarro, J.M., Staehelin, L.A. (2005): Quantitative analysis of changes in spatial distribution and plus-end geometry of microtubules involved in plant-cell cytokinesis. J Cell Sci. **118**:3895-903.

Azimzadeh, J., Traas, J. and Pastuglia, M. (2001): Molecular aspects of microtubule dynamics in plants. Current Opinion in Plant Biology **4**, 513-519.

Barroco, R.M., De, Veylder. L., Magyar, Z., Engler, G., Inze, D., Mironov, V. (2003): Novel complexes of cyclin-dependent kinases and a cyclin-like protein from Arabidopsis thaliana with a function unrelated to cell division. Cell Mol Life Sci. **60**:401-12

Barroso C, Chan J, Allan V, Doonan J, Hussey P, Lloyd C. (2000) Two kinesin-related proteins associated with the cold-stable cytoskeleton of carrot cells: characterization of a novel kinesin, DcKRP120-2. Plant J. **24**:859-68.

Barthels, N., van der Lee, F.M., Klap, J, Goddijn, O.J.M., Karimi, M., Puzio, P., Grundler, F.M.W., Ohl, S.A., Lindsey, K., Robertson, L., Robertson, W.M., Van Montagua M., Gheysen, G. and Sijmons P.C. (1997): Regulatory sequences of arabidopsis drive reporter gene expression in nematode feeding structures. Plant Cell **9**, 2119-2134.

Bogre, L., Calderini, O., Binarova, P., Mattauch, M., Till, S., Kiegerl, S., Jonak, C., Pollaschek, C., Barker, P., Huskisson, N.S., et al (1999): A MAP kinase is activated late in plant mitosis and becomes localized to the plane of cell division. Plant cell **11**: 101-113.

Bowser, J. and Reddy, A.S.N. (1997): Localization of a kinesin-like calmodulin-binding protein in dividing cells of Arabidopsis and tobacco. Plant Physiology **114**,1417-1417.

Bulinski, J.C., Odde, D.J., Howell, B.J., Salmon, T.D. and Waterman-Storer, C.M. (2001): Rapid dynamics of the microtubule binding of ensconsin in vivo. J. Cell Sci. **114**, 3885-3897.

Burns, R.G. and Surridge, C.D. (1994): Tubulin: conservation and structure. In: *Microtubules*, (ed. J.S. Hyams and C.W Lloyd), pp. 3-31. New York: Wiley-Liss.

Cullen, C.F., Deak, P., Glover, D.M., Ohkura, H.(1999): mini spindles: A gene encoding a conserved microtubule-associated protein required for the integrity of the mitotic spindle in Drosophila. J Cell Biol. **146**:1005-18.

Garcia, M.A., Vardy, L., Koonrugsa, N., Toda, T.(2001): Fission yeast ch-TOG/XMAP215 homologue Alp14 connects mitotic spindles with the kinetochore and is a component of the Mad2-dependent spindle checkpoint. EMBO J. **20**:3389-401.

Goddard, R. H., Wick, S. M., Silflow, C. D., Snustad, D. P. (1994): Microtubule components of the plant cell cytoskeleton. Plant Physiol, **104**:1-6

Buschmann, H., Fabri, C.O., Hauptmann, M.,Hutzler P., Laux, T., Lloyd, C. W., and Schaffner, A. R.(2004): Helical growth of the Arabidopsis mutant tortifolial reveals a plant specific microtubule-associated protein. Curr. Biol. **14**, 1515-1521.

Calderini, O., Glab, N., Bergounioux, C., Heberle-Bors, E., and Wilson, C. (2001): A novel tobacco mitogen-activated protein (MAP) Kinase kinase, NtMEK1, activates the cell cycle-regulated p43Ntf6 MAP kinase. *J. Biol. Chem.* **276**: 18139-18145.

Chan, J., Rutten, T. and Lloyd, C. (1996): Isolation of microtubule-associated proteins from carrot cytoskeletons: A 120 kDa map decorates all four microtubule arrays and the nucleus. Plant J. **10**; 251-259.

Chan, J., Calder, G.M., Doonan, J.H. and Lloyd, C.W. (2003): EB1 reveals mobile microtubule nucleation sites in *Arabidopsis*. Nat. Cell Biol. **5,** 967-971.

Chan, J., Jensen, C.G., Jensen, L.C.W., Bush, M., and Lloyd, C.W. (1999): The 65-kDa carrot microtubule-associated protein forms regularly arranged filamentous cross-bridges between microtubules. Proc. Natl. Acad. Sci. USA **96**, 14931-14936.

Chan, J., Calder, G.M., Doonan, J.H. and Lloyd, C.W. (2003a): EB1 reveals mobile microtubule nucleation sites in *Arabidopsis*. Nat. Cell Biol. **5,** 967-971.

Chan, J., Mao, G., Smertenko, A., Hussey, P.J., Naldrett, M., Bottrill, A., and Lloyd, C.W. (2003b): Identification of a MAP65 isoform involved in directional expansion of plant cells. FEBS Lett. **534**, 161-163.

Chang, H. Y., Smertenko, A.P., Igarashi, H., Dixon, D. P., Hussey, P. J. (2005): Dynamic interaction of NtMAP65-1a with microtubules in vivo. Journal of Cell Science **118**, 3195-3201.

Charrasse, S., Schroeder, M., Gauthier-Rouviere, C., Ango, F., Cassimeris, L., Gard, D.L., Larroque, C.(1998): The TOGp protein is a new human microtubule-associated protein homologous to the Xenopus XMAP215. J Cell Sci. **111**:1371-83.

Chen, C., Marcus, A., Li, W., Hu, Y., Calzada, J. P., Grossniklaus, U., Cyr, R. J., Ma, H.(2002): The arabidopsis ATK1 gene is required for spindle morphogenesis in male meiosis. Development **129**,2401-2409.

Chen, A., Gibson, T.B., Robinson, F., Silvestro, L., Pearson, G., Xu, B., Wright, A., Vanderbilt, C., and Cobb, M. H. (2001): MAP kinase. Chem. Rev. **101**:2449-2476.

Cleary, A.L., Smith L.G. (1998): The tangled 1 gene is required for spatial control of cytoskeleton arrays associated with cell division during maize leaf development. Plant cell. **10**:1875-1888.

Clough, S.J., and Bent, A.F. (1998): Floral dip: a simplified method for *Agrobacterium*-mediated transformation of *Arabidopsis thaliana*. Plant J. **16**, 735-743.

Compton D. A. (2000): Spindle assembly in animal cells. Annu Rev Biochem. **69**:95-114.

Dagenbach, E. M., Endow S. A. (2004): A new kinesin tree. J. Cell Sci.,**117**, 3-7.

Dhonukshe, P, Gadella TWJ (2003): Alteration of microtubule dynamic instability during preprophase band formation revealed by yellow fluorescent protein-CLIP170 imcortubule plus –end labeling. Plant Cell, **15**:596-611.

Doi, Y., Higashida, M. and Kido, S. (1987): Plasma gelsolin binding sites on the actin sequence. Eur. J. Biochem. **164**, 89-94.

Dong, C.-H., Xia, G-X., Hong, Y., Ramachandran, S., Kost, B.& Chua, N.-H. (2001): ADF proteins are involved in the control of flowering and regulate F-actin organization , cell expasion, and organ growth in *Arabdopsis*. Plant cell **13**, 1-15

Compton D. A. (2000): Spindle assembly in animal cells.

Eleftheriou, E. P., Baskin T. I., Hepler P. K. (2005): Aberrant cell plate formation in the Arabidopsis thaliana microtubule organization 2 mutant. Plant cell physiol.

Endwo, S. A. (1999): Determinants of molecular motor directionality. Nat. Cell Biol. **1**, E163-E167.

Erhardt, M., Stoppin-Mellet V., Campagne S., Canaday J., Muteerer J., Fabian T., Sauter M., Muller T., Peter C., Lambert A. M., and Schmit A. C., (2002): The plant Spc98p homologue colocalizes with γ-tubulin at microtubule nucleation sites and is required for microtubule nucleation. Journal of cell science **115**, 2423-2431.

Euteneuer, U., Jackson, W.T., McIntosh, J.R. (1982): Polarity of spindle microtubules in Haemanthus endosperm. J Cell Biol. **94**:644-53.

Fang, G., Yu, H. and Kirshner, M.W. (1998): Direct binding of CDC20 protein family members activates the anaphase-promoting complex in mitosis and G1. Mol. Cell **2**:163-171.

Fellous A, Kubelka M, Thibier C, Taieb F, Haccard O., Jessus C (1994) Association of p34(cdc2) kinase and map kinase with microtubules during the meiotic maturation of xenopus oocytes. Int. J. Dev. Biol. **38**, 651-659.

Filonova, L.H., Bozhkov, P.V., and Von Arnold, S., (2000): Developmental pathway of somatic embryogenesis in Picea abies as revealed by time-lapse tracking. J. Exp Bot. **51**:249-64.

Filonova, L.H., Von Arnold, S., Daniel, G., and Bozhkov, P.V. (2002): Programmed cell death eliminates all but one embryo in a polyembryonic plant seed. Cell Death and Differentiatoin **9**: 1057-1062.

Fisher, D.D. & Cyr, R. J. (1998): Extending the microtubule/microfibril paradigm-Cellulose synthesis is required for normal cortical microtubule alignment in elongating cells. Plant Phsiology **116**, 1043-1051.

Fischer, J.A. (2000): Molecular motors and developmental asymmetry. Curr. Opin. Genet. Dev. **10**, 489-496.

Fiammetta, V., Somma, M.P., Gunsalus, K.C., Bonaccorsi, S., Belloni, G., Goldberg, M. L., and Gatti, M. (2004): Feo, the *Drosophila* homolog of PRC1, is required for central-spindle formation and cytokinesis. Current Biology, **14**, 1569-1575.

Furutani, L., Watanabe Y., Prieto R., Masukawa M., Suzuki K., Naoi K., Thitamadee S., Shikanai T., and Hashimoto T. (2000): The SPIRAL genes are required for directional central of cell elongation in Arabidopsis thaliana. Development **127**, 4443-4453.

Gachet, Y., Tournier, S., Millar, J. B. A., Hyams, J.S. (2001): A MAP kinase-dependent actin checkpoint ensures proper spindle orientation in fission yeast. Nature **12**,352-355.

Ganem, N.J., Upton, K., and Compton, D. A. (2005): Efficient mitosis in human cells lacking pole ward microtubule flux. Current Biology 15: 1827-1832.

Gard, D.L. and Kirschner, M.W. (1987): A microtubule-associated protein from Xenopus eggs that specifically promotes assembly at the plus-end. Journal of Cell Biology **105**: 2203-2215.

Gardiner, J and Marc, J. (2003): Putative microtubule-associated proteins from the *Arabidopsis* genome. Protoplasma **222**, 61-74.

Geelen, D.N.V. and Inze' D.G. (2001): A bright future for the BrightYellow-2 cell culture. Plant Physiol. **127**, 1375–1379.

Giddings,T.H., Staehelin,L.A.(1991):Microtubule-mediated control of microfibril deposition; a re-examination of the hypothesis. In: Lloyd CW (eds) The cytoskeletal basis of plant growth and form. Academic, San Diego, CA, pp 85–100

Glotzer, M., Murray, A.W,, Kirschner, M.W. (1991): Cyclin is degraded by the ubiquitin pathway. Nature **349**:132-8.

Graf R, Daunderer C, Schliwa M.(2000): Dictyostelium DdCP224 is a microtubule-associated protein and a permanent centrosomal resident involved in centrosome duplication. J Cell Sci. **113**:1747-58.

Graves, L.M., Guy, H.I., Kozlowski, P., Huang, M., Lazarowski, E., Pope, R.M., Collins, M.A., Dahlstrand, E.N., EarpIII, H.S., and evans, D.R. (2000): Regulation of carbamoyl phosphate synthetase by MAP kinase. Nature **403**: 328-332.

Grishchuk, E. L., Molodtsov, M.I., Ataullakhanov, F. I., and McIntosh, J. R. (2005): Force production by disassembling microtubules. Nature **438**:384-388.

Green,P.B.(1962): Mechanism for plant cellular morphogenesis. Science 138:1404–1405

Gunawardane R. N., Martin O. C., Cao K., Zhang K., Iwamatsu D. A., and Zheng Y. (2000): Characterization and reconstitution of *Drosophila* gamma-tubulin ring complex subunits J. Cell Bol. **151**, 1513-1523.

Hamada, T., Igarashi H., Ttoh T. J., Shimmen T., and Snobe S. (2004): Characterization of a 200kDa microtubule-associated protein of tobacco BY-2 cells, a member of the XMAP215/MOR1 family. Plant Cell Physiol.**45**, 1233-1242.

Hashimoto, T. (2002): Molecular genetic analysis of left-right handedness in plants. Philos Trans R Soc Lond B Biol Sci. **357**,799-808

Havlicek L, Hanus J, Vesely J, Leclerc S, Meijer L, Shaw G, Strnad M (1997) :Cytokinin-derived cyclin-dependent kinase inhibitors: synthesis and cdc2 inhibitory activity of olomoucine and related compounds. J. Med. Chem. 40(4):408-12

Hayden, J.H., Bowser, S.S., Rieder, C.L. (1990): Kinetochores capture astral microtubules during chromosome attachment to the mitotic spindle: direct visualization in live newt lung cells. J Cell Biol. **111**:1039–1045.

Heald, R., Tournebize, R., Blank, T., Sandaltzopoulos, R., Becker, P., Hyman, A., Karsenti, E. (1996): Self-organization of microtubules into bipolar spindles around artificial chromosomes in Xenopus egg extracts. Nature. **382**:420-5.

Heald, R., Tournebize, R., Habermann, A., Karsenti, E., Hyman, A. (1997): Spindle assembly in Xenopus egg extracts: respective roles of centrosomes and microtubule self-organization. J Cell Biol. **138**:615-28

Heidemann SR, McIntosh JR. (1980): Visualization of the structural polarity of microtubules. Nature **286**:517-9.

Hoshino, H., Yoneda, A., Kumagai, F., and Hasezawa, S. (2003) Role of actin-depleted zone and preprophase band in determining the division site of higher-plant cells, a tobacco BY-2 cell line expressing GFP-tubulin. Protoplasma **222**,157-165.

Horio, T. and Hotani, H. (1986): Visualization of the dynamic instability of individual microtubules by dark-filed microscopy. Nature, **321**:605-607.

Hulskamp, M., Misra, S., Jurgens, G. (1994) Essential role of a kinesin-like protein in Arabidopsis trichome morphogenesis. Cell **76**:555-66.

Hush, J.M, Wadsworth, P., Callaham, D.A. and Hepler, P.K. (1994): Quantification of microtubule dynamics in living plant cells using fluorescence redistribution after photobleaching. J Cell Sci. **107**, 775-784.

Hussey, P.J., Hawkins, T.J., Igarashi, H., Kaloriti, D., and Smertenko, A. (2002): The plant cytoskeleton: recent advances in the study of the plant microtubule-associated proteins MAP-65, MAP-190 and the *Xenopus* MAP215-like protein, MOR1. Plant Mol

Biol. **50**, 915-924.

Hussey, P.J. (2004): The plant cytoskeleton in cell differentiation and development. (Blackwell Publishing).

Hyams, J. S. and Lloyd, C. W. (1993): *Microtubules* . Wiley-liss, New York. 439pp. Nature, **312**:237-242

H. Yasuhara, S. Sonobe and H. Shibaoka (1993): Effects of taxol on the development of the cell plate and of the phragmoplast in tobacco BY-2 cells. Plant Cell Physiol. **34**:21-29.

Ichimura, K., shinozaki, K., Tena, G., Sheen, J., Henry, Y., Champion, A., Kreis, M., Ahang, S., Hirt, H., Wilson, C., et al. (2002) Mitogen-activated protein kinase cascades in plants: A new nomenclature. Trends Plant Sci. 7:301-308.

Igarashi, H., Orii, H., Mori, H., Shimmen, T. and Sonobe, S. (2000): Isolation of a novel 190 kDa protein from tobacco BY-2 cells:possible involvement in the interaction between actin filaments and microtubules. Plant Cell Physiol. **41**:920-931.

Irigoyen, J. P., Besser, D., Nagamine, Y. (1997): Cytoskeleton reorganization induces the urokinase-type plasminogen activator gene via Ras/Extracellular singal-regulated kinase (ERK) singnaling pathway. Journal of biological chemistry **272**, 1904-1909.

Isabelle, L., Jame S., Thanuja Gangi-Setty, Nam-Phuong T Nguyen, Anne Paoletti, and P. T. Tran (2005): Ase1p organizes anti-parallel microtubule arrays during interphase and mitosis in fission yeast. Mol Biol Cell.

Ishikawa, M., Soyano, T., Nishihama, R., Machida, Y. (2002): The NPK1 mitogen-activated protein kinase kinase kinase contains a functional nuclear localization signal at the binding site for the NACK1 kinesin-like protein. Plant J. **32**:789-98.

Itoh, T. J. and Hotani, H. (1994):Mirotubule-stabilizing activity of mirotubule-associated protein (MAPs) is due to increase in frequency of rescue in dynamic instability: shortening length decrease with binding of MAPs onto microtubules. Cell Struct. Funct., **19**:279-290.

Janson ME, Setty TG, Paoletti A, Tran PT. (2005): Efficient formation of bipolar microtubule bundles requires microtubule-bound gamma-tubulin complexes. J Cell Biol. **169**:297-308.

Jeffrey, P.D., Russo, A.A., Polyak, K., Gibbs, E., Hurwitz, J., Massague, J., Pavletich, N.P. (1995): Mechanism of CDK activation revealed by the structure of a cyclinA-CDK2 complex
Nature. **376**:313-20.

Jiang, C. J. and Sonobe, S., (1993): Identification and preliminary characterization of a 65 kDa higher-plant microtubule-associated protein. J. Cell Sci. **105**: 891-901.

Jiang, W., Jimenez, G., Wells, N.J., Hope, T.J., Wahl, G. M., Hunter T. and Fukunaga, R. (1998): PRC1: a human mitotic spindle associated CDK substrate protein required for cytolinesis. Mol. Cell **2**:877-885.

Joubes, J., Chevalier, C., Dudits, D., Heberle-Bors, E., Inze, D., Umeda, M., Renaudi, J.P. (2000): CDK-related protein kinases in plants. Plant Mol Biol. **43**:607-20.

Jonak, C., Okresz, L., Bogre, L., and Hirt, H., (2002) NPK, an MEKK1-like mitogen-activated protein kinase kinase kinase, regulates innate immunity and development in plants. Curr., Opin. plant Biol. **5**:415-424.

Juang, Y-L., Huang, J., Peters, J.-M., Mclaughlin, M.E., Tai, Ch. –Y. and Pellman, D. 1997. APC-mediated proteolysis of Ase1 and the morphogenesis of the mitotic spindle. Nature **275**:1311-1314.

Khodjako A., and Kapoor, T. (2005): Microtubule flux: what is it good for? Current Biology 15: 966-969.

King, R.W., Glotzer, M., and Kirschner, M.W. (1996): Mutagenic analysis of the destruction signal of mitotic cyclins and structural characterization of ubiquitintaed intermediates. Mol. Biol. Cell **7**: 1343-1357.

Korolev, A. V., Chan, J., Naldrett, M. J., Doonan, J. H., and Lloyd C. W.(2005): Idetification of a novel family of 70kDa microtubule-associated proteins in Arbidopsis cells. The Plant Journal **42**, 547-555.

Knop, M., and Schiebel, E. (1997): Spc98p and Spc97p of the yeast γ-tubulin complex mediate binding to the spindle pole body via interaction with Spc110p. EMBO J.**16**, 6985-6995.

Kreis, T. and Vale, R. (1993): Guide book to the cytoskeletal and motor proteins. Oxford University Press.

Kurasawa, Y., Earnshaw, W.C., Mochizuki, Y., Dohmae, N. and Todokoro, K. (2004): Essential roles of KIF4 and its binding partner PRC1 in organized central spindle midzone formation. EMBO J. **23**, 3237-3248.

Ledbetter MC, Porter KR (1963): A "microtubule" in plant cell fine structure. J. Cell Biol. 19:239–250

Lee, Y.R.J. and Liu, B. (2000): Identification of a phragmoplast-associated kinesin-related protein in higher plants. Current Biology **10**, 797-800.

Lee, Y.R.J. and Lui, B. (2004): Cytoskeletal motors in Arabidopsis. Sixty-one kinesins and seventeen myosins. Plant Physiology **136**, 3877-3883.

Lee, Y.R.J., Giang HM, Liu B. (2001): A novel plant kinesin-related protein specifically associates with the phragmoplast organelles. Plant Cell. **13**(11):2427-39.

Lloyd, C. and Hussey, P. (2001): Microtubule-associated proteins in plants:why we need a MAP. Nature Rev. **2**:40-47.

Lloyd, C.W., Hussey, P.J. and Chan, J. (2004): Microtubules and microtubule-associated proteins. In The plant cytoskeleton in cell differentiation and development, P.J.Hussey, ed (Blackwell Publishing), pp. 3-31.

Maddox, P., Straight, A., Coughlin, P., Mitchison, T. J. and Salmon, E. D. (2003). Direct observation of microtubule dynamics at kinetochores in *Xenopus* extract spindles: implications for spindle mechanics. J. Cell Biol. **162**, 377-382

Margolis, R. L. and Wilson, L. (1981): Microtubule treadmills: possible molecular machinery. Nature **293**, 705-711

Mao, T., Jin L., Li H., Liu B., Yuan M. (2005): Two microtubule-associated proteins of the Arabidopsis MAP65 family function differently on microtubules.Plant physiology.

Mao, G., Chan, J., Calder, G., Doonan, J. H., and Lloyd, C.W.(2005): Modulated targeting of GFP-AtMAP65-1 to central spindle microtubules during division. The plant Journal **43**, 469-478.

Marcus, A. I., Li, W., Ma, H., and Cyr, R. J. (2002): A kinesin mutant with an atypical bipolar spindle undergoes normal mitosis. Mol. Bio. of the Cell **14**, 1717-1726.

Marcus, A.I., Dixit, R., and Cyr, R.J. (2005) Narrowing of the preprophase microtubule band is not required for cell division plane determination in cultured plant cells. Protoplasma **226**:169-174.

Mathur J., Mathur N., Kernebeck B., Srinivas B. P., Hulskamp M. (2003): A novel localization pattern for an EB1-like protein links microtubule dynamics to endomembrane organization. Curr. Biol., **13**, 1991-1997.

Martin, O. C., Gunawardane, R. N., Iwamatsu, A. and Zheng, Y. (1998): Xgrip 109: a γ-tubulin associated protein with an essential role in γ-tubulin ring complex (γ-TuSC) assembly and centrosome function. J. Cell. Biol. **141**. 675-687.

Masahide Sawano, Teruo Shimmen and Seiji Sonobe, (2000): Possible involvement of 65 kDa MAP in Elongation growth of Azuki bean Epicotyls. Plant cell physiol. **41**:968-976.

Mastronarde, D.N., McDonald, K.L., Ding, R., McIntosh, J.R. (1993): Interpolar spindle microtubules in PTK cells. J Cell Biol. **123**:1475-89.

McNally, F.J., Vale, R.D. Identification of katanin, an ATPase that severs and disassembles stable microtubules. Cell **75**:419-29.

Menges, M., Hennig L., Gruissem, W. and Murrey J.A.H (2003): Genome-wide gene expression in an *Arabidopsis* cell suspension. Plant Mol. Biol. **53**, 423-442.

Merdes A, Heald R, Samejima K, Earnshaw WC, Cleveland DW. (2000): Formation of spindle poles by dynein/dynactin-dependent transport of NuMA. J Cell Biol. **149**:851-62.

Mineyuki, Y. & Gunning, B.E.S. (1990): A role for preprophase band of microtubules in maturation of new cell walls, and a general proposal on the function of preprophase band sites in cell-division in higher-plants. Journal of Cell Science **97**, 527-537.

Mineyuki, Y. (1999) the preprophase band of microtubules: its function as a cytokinetic apparatus in higher plants. Int. Rev. Cytol. 187:1-49.

Minshull, J., Sun, H., Tonks, N.K., and Murray, A. W. (1994) A MAPkinase-dependent spindle assembly checkpoint in *Xenopus* egg extracts. Cell **79**:475-486.

Mitchison, T. and Kirschner, M. (1984): Dynamic instability of microtubule growth. Nature **312**: 237-242.

Mitchison, T., Evans, L., Schulze, E., and Kirschner, M. (1986): Sites of microtubule assembly and disassembly in the mitotic spindle, Cell **45**:515–527

Mitsui, H., Yamaguchi-Shinozaki K., Shinozaki, K., Nishikawa, K., Takahashi, H. (1993): Identification of a gene family (kat) encoding kinesin-like proteins in arabidopsis thaliana and the characterization of secondary structure of KatA. Mol. Gen. Genet. **238**, 362-368.

Mollinari, C., Kleman, J.P., Jiang, W., Schoehn, G., Hunter, T., and Margolis, R.L. (2002): PRC1 is a microtubule binding and bundling protein essential to maintain the mitotic spindle midzone. J. Cell Biol. **157**, 1175-1186.

Molodtsov MI, Grishchuk EL, Efremov AK, McIntosh JR, Ataullakhanov FI.(2005): Force production by depolymerizing microtubules: a theoretical study. Proc Natl Acad Sci U S A. **102**:4353-8.

Moore, R.C., Zhang, M., Cassimeris, L. and Cyr, R.J. (1997): In vitro assembled plant

microtubules exhibit a high state of dynamic instability. Cell Motil. Cytoskel. **38**: 278-286.

Morgan, D.O. (1995): Principles of CDK regulation. Nature. **374**:131-4.

Müller, S., Fuchs, E., Ovecka, M., Wysocka-Diller, J., Benfey, P.N., and Hauser M.-T. (2002): Two new loci, *PLEIADE* and *HYADE*, implicate organ-specific regulation of cytokinesis in Arabidopsis. Plant Physiol. **130**, 312-324.

Müller, S., Smertenko, A., Wagner, V., Heinrich, M., Hussey, P.J. and Hauser M.-T. (2004): The plant microtubule associated protein, AtMAP65-3/PLE, is essential for cytokinetic phragmoplast function. Current Biol. **14**, 412-417.

Murata, T., and Wada, M., (1991): Expreimental obliteration of the preprophase band alters the site of cell division, cell plate orientation and phragmoplast expansion in *Adiantum protonemata*. J. Cell Sci. **100**:551-557.

Nagata, T. and Kumagai, F.(1999): Plant cell biology through the window of the highly synchronized tobacco BY-2 cell line. Methods Cell Sci **21**:123-7.

Nakajima, K., Furutani, I., Tachimoto, H., Matsubara, H., and Hashimoto, T. (2004): SPIRAL1 encodes a plant-specific microtubule-localized protein required for directional control of rapidly expanding arabidopsis cells. The plant cell **16**, 1178-1190.

Neant, I., and Guerrier, P. (1988): 6-Dimethylaminopurine blocks starfish oocyte maturation by inhibiting a relevant protein kinase activity. Exp. Cell Res. 176, 68.

Nick, P. (1998): Signaling to the microtubular cytoskeleton in plants. Int. Rev. Cyt. **184**: 33-80.

Nigg EA.(1995): Cyclin-dependent protein kinases: key regulators of the eukaryotic cell cycle. Bioessays. 17:471-80.

Nishihama Ryuichi and Machida Yasunori (2001): Expansion of the phragmoplast during plant cytokinesis: a MAPK pathway may MAP it out. Curr. Opin. Plant Biol.

4:507-512.

Nishihama, R., Ishikawa, M., Araki, S., Soyano, T., Asada, T., and Machida, Y. (2001): The NPK mitogen-activated protein kinase kinase kinase is a regulator of cell-plate formation in plant cytokinesis. Genes & Dev. 15: 352-363.

Nishihama, R., Soyano, T., Ishikawa, M., Araki, S., Tanaka, H., Asada, T., Irie, K., Ito, M., Terada, M., Banno, H., et al. (2002): Expansion of the cell plate in plant cytokinesis requires a kiinesin-like protein/MAPKKK complex. Cell **109**: 87-99.

O'Connell, K.F., Leys, C.M., and White, J.G. (1998): A genetic screen for temperature-sensitive cell-division mutant of Caenorhabditis elegans. Ggenetics **149**, 1303-1321.

Oegema, K., Wiese, C., Martin, O. C., Miligan, R. A., Iwamatzu, A., Mitchinson, T. J. and Zheng, Y. (1999). Characterizaion of two related Drosophila gamma-tubulin complexes that differ in their ability to nucleate microtubules. J. Cell. Biol. **144,** 721-733

Ohkura, H., Adachi, Y., Kinoshita, N., Niwa,O., Toda, T., and Yanagida, M.(1988): Cold-sensitive and caffeine-supersensitive mutant of the Schizosaccharomyces-Pombe Dis genes implicated in sister chromatid separation during mitosis. Embo Journal **7**:1465-1473.

Oka, M., Yanagawa, Y., Asada, T., Yoneda, A., Hasezawa, S., Sato, T., Nakagawa, H.(2004): Inhibition of proteasome by MG-132 treatment causes extra phragmoplast formation and cortical microtubule disorganization during M/G1 transition in synchronized tobacco cells. Plant Cell Physiol. **45**:1623-32

Ookata, K., Hisanaga, S., Bulinski, J.C., Murofushi, H., Aizawa, H., Itoh, T.J., Hotani, H., Okumura, E., Tachibana, K. and Kishimoto, T. (1995): Cyclin B interaction with microtubule-associated protein 4 (MAP4) targets p34cdc2 kinase to microtubules and is a potential regulator of M-phase microtubule dynamics. J.Cell. Biol. **128**:849-886.

Ostergren, G. (1950). Consideration of some elementary features of mitosis. *Hereditas* **36**, 1-19.

Ovechkina, Y., Wordeman, L. (2003): Unconventional motoring: an overview of the Kin C and Kin I kinesins. Traffic **4**, 367-375.

Pages, G., Lenormand, P., L'Allemain, G., Chambard, J.C., Meloche, S., and Pouyssegur, J. (1993) Mitogen-activated protein kinases p42mapk and p44mapk are required for fibroblast proliferation. Proc. Nat. Acad. Sci.**90**: 8319-8323.

Panteris, E., Apostolakos, P., Graf, R., and Galatis, B. (2000): Gamma-tubulin colocalizes with microtubule arrays and tubulin paracrystals in dividing vegetative cells of higher plant. Protoplasma **210**: 179-187.

Patel S, Rose A, Meulia T, Dixit R, Cyr RJ, Meier I.(2004): Arabidopsis WPP-domain proteins are developmentally associated with the nuclear envelope and promote cell division. Plant Cell **16(12)**:3260-73

Pellman, D., Bagget, M., Tu, H., and Fink, G. R. (1995): Two mirotubule-associated proteins required for anaphase spindle movement in *Saccharomyces cerevisiae*. J. Cell. Biol. **130**: 1373-1385.

Perez F, Diamantopoulos GS, Stalder R, Kreis T.E. (1999): CLIP-170 highlights gowing microtubules ends in vivo. Cell **96**:517-527.

Pfleger, C.M., Kirschner, M.W. The KEN box: an APC recognition signal distinct from the D box targeted by Cdh1. Genes Dev **14**:655-65.

Popov, A.V., Severin, F., and Karsenti, E. (2002): XMAP215 is required for the microtubule-nuleating activity of centrosomes. Curr. Biol. **12,** 1326-1330.
Schuyler, Scott, C., S.C., Liu, J.Y. and Pellman, D.J. (2003): The molecular function of Ase1p: evidence for a MAP-dependent midzone-specific spindle matrix. J. Cell Biol. **160**, 517-528.

Preuss, M.L., Kovar, D.R., Lee, Y.R., Staiger, C.J., Delmer, D.P., Liu, B. (2004): A plant-specific kinesin binds to actin microfilaments and interacts with cortical microtubules in cotton fibers. Plant Physiol. **136**,3945-55.

Reddy, A.S., Safadi, F., Narasimhulu, S.B., Golovkin, M., Hu, X.(1996): A novel plant calmodulin-binding protein with a kinesin heavy chain motor domain. J Biol Chem.

271:7052-60.

Reddy, A. S. (2000): Molecular motors and their fuctions in plants. Int. Rev. Cytol. **204,** 97-178.

Rieder, C.L. (1981): The structure of the cold-stable kinetochore fiber in metaphase PtK1 cells. Chromosoma. **84**:145-58.

Renaudin, J. P., Doonan, J. H., Freeman, D., Hashimoto, J., Hirt, H., Inze, D., Jacobs, T., Kouchi, H., Rouze, p., Squter, M., et al (1996): Plant cyclins: a unified nomenclature for plant A-, B- and D-type cyclins based on sequence organization. Plant Mol Biol **32**:1003-1018.

Reszka, A.A., Seger, R., Diltz, C.D., Krebs, E.G., Fischer, E.H. (1995). Association of mitogen-activated protein-kinase with the microtubule cytoskeleton. PNAS of USA **92,** 8881-8885.

Samuels, A. L., Giddings, J. H., Jr, Staehelin, L.A. (1995): Cytokinesis in tobacco BY-2 and root tip cells: a new model of cell plate formation in higher plants. J Cell Biol. **130**:1345-57.

Schoch, C., Aist, J., Yode,r O., and Turgeon, B. (2003): A complete inventory of fungal kinesins in representative filamentous ascomycetes. Fungal Genet. Biol. **39**, 1-15.

Sedbrook, J. C., Ehrhardt, D. W., Fishe, S. E., Scheible, W. R., and Somerville, C. R. (2004) The Arabidopsis sku6/spiral1 gene encodes a plus end-localized microtubule-interacting protein involved in directional cell expension. Plant Cell. **16,** 1506-1520.

Sedbrook, J. C. (2004): MAPs in plant cells: delineating microtubule growth dynamics and organization. Curr. Opi. in Plant Biol., **7**: 632-640.

Shapiro, P.S., Vaisberg, E., Hunt, A.J., Tolwinski, N.S., Whalen, A.M., McIntosh J.R., and Ahn, N.G. (1998): Activation of the MKK/ERK pathway during somatic cell mitosis: Direct interactions of active ERK with kinetochores and regulation of the mitotic 3F3/2 phosphoantigen. J. Cell. Biol. **142**:1533-1545.

Shaw, S.L., Kamyar, R. and Ehrhardt, D.W. (2003): Sustained microtubule treadmilling in arabidopsis cortical arrays. Science **300**, 1715-1718.

Shelanski, M.L., Gaskin, F. And Cantor, C.R. (1973): Microtubule assembly in absence of added nucleotides. Proc. Natl. Acad. Sci. USA **70**, 765-768.

Shiebele. (2000): γ-tubulin complexes: binding to the centromsome, regulation and microtubule nucleation. Curr. Opin. Cell Biol. **12**,113-118.

Sherryl, R., Bisgrove, Whitney, E., Hable, and Darryl, L. Kropf. (2004): +TIPs and microtubule regulation. The beginging of the plus ends in plants. Plant Physiology **136**, 3855-3836.

Shoji, T., Narita, N. N., Hayashi, K, Asada, J., Hamada, T., Sonobe, S., Nakajima, K., and Hashimoto, T. (2004): Plant-specific microtubule-associated protein SPIRAL2 is required for anisotropic growth in Arabidopsis. Plant Physiol. **136**, 3933-3944.

Smertenko, A., Saleh, N., Igarashi, H., Mori, H., Hauser-Hahn, I., Jiang, C.J., Sonobe, S., Lloyd, C.W., and Hussey, P.J. (2000): A new class of microtubule-associated proteins in plants. Nat. Cell Biol. **2**, 750-753.

Smertenko, A.P., Bozhkov, P.V., Filonova, L.H., von Arnold, S. and Hussey, P.J. (2003): Re-organisation of the cytoskeleton during developmental programmed cell death in *Picea abies* embryos. Plant J. **33**, 813-824.

Smertenko, A.P., Chang, H.Y., Wagner, V., Kaloriti, D., Fenyk, S., Sonobe, S., Lloyd, C., Hauser, M.T. and Hussey, P.J. (2004): The *Arabidopsis* microtubule-associated protein AtMAP65-1: Molecular analysis of its microtubule bundling activity. Plant Cell, **16**: 2035-2047.

Smertenko, A.P., Chang, H.Y., Sonobe, S., Fenyk S. I., Weingartner, M., Bogre, L., Hussey, P. J., (2006): Control of the AtMAP65-1 interactoin with microtubules through the cell cycle. Journal of Cell Science. 119, 3227-3237.

Smirnova, E.A., and Bajer, A.S. (1994): Microtuble converging centers and reorganization of the interphase cytoskeleton and the mitotic spindle in higher-plant

Haemanthus. Cell motility and the cytoskeleton **27**, 219-233.

Smith L.G., Hake S., and Sylvester A. W. (1996): The *tangled 1* mutation alters cell division orientations throughout maize leaf development without altering leaf shape. Development **122**, 481-489.

Smith, L.G., Gerttula, S.M., Han, S., Levy, J. (2001): Tangled 1: a microtubule binding protein required for the spatial control of cytokinesis in maize. J. Cell Biol. **52:**231-236.

Sollner, R., Glasser, G., Wanner, G., Somerville, C.R., Jurgens, G. and Assaad, F.F. (2002): Cytokinesis-defective mutants of Arabidopsis. Plant Physiol. **129**, 678-690.

Sollner, R., Glasser, G., Wanner, G., Somerville, C.R., Jurgens, G. and Assaad, F.F. (2002): Cytokinesis-defective mutants of Arabidopsis. Plant Physiol. **129**, 678-690.

Sorensen, M.B., Mayer, U., Lukowitz, W., Robert, H., Chambrier, P., Jurgens, G., Somerville, C., Lepiniec, L. and Berger, F. (2002): Cellularisation in the endosperm of *Arabidopsis thaliana* is coupled to mitosis and shares multiple components with cytokinesis. Development, **129**, 5567-5576.

Stals, H., Bauwens, S., Traas, J., VanMontagu, M., Engler,G., and Inze, D.(1997): Plant CDC2 is not only target to the pre-prophase band, but also co-localizes with the spindle, phramoplast, and chromosomes. Feb Letters **418**, 229-234.

Stoppin, V., Vantard, M., Schmit, A. C. and Lambert, A.M. (1994): Isolated plant nuclei nucleate microtubule assembly-the nuclear-surface in higher-plants has centrosome-like activity. Plant Cell **6**,1099-1106.

Stoppin-Mellet, V., Gaillard, J. and Vantard, M. (2002): Functional evidence for *in vitro* microtubule severing by the plant katanin homologue. Biochem. J. **365**: 337-342.

Su, L.K., Burrell, M., Hill, D. E., Gyuris, J., Brent, R., Wiltshire, R., Trent, J., Vogelstein, B., Kinzler, K.W.(1995) APC binds to the novel protein EB1. Cancer Res **55**: 2972–2977

Sugimoto, K., Williamson, R.E., Wasteneys, G.O. (2001): Wall architecture in the cellulose-deficient rsw1 mutant of *Arabidopsis thaliana*: microfibrils but not

microtubules lose their transverse alignment before microfibrils become unrecognizable in the mitotic and elongation zones of roots. Protoplasma 215:172–183

Sugimoto, K., Himmelspach, R., Williamson, R.E., Wasteneys, G.O. (2003): Mutation or drug-dependent microtubule disruption causes radial swelling without altering parallel cellulose microfibril deposition in *Arabidopsis* root cells. Plant Cell 15:1414–1429

Takahashi, Y., Soyano, T., Sasabe, M., Machida, Y. (2004): A MAP kinase cascade that controls plant cytokinesis. J Biochem (Tokyo).**136**:127-32.

Takenaka, K., Gotoh, Y., and Nishida, E. (1997): MAP kinase is required for the spindle assembly checkpoint but is dispensable for the normal M phase entry and exit in *Xenopus* egg cell cycle extracts. J. Cell Biol.**136**: 1091-1097.

Takenaki, K., Moriguchi, T., and Nishida, E. (1998): Activation of the protein kinase p38 in the spindle assembly checkpoint and mitotic arrest. Science **280**:599-602.

Tassin, A. M., Celati, C., Paintrand,M., and Bornens, M. (1998): Identification of the humanhomologue of the yeast spc98 and its association with γ-tubulin. *J. Cell Biol.* **141**, 689-701.

Tatsuya, A., Siripong, T., and Takash,i H. (2004): Microtubule defects and cell morphogenesis in the lefty1lefty2 tubulin mutant of Arabidopsis thaliana. Plant cell phsio. **45**, 211-220.

Timauer, J. S., Grego, S., Salmon, E. D., Mitchison, T. J. (2002): EB1-microtubule interactions in Xenopus egg extracts: role of EB1 in microtubule stabilization and mechanisms of targeting to microtubules. Mol Biol Cell **13**, 3614-3626.

Titus, M.A. & Gibert, S.P.(1999): The diversity of molecular motors: an overview. Cell mol. Life. Sci. **56**, 181-183.

Mathur, J., Mathur, N., Kernebeck, B., Srinivas, B. P., and Hulskamp, M. (2003): A novel Localization pattern for an EB1-like protein links microtubule dynamics to

endomembrane organization. Current Biology **13**, 1991-1997.

Meggio F, Donella Deana A, Ruzzene M et al. (1995) "Different susceptibility of protein kinases to staurosporine inhibition. Kinetic studies and molecular bases for the resistance of protein kinase CK2". Eur J Biochem. 234(1):317-22

Tournebize, R., Popov, A., Kinoshita, K., Ashford, A.J., Rybina, S., Pozniakovsky, A., Mayer, T.U., Walczak, C.E., Karsenti,E., and Hyman,A. A. (2000) Control of microtubule dynamics by the antagonistic activities of XMAP215 and XKCM1 in *Xenopus* egg extracts. Nat. Cell. Biol. **2**, 13-19.

Topping, J.F., Wei, W.B. and Lindsey, K. (1991): Functional tagging of regulatory elements in the plant genome. Development **112**, 1009-1019.

Twell, D., Park, S.K., Hawkins, T.J., Schubert, D., Schmidt, R., Smertenko, A. and Hussey, P.J. (2002): MOR1/GEM1 has an essential role in the plant-specific cytokinetic phragmoplast. Nat. Cell Biol. **4**, 711-714.

Tournebize, R., Popov, A., Kinoshita, K., Ashford, A.J., Rybina, S., Pozniakovsky, A., Mayer, T.U., Walczak, C.E., Karsenti E. and Hyman, A.A.2000. Control of microtuule dynamics by the antagonistic activities of XMAP215 and XKCM1 in *Xenopus* egg extracts. Nat. Cell Biol. **2**:13-19.

Ueda, K. and Matsuyama, T. (2000): Rearrangement of cortical microtubules from transverse to oblique or longitudinal in living cells of transgenic *Arabidopsis thaliana.* Protoplasma, **213**, 28-38.

Vallee, R. B. (1982): A taxol- dependent procedure for the isolation of microtubules and microtubule-associated proteins (MAPs). J. Cell. Biol. **92**:435-442.

Vasquez, R.J., Gard, D.L., Cassimeris, L. Phosphorylation by CDK1 regulates XMAP215 function in vitro. Cell Motil Cytoskeleton. **43**:310-21.

Verbrugghe, Koen, J. C., and White, J. G., (2004): SPD-1 is required for the formation of the spindle midzone but is not essential for the completion of cytokinesis in *C.*

elegans embryos. Current biology **14:** 1755-1780.

Von Arnold, S., Sabala, I., Bozhkov, P., Dyachok, J. and Filonova, L. (2002): Developmental pathways of somatic embryogenesis. Plant Cell Tissue and Organ Culture **69**:233-249.

Wang, X.M., Ahai, Y., and Ferrell, J.E. (1997): A role for mitogen-activated protein kinase in the spindle assembly checkpoint in XTC cells. J. Cell. Biol. **137**:433-433.

Wang, P.J., Huffaker, T.C. (1997): Stu2p: A microtubule-binding protein that is an essential component of the yeast spindle pole body. J Cell Biol. **139**:1271-80.

Wasteneys, G.O. and Williamson, R.E. (1989): Reassembly of microtubules in *Nitella tasmanica*-Assembly of cortical microtubules in branching clusters and its relevance to steady-state microtubule assembly. J. Cell Sci. **93**:705-714.

Wasteneys, G.O. (2000): The cytoskeleton and growth polarity. Curr. Opin. Plant Biol. **3**,503-511.

Wasteneys, G. O. (2002): Microtubule organization in the green kingdom: chaos or selforder? Journal of Cell Science **115**, 1345-1354.

Wasteneys, G.O. (2004): Progress in understanding the role of microtubules in plant cells. Curr Opin Plant Biol 7:651–660

Weingartner, M., Binarova, P., Drykova, D., Schweighofer, A., David, J.P., Heberle-Bors, E., Doonan, J., Bogre, L.(2001): Dynamic recruitment of Cdc2 to specific microtubule structures during mitosis. : Plant Cell **13(8)**:1929-43.

Wen, Y., Eng, C.H., Schmoranzer, J., Cabrera-Poch, N., Morris, E.J., Chen, M., Wallar, B.J., Albertsm, A.S., Gundersen, G.G. (2004): EB1 and APC bind to mDia to stabilize microtubules downstream of Rho and promote cell migration. Nat Cell Biol **6**: 820–830

Whittington, A.T., Vugrek, O., Wei, K.-J., Hasenbein, N.G., Sugimoto, K., Rashbrooke, M.C. and Wasteneys, G.O. (2001): MOR1 is essential for organization cortical mocrotubules in plants. Nature **411**:610-613.

Wicker-Planquart, C., Stoppin-Mellet, V., Blanchoi, L. and Vantard, M. (2004): Interactions of tobacco microtubule-associated protein MAP65-1b with microtubules. Plant J. **39**, 126-134.

Wright, J.H., Munar, E., Jameson, D.R., Andreassen, P. R., Margolis, R.L., Seger, R., and Krebs, E.G.(1999): Mitogen-activated protein kinase kinase activity is required for the G2/M trasition of the cell cycle in mammalian fibroblasts. Proc. Nat. Acad. Sci. **96**: 11335-11340.

Wymer, C., and Lloyd, C. W. (1996): Dynamic microtubules: Implications for cell wall patterns. Trends in Plant Science **1**, 222-228.

Yamaguchi, M., Fabian, T., Sauter, M., Bhalerao, R.P., Schrader, J., Sandberg, G., Umeda M, Uchimiya H.(2000): Activation of CDK-activating kinase is dependent on interaction with H-type cyclins in plants. Plant J. **24**:11-20

Yamashita, A., Sato, M., Fujita, A., Yamamoto, M., and Toda, T., (2005):The roles of fission yeast in mitotic cell division, meiotic nuclear oscillation and cytokinesis checkpoint signaling. Mol Biol Cell

Yasuhara, H., Muraoka, M., Shogaki, H., Mori, H. and Sonobe, S. (2002): TMBP200, a microtubule bundling polypeptide isolated from telophase tobacco BY-2 cells is a MOR1 homologue. Plant Cell Phys. **43**, 595-603.

Yuan, M., Shaw, P.J., Warn, R.M., and Lloyd, C.W. (1994): Dynamic reorientation of cortical microtubules, from transverse to longitudinal in living plant cells. Proc. Nat. Acad. Sci. USA **91**, 6050-6053.

Zabala, J.C. and Cowan, N.J. (1992): Tubulin dimer formation via the release of α- and β-tubulin monomers from multimolecular complexes. Cell Motil. And Cytoskeleton **23**, 222-230.

Zecevic, M., Catling, A.D., Eblen, S.T., Renzi, L., Hittle, J.C., Yen, T.J., Gorbsky, G.J., and Weber, M.J.(1998): Active MAP kinase in mitosis: Localization at kinetochores and association with the motor protein CENP-E. J. Cell Biol. 142; 1547-1558.